Università degli studi Roma Tre
Facoltà di SMFN
Dipartimento di Fisica "E. Amaldi"

Flavor-changing processes of quarks and leptons as indirect probes of physics beyond the Standard Model

Gianluca Blankenburg

SCUOLA DI DOTTORATO DI RICERCA IN FISICA

CICLO XXV

Supervisore interno: Prof. GUIDO ALTARELLI

Supervisore esterno: Dott. GINO ISIDORI

January, 2013

Contents

Introduction and Outline

The deepest knowledge of the nature behavior is today represented by Standard Model (SM) of particle physics. This quantum field theory is briefly presented in Chapter 1, where we discuss its foundations in terms of particles and gauge symmetries. In particular we focus on the scalar and flavor sector, that are the main concern of this Thesis. We show that the elegance of the theory seems to be completely lost when we consider the ultra-high sensitivity to the short-distance effects in the scalar mass term (hierarchy problem) or when we try to explain the peculiar patterns of masses and mixings that we observe in quarks and leptons (flavor puzzle).

Anyway if the hierarchy problem seems to indicate that some unknown completion of the SM should be at the TeV scale, the experimental data agree with high precision with the SM. For this reason we know that if some New Physics (NP) is close it must be highly non-generic, specially in its flavor sector (flavor problem). After quantifying this considerations in Chapter 2, we present a possible solution to this problem (at least from the flavor point of view), that is the Minimal Flavor Violation hypothesis.

In Section 2.3 we present one of the most prominent candidates for a theory beyond the SM, that is the supersymmetry. We again discuss with particular attention the Higgs and flavor sector of the Minimal Supersymmetry Standard Model. In particular we show that within the minimal framework of this theory the recent LHC results are pushing higher and higher the scale of the supersymmetric particles, stepping away from the naturalness expectations.

Nevertheless, some new ideas able to explain what has been observed so far have emerged. For example the squarks of the first two families can be significantly heavier than the third generations (split-family SUSY), explaining the fact that we haven't seen any supersymmetric particle and keeping the theory natural at the same time. This possibility is analyzed in Chapter 3, where we present a specific flavor model compatible with such a scenario and based on a $U(2)^3$ flavor symmetry. We show that this symmetry is not only able to give the desired suppression to Flavor Changing Neutral Currents, but it can also provide some insight into the SM flavor puzzle. However the $U(2)^3$ model is able to describe only the quark sector, while in a complete theory we need to enlarge

the description also to leptons. This goal is achieved in [1] and presented in Section 3.2. Starting from the maximal $U(3)^5$ symmetry we show how it is possible to obtain a two steps breaking leading to $O(3)$ in the neutral sector and to $U(2)^5$ in the charged sector, to be able to provide a good description of the lepton sector and keeping the (s)quark as in the original $U(2)^3$ model. We also calculate the Lepton Flavor Violation processes, testing the goodness of the model in this respect.

The same model is analyzed also in Section 3.3, where we assume the $U(2)^3$ flavor symmetry to be broken at a very high scale, instead of being directly applied at the electroweak scale [2]. We present the Renormalization Group Equations effects on the low-energy parameter space. For example we check under which conditions it is possible to obtain a splitted squark spectrum and if the typical $U(2)^3$ mixing properties are preserved by the running. We also study possible deviations from the minimal breaking patter of the flavor symmetry and the effects of some usually neglected $\Delta F = 2$ operators.

Beside supersymmetry, other New Physics theories have been proposed in order to solve (at least in part) the problems of the SM. In the second part of this Thesis we take a more general approach: we analyze in a model-independent way a few phenomenological consequences of possible deviations from the SM Higgs sector. In fact almost all the SM problematic aspects are in its scalar sector (hierarchy problem, flavor puzzle, vacuum stability, neutrino masses and also cosmological constant problem) and for this reason a motivated NP Higgs sector usually introduces several new features not present in the SM.

Thus, the recent LHC discovery of a new scalar neutral particle gives us the important opportunity to probe the SM and its possible completions in one of their crucial aspects. In Section 4.1 we present a general analysis where we i) analyze the indirect constraints on possible flavour-violating couplings of the Higgs set by low-energy flavour-changing transitions, ii) analyze the consequences of these constraints on possible flavour-violating decays of the Higgs boson [3]. In particular we show which are the flavor-changing decays that could be observed with the LHC sensitivity.

In Section 4.2 and 4.3 instead, we focus on a class of theories beyond the SM, that is the 2 Higgs Doublets Model. In this framework we analyze the B-physics phenomenology and in particular the decay $B \to \tau\nu$ that seems to show a slight tension with the SM expectation [4]. We present under which conditions it is possible to obtain an enhancement in the decay rate assuming Minimal Flavor Violation and considering all the other flavor processes relevant at large $\tan\beta$. We also show a preliminary study, where we compare the discovery potential of the processes $B \to \tau\nu$ and $B_s \to \mu\mu$, in view of the experimental prospects of LCHb and a possible superB machine [5].

Chapter 1

Standard Model and open questions

1.1 The Standard Model

The ultimate description of all the known natural phenomena can be given in terms of fundamental particles and their interactions. The elementary particles are the constituent elements of matter and radiation and their dynamic is governed by four different types of interactions: *electromagnetic, weak, strong* and *gravity*. Between the latter, gravity plays a special role because its quantum effects become important only for very high energy densities, that are not in practice accessible to experiments in laboratories. Therefore our deepest knowledge of the nature behavior is given today by the Standard Model, which is a quantum field theory giving an accurate description of all the known particle physics phenomenology at the current experimental energy scales.

Particles and gauge symmetries

The SM is a quantum field theory based on the invariance under the gauge symmetry group

$$G_{SM} = SU(3)_c \times SU(2)_L \times U(1)_Y \,. \tag{1.1}$$

The matter fields are spin 1/2 particles, that differ according to their transformation properties under the symmetry group, as shown in Tab. 1.1; in particular *quarks* are charged under $SU(3)_c$ while *leptons* are not, left-handed fields are in $SU(2)_L$ doublets and there are no right-handed neutrinos.

$SU(3)_c$ is the colour group of the strong interaction, described by a theory called QCD; it has 8 generators corresponding to the spin zero force mediators, called *gluons*. The non-Abelian structure of this gauge group gives the main properties of QCD: aymptotic freedom and confinement. The effects of the gluon self interactions renders negative the β function of QCD and this causes that at low energies the quarks are bound in composite structures called *mesons* and *baryons*, while at high energies the theory becomes weakly

	Q_L	d_R	u_R	L_L	e_R
$U(1)_Y$	$\frac{1}{6}$	$\frac{1}{3}$	$-\frac{2}{3}$	$-\frac{1}{2}$	1
$SU(2)_L$	**2**	**1**	**1**	**2**	**1**
$SU(3)_c$	**3**	$\overline{\mathbf{3}}$	$\overline{\mathbf{3}}$	**1**	**1**

Table 1.1: Quantum numbers of the matter fermion fields of the SM.

coupled. A combination of $SU(2)_L \times U(1)_Y$ gives the electroweak interactions, described by the QED. In particular $SU(2)_L$ is the weak force group, it has 3 generators T_i and it acts only on the left-handed fermions. A combination of two of these generators gives the charged $W^{\pm}$ gauge bosons, while the third one mixes with the $U(1)_Y$ generator Y to form the neutral Z boson and the photon γ. The electric charge is therefore given by $Q = T_3 + Y/2$.

The gauge invariant Lagrangian is given by

$$\mathcal{L}_K = \sum_{i\,m} \left(i\bar{\psi}_i \not{D} \psi_i - \frac{1}{4} F^A_{m\,\mu\nu} F^{\mu\nu\,A}_m \right) , \tag{1.2}$$

$$D_\mu = \partial_\mu + i\, g_m V_{m\,\mu} \,, \tag{1.3}$$

$$F^A_{m\,\mu\nu} = \partial_\mu V^A_{m\,\nu} + \partial_\nu V^A_{m\,\mu} - g\, C_{ABC} V^B_{m\,\mu} V^C_{m\,\nu} \,, \tag{1.4}$$

where the sum is extended to all the fermions ψ_i and all the interactions g_m with the corresponding generators $V^A_{m\,\mu}$.

Electroweak symmetry breaking

The SM Lagrangian can be written as

$$\mathcal{L}_{SM} = \mathcal{L}_K + \mathcal{L}_Y + \mathcal{L}_H \,, \tag{1.5}$$

where $\mathcal{L}_K$ contains the kinetic terms and the gauge interactions given in Eq. (1.2) (with the addition of the ϕ kinetic term), $\mathcal{L}_Y$ gives the Yukawa interactions and $\mathcal{L}_H$ is the scalar potential. The whole $\mathcal{L}_{SM}$ is G_{SM} invariant but the minimum in $\mathcal{L}_H$ is not and this generates the spontaneous breaking of $SU(2)_L \times U(1)_Y \to U(1)_Q$. To be more precise, given the simplest form of $\mathcal{L}_H$

$$\mathcal{L}_H = -\mu^2 \phi^\dagger \phi - \lambda (\phi^\dagger \phi)^2 \,, \tag{1.6}$$

it gives a continuum of degenerate states of minimum energy, that all together are symmetric, though the single minimum states are not. The fact that the system is found in one particular minimum generates the spontaneous breaking of the symmetry. This means that the interactions are kept symmetric, while the mass spectrum violates the symmetry. In particular in Eq. (1.6) the negative squared mass doublet ϕ in the unitary gauge takes the vacuum expectation value (vev)

$$\langle 0|\phi(x)|0\rangle = \begin{pmatrix} 0 \\ v/\sqrt{2} \end{pmatrix} , \qquad v = (-\mu^2/\lambda)^{1/2} \,. \tag{1.7}$$

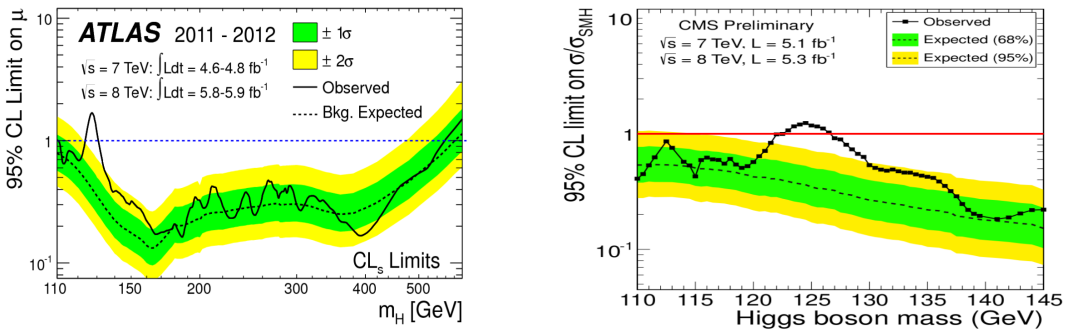

Figure 1.1: Observation of a new particle in the search for the Standard Model Higgs boson with the ATLAS (left) and CMS (right) detectors.

After a shift of the fields around the minimum, this gives three Goldstone bosons that become the longitudinal components of the massive $W^{\pm}$ and Z, and one additional scalar neutral particle, called the *Higgs* boson, h.

Even if the mass of h is not determined by the theory, the Electro Weak Precision Test and the non-observation of h at LEP2 suggest that in the SM [6]

$$114 \text{ GeV} < m_h < 171 \text{ GeV} \qquad (95\% \text{ c.l.}) \,. \tag{1.8}$$

This uncertainty on m_h is now disappeared after the 4^{th} of July 2012, when ATLAS and CMS announced the discovery of a neutral scalar particle compatible with the SM Higgs boson, with mass

$$m_h = 125.3 \pm 0.9 \qquad (\text{CMS [7]}) \,, \tag{1.9}$$
$$m_h = 126.0 \pm 0.8 \qquad (\text{ATLAS [8]}) \,, \tag{1.10}$$

as shown in Fig. 2.1. May be it is still too early to assert that the SM Higgs mechanism is at work, but certainly the agreement between the SM expectation in Eq. (1.8) and the experimental values in Eqs. (1.9) and (1.10) is promising.

The flavor sector

Quarks and leptons are present in three generations with equal quantum numbers but with different masses. The origin of this triple replication of the SM fermion content is one of the most mysterious aspects of the theory.

As far as the masses are concerned, the chiral nature of the $SU(2)_L$ gauge symmetry prevents a direct fermion mass term in the Lagrangian. Such term arises through the Yukawa interactions with the Higgs field in

$$\mathcal{L}_Y = (Y_u)_{ij} \bar{Q}_{Li} u_{Rj} \tilde{\phi} + (Y_d)_{ij} \bar{Q}_{Li} d_{Rj} \phi + (Y_e)_{ij} \bar{L}_{Li} e_{Rj} \phi \,, \tag{1.11}$$

where $\tilde{\phi} = -i(\phi^\dagger \tau_2)^T$ and ij are generation indices. After the electroweak symmetry breaking the neutral component of Higgs doublet can be written as $\phi_2 = (v+h)/\sqrt{2}$, where the term proportional to v gives the fermion masses

$$(M_u)_{ij}\bar{u}_{Li}u_{Rj} + (M_d)_{ij}\bar{d}_{Li}d_{Rj} + (M_e)_{ij}\bar{e}_{Li}e_{Rj}, \qquad M_i = Y_i\frac{v}{\sqrt{2}}\,, \tag{1.12}$$

while the piece with h gives the interactions between fermions and the physical Higgs boson.

In general the Yukawa matrices are non-diagonal in the interaction basis and therefore it could be possible that the gauge or kinetic terms mix the mass eigenstates. Within the SM this is the case only for the weak interaction, which is the only force that couples up and down sectors. Note that in the Higgs sector the mixing between left and right components could also generate non-diagonal interactions, but this does not happen in the SM where there is only one Higgs doublet and then the masses and the couplings with h correspond. In the quark sector, being $U_L^u, U_L^d, U_R^u, U_R^d$ the unitary transformations that diagonalize Y_u and Y_d, it results that in the mass basis the weak current becomes*

$$J_\mu = \bar{u}_L\gamma_\mu d_L \rightarrow \bar{u}_L {U_L^u}^\dagger U_L^d \gamma_\mu d_L\,, \tag{1.13}$$

giving the Cabibbo-Kobayashi-Maskawa (CKM) mixing matrix

$$V_{CKM} = {U_L^u}^\dagger U_L^d \equiv \begin{pmatrix} V_{ud} & V_{us} & V_{ub} \\ V_{cd} & V_{cs} & V_{cb} \\ V_{td} & V_{ts} & V_{tb} \end{pmatrix}. \tag{1.14}$$

With a proper rephasing of the fields it possible to show that V_{CKM} contains 4 independent parameters, 3 angles and 1 phase. An important observation is that the phase, δ_{CKM}, is the only source of CP violation in the SM. †

1.2 Open questions

The SM has been tested in the past decades to a very good precision in both direct and indirect searches at particle colliders. It showed a very good agreement with the data, except for some small anomalies that are still under discussion. Nevertheless the SM can not be the "ultimate" theory of nature, due to the following arguments:

- Only three of the four fundamental forces are considered in the theory. This is a very robust approximation at the current experimental energies, but at very high scales gravity effects become important.
- Almost 23% of the Universe is composed by non-ordinary baryonic matter, called Dark Matter (DM). This means that new quantum excitations must enter into the play at some energy scales.

*In this notation ${U_L^u}^\dagger Y_u U_R^u = \mathrm{diag}(y_u, y_c, y_t)$ and ${U_L^d}^\dagger Y_d U_R^d = \mathrm{diag}(y_d, y_s, y_b)$

†Another possible source of CPV is the θ_{QCD} term that will be discussed in the next Section.

- Charge quantization and anomaly cancellation appear in the SM as an accident and a more fundamental explanation is missing. For example in Grand Unified Theories (GUT) the down quark electric charge is 1/3 of the electron charge because of the quarks are present in three different colors.
- Matter/Antimatter asymmetry in the universe can not be explained within the SM.
- Neutrinos are not massless and the smallness of their masses seem to point to a very high scale in which the Lepton Number is violated, for example given by the ν_R Majorana mass scale in the see-saw mechanism.
- The flavor structures of the SM span over several orders of magnitude without any apparent reason (flavor puzzle).
- The Higgs potential is quadratically sensitive to the cut off of the theory in the quantum corrections (hierarchy problem).

The last two points are the main motivations for this Thesis and so they deserve a separate description.

1.2.1 Flavor puzzle

One of the more unclear aspects of the SM is the Yukawa sector. For example in the charged sector the observed pattern of masses and mixings is strongly hierachical, with some Yukawa couplings being very small without any apparent reason. It is therefore plausible that a more fundamental theory could explain this hierarchy.

This can be easily achieved with the introduction of a *flavor symmetry*, that could distinguish between the different generations. In the Froggatt-Nielsen mechanism [11], for example, the basic idea is that the small mass terms are given by non renormalizable operators involving, in addition to the regular Higgs field H, exotic matter states χ and new scalar fields θ called flavons, as shown in Fig. 1.2. The number of flavon insertions corresponds to the charge of the fermion ψ with respect to a new flavor symmetry, $U(1)_{FN}$, and the suppression of the mass is proportional to the dimension of the operator:

$$m_\psi \simeq \left(\frac{\langle\theta\rangle}{M_\theta}\right)^n \frac{v}{\sqrt{2}}\,. \tag{1.15}$$

Otherwise another typical approach is given by models with Extra Dimension [12], where the hierarchy of fermion masses is generated from the different distributions of the particles in the bulk: the heaviest fermions correspond to the ones closest to the brane where the Higgs is located. Anyway in this Thesis we will concentrate more on the first possibility.

On the contrary in the neutrino sector the hierarchy of the masses is milder and some mixing angles are large. In particular the neutrino mixings can be described with an *anarchic* approach [13] or with a broken *discrete* flavor symmetry [14], in which large

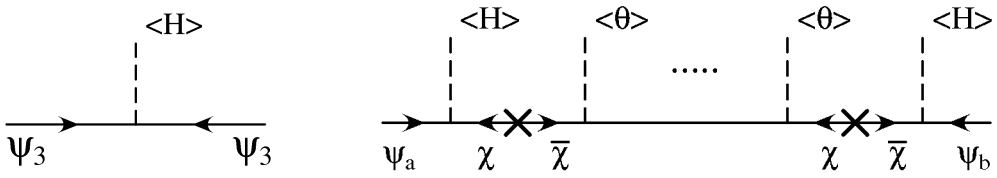

Figure 1.2: Schematic diagrams for Froggatt-Nielsen mechanism. Here a and b are the family indices. $(\chi, \bar{\chi})$ are the vector-like Froggatt-Nielsen fields. Left: the tree level diagram generating the mass of the third family. Right: higher order diagram generating the mass of the lighter matter fields of order $\sim (\frac{\langle\theta\rangle}{M})^n$.

mixings are automatically generated. The mass spectrum can be quasi degenerate, or with normal or inverted hierarchy, depending on the absolute neutrino mass scale which has not been measured jet. Several future experiments based on β-decay [15], $0\nu\beta\beta$ [76] and cosmology [77] are designed to measure this quantity.

1.2.2 Hierarchy problem

As already discussed the spontaneous breaking of $SU(2)_L \times U(1)_Y$ generates the $W^\pm$ and Z bosons masses. This implies that the physical μ parameter in the Higgs potential should be of the same order of magnitude of $m_{W^\pm}$ and m_Z, ie

$$-\mu^2 \sim (100 \text{ GeV})^2 \,. \tag{1.16}$$

Unfortunately $-\mu^2$ is the mass square of a scalar field that receives quadratically divergent quantum corrections. This very high sensitivity to the short-distance effects makes the theory very unstable and unnatural. In practice this problem can be seen in the Higgs mass. In fact its bare value is

$$m^2_{h|\text{bare}} = -2\mu^2 \tag{1.17}$$

and it gets dominant corrections from a top loop, that gives

$$m^2_{h|\text{physical}} = m^2_{h|\text{bare}} + \delta m^2_{h|\text{top}} \,, \qquad \delta m^2_{h|\text{top}} \sim -\frac{3G_F}{2\sqrt{2}\pi^2} m_t^2 \Lambda^2 \,, \tag{1.18}$$

where Λ is momentum cut-off introduced to regularize the loop integral. The problem is that if the SM is assumed to be valid up to M_{GUT} for example, then $\Lambda = M_{GUT}$ and a huge cancellation is needed between the loop correction $\delta m^2_{h|\text{top}}$ and the bare mass $m^2_{h|\text{bare}}$ in order to reproduce $m_{h|\text{physical}} \simeq 125$ GeV. Otherwise, if we demand that the quantum corrections do not exceed the physical Higgs mass, Λ must be close to the TeV scale and within the reach of LHC.

Note that the same argument does not apply to the other particles of the theory because they are protected by extra symmetries (chiral symmetry for fermions and gauge symmetry for γ and g), forcing the quantum corrections to be only logarithmic.

Chapter 2

The flavor problem and supersymmetry

Among the open questions of the SM, the hierarchy problem seems nowadays the most pressing. In fact, differently from the other issues, its solution requires that new degrees of freedom, that we call New Physics, must be very close, at the TeV scale. For this reason in the recent decades the physics community has focused on the development of a low-energy extension of the SM and on the study of its phenomenology. It is fair to mention, however, that other alternative approaches to the hierachy problem exist:

- The SM can be assumed to be the ultimate theory of nature or at most, if there exist any other fundamental scale, it is totally decoupled from the SM (in spite of the presence of gravity).

- Infinite realizations of the Universe exist and we live in one of the few in which the high finetuning of the parameters allows our existence (for example with a higher value of m_h the atoms could not have existed). This is the anthropic solution.

These positions are certainly respectable and, for instance, the latter is usually considered a plausible solution for the cosmological constant problem. Anyway in the past centuries every "unnatural" phenomenon has been understood in terms of a more fundamental theory. Therefore in this Thesis we will not consider these approaches, but we will concentrate on the low-energy phenomenology of theories beyond the SM.

In this respect, if new degrees of freedom are relatively close we could measure them in two different ways. First we could produce directly some new resonances at the high energy colliders, such as the LHC, second we could measure their indirect effects in the quantum corrections to the low energies observables. In this Section we concentrate on the latter possibility, showing that the flavor physics gives an interesting testing ground for the SM and for the new theories.* At the end of the Section we also comment on one of the more motivated SM extensions, supersymmetry (SUSY), also in relation to the

*Interesting reviews on this subject can be found in [17–19].

flavor problem.[†]

2.1 Flavor and CP violation in the SM

The term flavor physics refers to the interactions that distinguish between the various generations. In the last decades flavor physics has shown a great development in both quark and lepton sectors. In fact, from the early years when the existence of the charm quark was inferred from the smallness of the ratio $\Gamma(K_L \to \mu\mu)/\Gamma(K^+ \to \mu\nu)$ and its mass predicted from the size of the mass difference $\Delta m_K = m_{K_L} - m_{K_S}$, passing through the nineties when the top mass value was indicated by Δm_B and to the latest LHCb results, flavor physics has been able to discover or probe New Physics before it could be directly observed in experiments. Moreover in the lepton sector the observation of neutrino oscillations has shown that neutrinos are not massless and has opened a window on energies close to unification scale.

In this Section we comment the main features of the SM flavor physics. In particular we show why the phenomena of Flavor Changing Neutral Currents (FCNC) and CP Violation (CPV) are particularly indicated for testing the SM and how all these informations are put together in the unitarity triangle fit.

2.1.1 FCNC

As already discussed in Sec. 1.1 within the SM the FCNC occur only at loop level and therefore are highly suppressed. For this reason these processes can be very sensitive to non-standard effects, which themselves usually contribute at loop level and are suppressed by the NP scale.

Consider for example neutral meson mixing, in which each flavor quantum number is changed by two units ($\Delta F = 2$). As shown in Fig. 2.1(a) for the Kaon case, this process is obtained from a *box* diagram and therefore presents the typical loop suppression $\alpha_{weak}/4\pi$. In addition, due to the unitarity of the CKM matrix, the total amplitude results proportional to the fermion masses circulating in the loop,[‡] giving in total the overall factor

$$A(K \to \bar{K}) \propto \frac{\alpha_{weak}}{4\pi} V^*_{u_i s} V_{u_i d} \, \frac{m_{u_i} m_{u_j}}{m_W^2} V^*_{u_j s} V_{u_j d} \,. \tag{2.1}$$

This is a very strong suppression for all the light quarks in the loop due to the ratio $m^2_{u_i}/m^2_W$ (*GIM suppression*) and also for the top loop due to the small CKM mixings with the third generation $(V^*_{ts}V_{td})^2$ (*CKM suppression*).

The same suppression is present also in all the neutral $\Delta F = 1$ processes. An illustrative example is given by the $b \to s\gamma$ transition given by the *penguin* diagram shown in Fig. 2.1(b), contributing, for example, to the $B \to X_s\gamma$ and $B_s \to \mu^+\mu^-$ decays. Also in

[†]For a review see [20, 21] or one of the various text books on the topic.

[‡]Each u_i-fermion line in the loop gives a contribution proportional to $\sum_i V^*_{u_i s} \frac{1}{\not{p} - m_{u_i}} V_{u_i d}$, that in the limit of equal masses is zero, given that $V^*_{u_i d_j} V_{u_i d_k} = \delta_{jk}$.

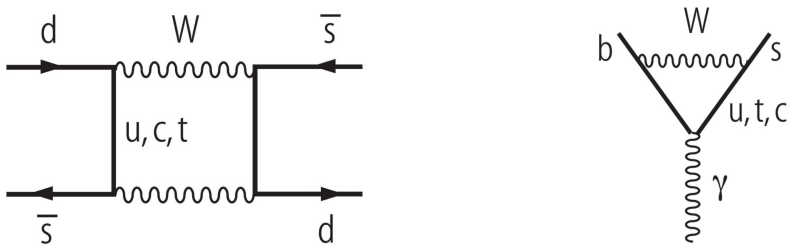

(a) $K - \bar{K}$ mixing (b) $b \to s\gamma$

Figure 2.1: FCNC responsible for $\Delta F = 2$ and $\Delta F = 1$ transitions. In the SM they are generated only at loop level.

the K sector, processes like $K \to \pi\nu\bar{\nu}$ are extremely rare. Even more interesting are the $\Delta F = 1$ transitions in the lepton sector, where processes like $\mu \to e\gamma$ and $\tau \to \mu\gamma$ result proportional to the neutrino masses and therefore they are completely negligible in the SM.

2.1.2 CP Violation

Another important feature of the SM is that the only source of CPV is within the CKM. This causes that flavor physics and CPV become strongly correlated, giving rise to tight predictions that, if not confirmed experimentally, can establish the presence of New Physics.

Considering the SM Lagrangian it is possible to show that $\mathcal{L}_K$ and $\mathcal{L}_H$ are real and therefore CP invariant. On the contrary the Yukawas bring complex parameters that violate CP. In fact if we make a CP transformation on one term in $\mathcal{L}_Y$ it gives (for example for the up quarks)

$$(Y_u)_{ij}\bar{Q}_{Li}u_{Rj}\tilde{\phi} \to (Y_u)_{ij}\bar{u}_{Rj}\tilde{\phi}^\dagger Q_{Li}\,, \tag{2.2}$$

that corresponds to its hermitian conjugate $(Y_u)^*_{ij}\bar{u}_{Rj}\tilde{\phi}^\dagger Q_{Li}$ (that is already contained in the Lagrangian) only if $Y_u = Y_u^*$. In particular it is possible to reabsorb all the phases but one, that, in the canonical mass basis, is given by the CKM phase δ_{CKM}.

CPV has been measured in decays, mixing and interference in K (ϵ_K, ϵ'/ϵ ...) and B ($S_{\psi K_s}$, $S_{\psi\phi}$ ...) physics [22] and recently also in D (Δa_{CP}) meson decays [23]. On the contrary no CPV has been yet observed in flavor diagonal processes, like in neutron and electron Electric Dipole Moments (EDMs) [22], in agreement with the SM expectation.

Note that we are neglecting the strong CP problem,[§] that is the fact that the gauge allowed term in the QCD $\mathcal{L}_K$

$$\theta_{QCD}\epsilon_{\mu\nu\rho\sigma}F_{\mu\nu}F^{\rho\sigma} \tag{2.3}$$

[§]For a review on the problem see [24] for example.

can be an additional source of CPV in flavor diagonal observables, such as in the EDMs. However from the experiments we know that it must be very small ($\theta_{QCD} < 10^{-9}$) without a natural explanation of it in the SM. In this work we simply assume that some unkown mechanism forbids this term.

2.1.3 Unitarity fit

The processes described in the previous Sections, together with several other transitions, give a unique chance to test the SM. In fact we have at disposal many observables depending only on four CKM paramters, that therefore can probe the CKM picture of flavor and CP violation or can estimate the room left for non-standard effects.

One way to do this is through the *unitarity triangle*. In fact the unitarity of the CKM matrix gives several constraints between the matrix elements that must hold. For example, from $(V_{CKM}^T V_{CKM}^*)_{13} = 0$ we obtain

$$V_{ud}V_{ub}^* + V_{cd}V_{cb}^* + V_{td}V_{tb}^* = 0\,, \tag{2.4}$$

that can be geometrically represented as a triangle in a complex plane (there are three of such triangles in total). Rescaling all the sides by $|V_{cb}V_{cb}^*|$, the length of the two complex sides become

$$R_u \equiv \sqrt{\rho^2+\eta^2} = \frac{1}{\lambda}\left|\frac{V_{ub}}{V_{cb}}\right|\,, \qquad R_t \equiv \sqrt{(1-\rho)^2+\eta^2} = \frac{1}{\lambda}\left|\frac{V_{td}}{V_{cb}}\right|\,, \tag{2.5}$$

while the three angles denoted by α, β and γ are

$$\alpha \equiv \arg\left[-\frac{V_{td}V_{tb}^*}{V_{ud}V_{ub}^*}\right]\,, \qquad \beta \equiv \arg\left[-\frac{V_{cd}V_{cb}^*}{V_{td}V_{tb}^*}\right]\,, \qquad \gamma \equiv \arg\left[-\frac{V_{ud}V_{ub}^*}{V_{cd}V_{cb}^*}\right]\,. \tag{2.6}$$

These quantities can be determined from several measurements, including

- R_u from the rates on semileptonic inclusive and exclusive charmless B decays.
- R_t from the ratio between the mass splitting in the B_d and B_s mixing, $\Delta M_b/\Delta M_s$.
- β from the CP asymmetry in $B \to \psi K_S$ ($S_{\psi K_S} = \sin 2\beta$).
- α from the rate of various $B \to \pi\pi, \rho\pi, \rho\rho$ decays.
- γ from the rate and CPV in $B \to DK$ decays.
- The CPV in K decays (ϵ') and mixing (ϵ_K) depends in a complicated way on ρ and η.

The area of all the triangles is the same and it gives a basis independent measure of the CPV of the system; it is given by $|J_{CMK}|/2$, defined as

$$Im(V_{ij}V_{kl}V_{il}^*V_{kj}^*) \equiv J_{CKM}\sum_{m,n=1}^{3}\epsilon_{ikm}\epsilon_{jln}\,. \tag{2.7}$$

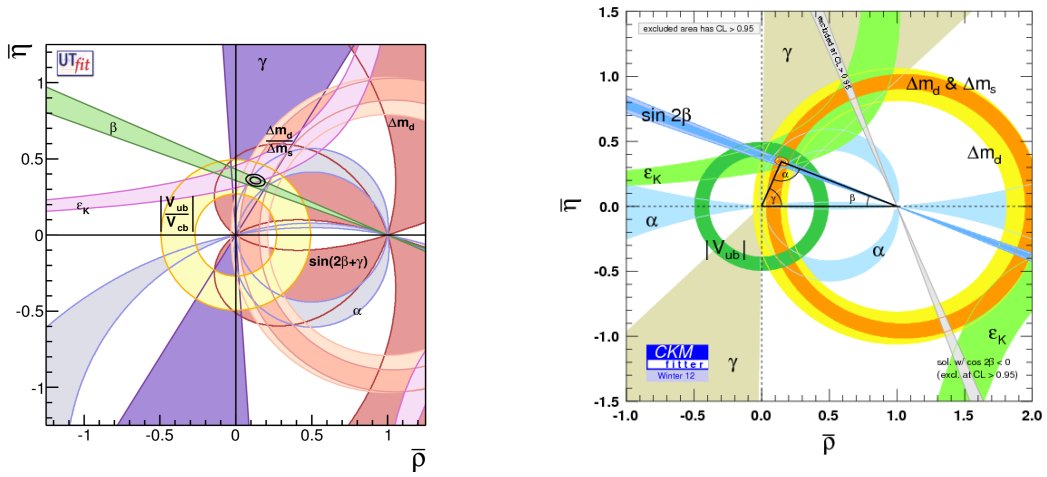

Figure 2.2: Standard Model unitarity fit performed by the UTfit (left) and CKMfitter (right) collaborations. The consistency of the fit is given by the overlapping of the various bars in the upper vertex of the triangle.

The consistency of the SM picture is tested extracting the CKM parameters from many different processes, as shown above, and checking if Eq. (2.4) is verified. Fig. 2.2 shows two different types of this analysis [25, 26] and, as can be seen, the consistency of the various constraints is impressive.

However, looking more closely, there are a few cases in which the agreement is not so good. Given the small statistical significance (1-2 σ effects) of these anomalies, we can not claim any discovery, but they can be treated as good starting points to investigate NP scenarios. Between these measurements, that are summarized for example in [27], we can report the tensions in $\sin 2\beta$, $B \to \tau\nu$ (even if this tension has been recently reduced) and the muon $g-2$, that will be discussed in this Thesis.

2.2 Effective theory

Following the analogy of the Fermi theory of the weak interactions, in a low-energy theory the heavy particles can be integrated out, ie they can be removed as physical degrees of freedom. The SM Lagrangian becomes the renormalizable part of a more general Lagrangian which includes an infinite series of non renormalizable terms

$$\mathcal{L}_{eff} = \mathcal{L}_{SM} + \sum_i \frac{c_i}{\Lambda_{NP}^{(d-4)}} O_i^{(d)}(\text{SM fields})\,. \tag{2.8}$$

The operators with dimension $d > 4$ are suppressed by $d-4$ powers of the cut-off, which represents the heavy physics scale. This approach, called Operator Product Expansion (OPE), is particularly useful for describing the low-energy flavor physics. In that case

one of the main theoretical difficulties is related to the QCD corrections. In fact, due to confinement, the real world is made of mesons and baryons instead of quarks and gluons and the hadronization process is governed by the low-energy QCD, that is non-perturbative. The virtue of the OPE is that it achieves a separation between the long-distance QCD contributions and the short-distance physics, as can be seen from the amplitude expression

$$A(i \to j)^{SM} = \sum_i \frac{c_i(\mu)}{\Lambda_{NP}^{(d-4)}} \langle j|O_i(\mu)^{(d)}|i\rangle \,. \tag{2.9}$$

In the previous equation μ is the low scale associated with the particular observable, it is arbitrarily chosen as the separation scale between the low and high energy physics (eg m_b for B decays, 2 GeV for K physics ...). The $c_i(\mu)$ are the perturbative Wilson coefficients containing all the short-distance effects. They are typically calculated at the cut-off scale (matching) and then evolved through the Renormalization Group Equations (RGE) at the energy μ. In this way the potentially large terms $\sim (\alpha_s \, log(\Lambda_{NP}/\mu))^n$ are safely resummed at all orders. The $\langle j|O_i(\mu)|i\rangle$ parameters are the matrix elements which parametrize the low-energy QCD effects.* They are calculated with non-perturbative methods, such as Lattice QCD, or in Chiral Perturbation Theory, Heavy Quark Expansion and so on. When these methods are particularly efficient the matrix elements result theoretically well known, like for $K \to \pi\nu\nu$ or $B_s \to \mu^+\mu^-$, and the relative processes become particularly indicated for investigating the physics beyond the SM.

2.2.1 An explicit example

As already discussed no relevant deviations from the SM expectations have been yet found. Accordingly it is possible to put bounds on the ratio $c_i/\Lambda_{NP}^{(d-4)}$ in Eq. (2.8). Consider for example the $\Delta S = 2$ (double variation of the strange quark number) processes introduced in Sec. 2.1.1. Two important non-standard contributions to such process come from $(LL)^2$ and $(RL)(LR)$ four fermion operators†

$$\mathcal{L}_{eff} \to \frac{c_1}{\Lambda_{NP}^2}(\bar{s}_L\gamma_\mu d_L)^2 + \frac{c_4}{\Lambda_{NP}^2}(\bar{s}_R d_L)(\bar{s}_L d_R) \,. \tag{2.11}$$

In particular the real part of these contributions gives Δm_K, while the imaginary part ϵ_K. Both these quantities are measured with high precision and the SM expectation is known very well (it can be obtained extracting the CKM parameters from the tree level flavor observables that are likely not affected by NP contributions). In particular from [30] we

*Consider the simplest case of pion decay constant f_π, defined through

$$\langle 0|\bar{u}_L\gamma_\mu d_L|\pi(q)\rangle \equiv i\sqrt{2} f_\pi q_\mu \,. \tag{2.10}$$

It represents the mismatch between the facts that the fields $\bar{u}_L$ and d_L create and destroy free particles, while the quarks are not free in the meson. It has been calculated in ChPT for example.

†A complete list of operators contributing to this process can be found in [29].

Operator	Bounds on Λ in TeV ($c_{ij}=1$)		Bounds on c_{ij} ($\Lambda=1$ TeV)		Observables
	Re	Im	Re	Im	
$(\bar{s}_L\gamma^\mu d_L)^2$	9.8×10^2	1.6×10^4	9.0×10^{-7}	3.4×10^{-9}	Δm_K; ϵ_K
$(\bar{s}_R\, d_L)(\bar{s}_L d_R)$	1.8×10^4	3.2×10^5	6.9×10^{-9}	2.6×10^{-11}	Δm_K; ϵ_K
$(\bar{c}_L\gamma^\mu u_L)^2$	1.2×10^3	2.9×10^3	5.6×10^{-7}	1.0×10^{-7}	Δm_D; $\lvert q/p\rvert, \phi_D$
$(\bar{c}_R\, u_L)(\bar{c}_L u_R)$	6.2×10^3	1.5×10^4	5.7×10^{-8}	1.1×10^{-8}	Δm_D; $\lvert q/p\rvert, \phi_D$
$(\bar{b}_L\gamma^\mu d_L)^2$	5.1×10^2	9.3×10^2	3.3×10^{-6}	1.0×10^{-6}	Δm_{B_d}; $S_{\psi K_S}$
$(\bar{b}_R\, d_L)(\bar{b}_L d_R)$	1.9×10^3	3.6×10^3	5.6×10^{-7}	1.7×10^{-7}	Δm_{B_d}; $S_{\psi K_S}$
$(\bar{b}_L\gamma^\mu s_L)^2$	1.1×10^2		7.6×10^{-5}		Δm_{B_s}
$(\bar{b}_R\, s_L)(\bar{b}_L s_R)$	3.7×10^2		1.3×10^{-5}		Δm_{B_s}

Table 2.1: Bounds on representative dimension-six $\Delta F=2$ operators. Bounds on Λ are quoted assuming the coefficients $c_{ij}=1$, or, alternatively, the bounds on the respective c_{ij} are obtained for $\Lambda=1$ TeV. Observables related to CPV are separated from the CP conserving ones with semicolons. In the B_s system is shown the bound on the modulo of the NP amplitude derived from Δm_{B_s}.

obtain:

$$C_{\Delta m_K} \equiv \frac{\Delta m_K^{exp}}{\Delta m_K^{SM}} = 0.93 \pm 0.32\,, \qquad C_{\epsilon_K} \equiv \frac{\epsilon_K^{exp}}{\epsilon_K^{SM}} = 0.92 \pm 0.14\,, \tag{2.12}$$

leaving very small room for the non-standard effects in Eq. (2.11). In fact it results that, if the NP physics scale is near, the Wilson coefficients must be very small [28]

$$\Lambda_{NP} = 1 \text{ TeV} \quad \rightarrow \quad \begin{cases} Re(c_1) < 1\times10^{-6} \\ Im(c_1) < 3\times10^{-9} \end{cases} \qquad \begin{cases} Re(c_4) < 7\times10^{-9} \\ Im(c_4) < 3\times10^{-11} \end{cases}\,, \tag{2.13}$$

or, with generic flavor parameters, the cut-off must be very heavy

$$c_1 = 1 \quad \rightarrow \quad \begin{cases} \Lambda_{NP} > 1\times10^3\,(\Delta m_K) \\ \Lambda_{NP} > 2\times10^4\,(\epsilon_K) \end{cases} \qquad c_4 = 1 \quad \rightarrow \quad \begin{cases} \Lambda_{NP} > 2\times10^4\,(\Delta m_K) \\ \Lambda_{NP} > 3\times10^5\,(\epsilon_K) \end{cases}\,. \tag{2.14}$$

Note that, due to the left-handed nature of the weak interactions only the $(LL)^2$ operators are generated in the SM, and that the bounds for the mixed chirality terms are usually the strongest due to larger hadronic matrix elements.

2.2.2 The flavor problem

Results similar to the ones shown in the previous Section are obtained also from D, B_d and B_s mixings and from various other flavor processes. The limits for various New Physics operators have been calculated in [28] and reported in Tab. 4.1. It is clear that if new degrees of freedom are in the energy range to solve the hierarchy problem (~ 1 TeV) their flavor structure must be very specific. This is the so called *flavor problem*.

Fortunately mechanisms exist keeping the flavor effects under control while saving the naturalness of the theory. They can be model dependent but in general they refer to three approaches

- Universality, the non-standard masses are flavor-blind and so proportional to the identity. The FCNC become suppressed due to the analogue of the GIM mechanism of the SM.
- Alignment, the new flavor sector has a non-trivial structure but it is arranged to be aligned with the Yukawa matrices. In this ways the NP masses become diagonal in the mass basis of the SM. For example this can be achieved if the same flavor symmetry is responsible for generating the SM and NP masses.
- Irrelevancy, the states that can potentially generate too large flavor effects are heavy and so their effects have not been seen yet. Note that if we want to preserve the naturalness of the model it is necessary that at least some new particles must be light. Therefore a non-trivial spreading of the NP spectrum is necessary.

2.2.3 Minimal Flavor Violation

Considering again the results in Tab. 4.1, it is possible to note that, for $\Lambda_{NP} = 1$ TeV, the limits on the Wilson coefficients are of the same size of other tiny quantities of the theory, that are the Yukawa couplings. It is therefore possible that a common mechanism could relate the two sectors, as assumed in Minimal Flavor Violation (MFV).

Consider again the SM Lagrangian in the quark sector. In absence of the Yukawa couplings it presents the global symmetry

$$U(3)_{Q_L} \times U(3)_{u_R} \times U(3)_{d_R}\,, \tag{2.15}$$

that is broken to Baryon Number $U(1)_B$ when introducing $\mathcal{L}_Y$. Therefore the Yukawas can be considered as non-dynamical *spurion* fields transforming as

$$Y_u \sim (3, \bar{3}, 1)\,, \qquad Y_d \sim (3, 1, \bar{3})\,, \tag{2.16}$$

under the symmetries in Eq. (2.15). The idea of MFV [31] (see also [32–34]) is that Y_u and Y_d are the only sources of $U(3)^3$ breaking also in the NP models. In this way the effective operators in Eq. (2.8) must be formally invariant under $U(3)^3$ and so the flavor-changing ones must be proportional to some combination of the Yukawas. For example, expanding in the small parameters of the Yukawas, the flavor-changing bilinears that give the non-standard operators in Eq. (2.11) becomes

$$\overline{Q}_L \gamma_\mu Q_L \;\rightarrow\; \overline{Q}_L Y_u Y_u^\dagger \gamma_\mu Q_L\,, \tag{2.17}$$

$$\overline{D}_R Q_L \;\rightarrow\; \overline{D}_R Y_d Y_u Y_u^\dagger Q_L\,, \tag{2.18}$$

that are very suppressed (in particular the corresponding ones in the up sector are negligible). The result is that the FCNC get the same suppression as in the SM and the bounds

Operator	Bound on Λ	Observables
$H^\dagger \left(\bar{D}_R Y^{d\dagger} Y^u Y^{u\dagger} \sigma_{\mu\nu} Q_L\right) (eF_{\mu\nu})$	6.1 TeV	$B \to X_s\gamma$, $B \to X_s\ell^+\ell^-$
$\frac{1}{2}(\bar{Q}_L Y^u Y^{u\dagger} \gamma_\mu Q_L)^2$	5.9 TeV	ϵ_K, Δm_{B_d}, Δm_{B_s}
$H_D^\dagger \left(\bar{D}_R Y^{d\dagger} Y^u Y^{u\dagger} \sigma_{\mu\nu} T^a Q_L\right) (g_s G^a_{\mu\nu})$	3.4 TeV	$B \to X_s\gamma$, $B \to X_s\ell^+\ell^-$
$\left(\bar{Q}_L Y^u Y^{u\dagger} \gamma_\mu Q_L\right) (\bar{E}_R \gamma_\mu E_R)$	2.7 TeV	$B \to X_s\ell^+\ell^-$, $B_s \to \mu^+\mu^-$
$i \left(\bar{Q}_L Y^u Y^{u\dagger} \gamma_\mu Q_L\right) H_U^\dagger D_\mu H_U$	2.3 TeV	$B \to X_s\ell^+\ell^-$, $B_s \to \mu^+\mu^-$
$\left(\bar{Q}_L Y^u Y^{u\dagger} \gamma_\mu Q_L\right) (\bar{L}_L \gamma_\mu L_L)$	1.7 TeV	$B \to X_s\ell^+\ell^-$, $B_s \to \mu^+\mu^-$
$\left(\bar{Q}_L Y^u Y^{u\dagger} \gamma_\mu Q_L\right) (eD_\mu F_{\mu\nu})$	1.5 TeV	$B \to X_s\ell^+\ell^-$

Table 2.2: Bounds on the scale of new physics (at 95% C.L.) for some representative $\Delta F = 1$ [135] and $\Delta F = 2$ [30] MFV operators (assuming effective coupling $\pm 1/\Lambda^2$), and corresponding observables used to set the bounds.

on Λ_{NP} become close to the TeV scale, as shown in Tab. 2.2 [28]. Particularly interesting is the case with more than one Higgs doublet, in which the ratio between the bottom and top Yukawa couplings is not fixed and it can be also close to the unity. In that case the MFV suppression is less efficient when considering insertions of the Yukawa couplings proportional to the large $(Y_{d\,(e)})_{33}$. This case will be considered in detail in Sec. 4.2 for the 2 Higgs Doublet Model.

As far as CPV is concerned, the MFV hypothesis gives the desired suppression in flavor-violating observables, but not in the flavor-conserving ones, such as the EDMs. For this reason it is usually assumed the more general $U(3)^3 \times \mathrm{CP}$ as the fundamental symmetry to be broken only by the Yukawa couplings.[‡]

The MFV assumption can be implemented in many NP models. In particular in weakly coupled theories with one Higgs doublet it gives the additional property that only the operators which play a significant role in the SM are the only relevant also in the NP sector. This case is called Constrained MFV (CMFV) [37].

2.3 Supersymmetry

As already discussed the hierarchy problem of the SM is given by the extremely high sensitivity to the cut-off scale in the scalar mass μ term in the Higgs sector, and consequently in m_h. On the other hand, the other particle masses are sensitive only logarithmically to the cut-off, because they are "protected" by extra symmetries. For the fermions this is the chiral symmetry, while for the neutral gauge bosons it is the gauge symmetry. The supersymmetric solution to the hierarchy problem consists into the introduction of a new symmetry, called supersymmetry, able to provide a similar protection to the scalar Higgs mass. Supersymmetry is an extension of the usual 4-dimensional space-time Poincaré group, in which new spin 1/2 generators are introduced, transforming bosons into fermions (and viceversa). We consider the simplest case with only one

[‡]For alternative realizations in explicit models see [35, 36].

of such generators ($\mathcal{N} = 1$). For each SM fermion (boson) a new boson (fermion) is introduced, with the same mass and the same guage quantum numbers (due to the fact that SUSY commutes with the Poincaré and gauge symmetries). However this symmetry can not be exact because we have not observed any of these new particles so far. The symmetry must be broken at some scale, in which the s-particles take a mass while the SM particles remain massless. This assumption is compatible with the fact that the SM fermion masses are forbidden by the gauge symmetries and therefore they are generated only when $SU(2)_L \times U(1)_Y$ is broken. The s-particle masses are instead related only to the SUSY-breaking scale. If this scale is low enough the hierarchy problem can be solved without requiring any particular fine-tuning between the parameters (at least compared with the SM), as we are going to explain.

In presence of a top scalar partner, called stop ($\tilde{t}$), the corrections to the Higgs self-energy in Eq. (1.18) become only logarithmically connected to the NP scale:

$$\delta m^2_{h|\text{top+stop}} \sim -\frac{3G_F}{\sqrt{2}\pi^2} m_t^4 \log \frac{m_{\tilde{t}_1}\, m_{\tilde{t}_2}}{m_t^2}\,. \tag{2.19}$$

The reason for this effect is that a scalar and a fermion contribute to the Higgs self-energy with an opposite sign, giving an exact cancellation in case of equal masses of the two particles or a logarithmic correction in case of a splitting between the two masses. Note that the cancellation of quadratic divergences can be lost in case of generic SUSY-breaking terms, while it is preserved choosing operators with dimension strictly less than four (unless in the minimal extension of the SM), called *soft*-breaking terms. In this latter case Eq. (2.19) holds and, as can be seen, if $m_{\tilde{t}_{1,2}}$ is not too heavy respect to m_t the fine-tuning between the parameters of the model is substantially reduced.*

2.3.1 Minimal Supersymmetric Standard Model

The Minimal Supersymmetric Standard Model (MSSM) is the SUSY extension of the SM with the minimal particle content. In particular every chirality state of the SM fermions is associated with a scalar partner (*sfermion*) and every SM gauge boson comes together with a Majorana spin 1/2 fermion (*gaugino*). Due to anomaly cancellation and the holomorphy of the supersymmetric potential, two Higgs doublets are needed: H_u giving mass to the up-quarks and H_d to the down-quarks. The SM vev is now given by $v = \sqrt{v_u^2 + v_d^2}$, where $v_{u(d)}$ is the minimum of $H_{u(d)}$ and their ratio is denoted as $\tan\beta = v_d/v_u$. Each component of the Higgs doublets is accompanied with a fermionic partner (*higgsino*).

Given the field content of the theory, the MSSM gauge and kinetic Lagrangian is fixed by the requirement of supersymmetric and gauge invariance (for example fermion-sfermion-gaugino interactions are the supersymmetric counterpart of the usual SM gauge

*Note that even if $m_{\tilde{t}_{1,2}} \sim M_{GUT}$ the dependence on the cut-off is reduced respect to the SM, being logarithmic instead of quadratic.

terms). The generalization of the Yukawa terms is given by the MSSM superpotential

$$W = Q_L\, Y_u u_R^c H_u + Q_L\, Y_d d_R^c H_d + L_L\, Y_e e_R^c H_d + \mu H_u H_d\,, \tag{2.20}$$

written in terms of chiral superfields. Two important considerations are in order. First, note that additional terms can contribute to Eq. (2.20). These are baryon (B) and/or lepton (L) number violating operators, which consequently must be very suppressed or vanishing. For this reason an additional symmetry of the Lagrangian forbidding such terms is usually assumed . It is called R-parity, defined as

$$P_R = (-1)^{3(B-L)+2s}\,, \tag{2.21}$$

where s is the spin of the particle.[†] A natural consequence of this symmetry is that the SUSY particles must be produced in couples and the lightest one, that is stable, is a good candidate for dark matter.

Second, the μ-term appears at the symmetric level and therefore we could expect it at any high energy scale. On the contrary, as we will show in the following, its value must be of the same order as the low-energy soft breaking terms (and $\sim v$), even if the two sectors are completely unrelated (μ-problem).[‡]

When we consider the soft sector of the MSSM the situation is more involved and a high number of parameters can enter into the play. Given the requirement of not reintroducing quadratic divergences, the soft Lagrangian can be written as

$$\begin{aligned}
\mathcal{L}_{soft} \;=\; & -\frac{1}{2}\left(M_3\tilde{g}\tilde{g} + M_2\tilde{W}\tilde{W} + M_1\tilde{B}\tilde{B} + c.c\right) \\
& -\left(\tilde{Q}_L\, A_u\, \tilde{u}_R^c H_u - \tilde{Q}_L\, A_d\, \tilde{d}_R^c H_d - \tilde{L}_L\, A_e\, \tilde{e}_R^c H_d + c.c\right) \\
& -\tilde{Q}_L^*\, m_{\tilde{Q}}^2\, \tilde{Q}_L^T - \tilde{L}_L^*\, m_{\tilde{L}}^2\, \tilde{L}_L^T - \tilde{u}_R^{c\dagger}\, m_{\tilde{u}}^2\, \tilde{u}_R^c - \tilde{d}_R^{c\dagger}\, m_{\tilde{d}}^2\, \tilde{d}^c - \tilde{e}_R^{c\dagger}\, m_{\tilde{e}}^2\, \tilde{e}^c \\
& - m_{H_u}^2 H_u^* H_u - m_{H_d}^2 H_d^* H_d - (b H_u H_d + c.c)\,.
\end{aligned} \tag{2.22}$$

The first line of the previous equation gives the gaugino masses. In this respect, it is interesting to note that one main feature of supersymmetry is that it provides an excellent coupling unification, better than in the SM (also the unification scale is heavier and this can help with the proton-decay limits). For this reason it is plausible that also the gaugino masses unify at M_{GUT}, accordingly to their couplings. This gives the additional relation

$$\frac{M_1}{g_1^2} = \frac{M_2}{g_2^2} = \frac{M_3}{g_3^2} = \frac{M_{1/2}}{g_U^2}\,, \tag{2.23}$$

valid at any RG scale (note that a redefinition of one of the gauge couplings is understood). The last three lines of Eq. (2.22) contribute to the flavor and Higgs sector of the MSSM, that are analyzed separately in the following.

[†] Alternatively recent works [38, 39] show that also the MFV assumption can be used to suppress B or L violating processes.

[‡] Also in the SM the electroweak scale is not dynamically predicted, but in SUSY the contribution of two unrelated sectors (SUSY-invariant and SUSY-breaking) to this scale makes the problem even more intriguing.

2.3.2 Higgs sector in the MSSM

Differently from the SM, in the MSSM Lagrangian the only allowed dimensionless terms are the gauge and Yukawa couplings. This means that the quartic Higgs coupling is not a free parameter, but it is just a fixed combination of the gauge couplings. Consequently the requirement of a stable potential giving the spontaneous symmetry breaking is not automatically satisfied, unless some of the soft terms in Eq. (2.22) are introduced satisfying the conditions

$$2b < 2|\mu|^2 + m_{H_u}^2 + m_{H_d}^2 \,, \tag{2.24}$$

$$b^2 > (|\mu|^2 + m_{H_u}^2)(|\mu|^2 + m_{H_d}^2) \,. \tag{2.25}$$

Interestingly the above equations can not be both realized if $m_{H_u} = m_{H_d}$ at the electroweak scale. Nevertheless, this relation can be taken at some high scale, like M_{GUT}. Then the running effects, dominated by the top Yukawa, can push m_{H_u} to small or negative values at electroweak scale, giving the *radiative* electroweak symmetry breaking.

The size of some of the above Lagrangian parameters can be inferred if, minimizing the scalar potential, we express them in terms of the measured masses. For example at first order in $\tan\beta$ we obtain

$$m_Z^2 = -2(m_{H_u}^2 + |\mu|^2) \,, \tag{2.26}$$

which, as already anticipated, shows that μ and m_{H_u} must be of the same order and close to the electroweak scale (barring finetuned cancellations). Moreover, as shown for example in [40], m_{H_u} gets quantum corrections from stop contributions at one loop and from gluinos at two loops

$$\delta m_{H_u|stop}^2 = -\frac{3}{8\pi^2} y_t^2 \left(m_{Q_3}^2 + m_{u_3}^2 + |A_t|^2\right) \log\left(\frac{\Lambda}{\text{TeV}}\right) \,, \tag{2.27}$$

$$\delta m_{H_u|gluino}^2 = -\frac{2}{\pi^2} y_t^2 \left(\frac{\alpha_s}{\pi}\right) |M_3|^2 \log^2\left(\frac{\Lambda}{\text{TeV}}\right) \,. \tag{2.28}$$

Therefore a "natural" Higgs sector requires light higgsino (directly related to μ), stop and gluino, with this order of importance. Note that the LHC bounds on these particles and the measured value of the Higgs mass (see in the following) already demand some cancellations between the supersymmetric parameters (*little hierarchy problem*). We will come back to this issue in Sec. 3.

Assuming a CP conserving Higgs sector, the full Higgs spectrum consists of two neutral scalars (h and H), one neutral pseudo-scalar (A) and two charged ($H^\pm$) Higgs particles, with masses

$$m_{A^0}^2 = 2b/\sin(2\beta) = 2|\mu|^2 + m_{H_u}^2 + m_{H_d}^2 \,, \tag{2.29}$$

$$m_{h^0,H^0}^2 = \frac{1}{2}\left(m_{A^0}^2 + m_Z^2 \mp \sqrt{(m_{A^0}^2 - m_Z^2)^2 + 4m_Z^2 m_{A^0}^2 \sin^2(2\beta)}\right) \,, \tag{2.30}$$

$$m_{H^\pm}^2 = m_{A^0}^2 + m_W^2 \,. \tag{2.31}$$

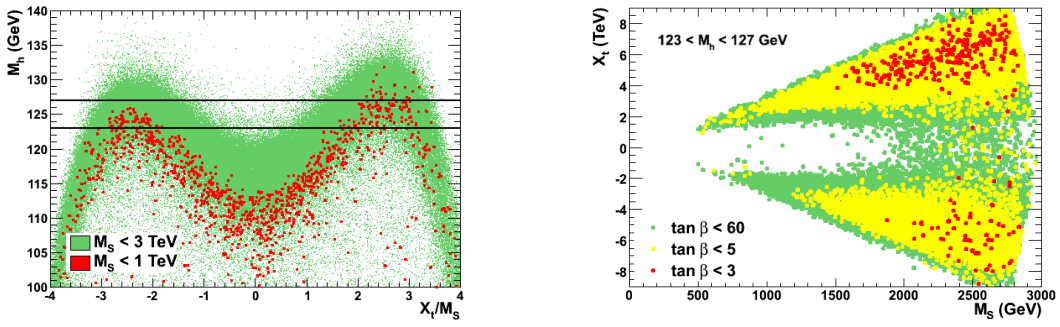

Figure 2.3: The maximal value of the Higgs boson mass as a function of X_t/M_S in the pMSSM (for the details on the SUSY parameter space see [42]) (left) and the contours for $123 < m_h < 127$ GeV in the $M_S - X_t$ plane for some selected range of $\tan\beta$ values (right).

In the limit $b \gg m_Z$ the $A\,, H$ and $H^\pm$ masses can be very large and only h remains light, looking exactly like the SM Higgs boson. Anyway there is a difference between the SM and the MSSM regarding the preferred value of m_h. In fact in the SM the Higgs mass is not directly predicted, instead in the MSSM, due to the absence of the $\lambda\phi^4$ term, we get the tree level relation

$$m_h < m_Z |\cos(2\beta)|\,. \tag{2.32}$$

Fortunately this relation gets sizable corrections from stop loops (as could have been argued from the fact that we have introduced SUSY to stabilize m_h through the stop contributions) pushing the Higgs mass to higher values.[§] In Fig. 2.3 are shown the preferred values of m_h in function of $X_t = A_t - \mu\cot\beta$ and the squark scale M_S, as reported in [42]. It is clear that, with a universal squark spectrum, $m_h \sim 125$ GeV can be obtained only for large A-term and/or for large squark masses (this last option contributes to the little hierarchy problem).

2.3.3 Flavor in the MSSM

Supersymmetric models provide new sources of flavor and CP violation in both the quark and lepton sector. In fact the soft masses in Eq. (2.22) are in general not universal and not aligned with the SM Yukawas. A useful basis to work with is the Super-CKM basis, in which the whole super-multiplets are rotated in the mass basis of the SM fermions. In this way the couplings to neutral gauginos are flavor diagonal and the supersymmetric flavor-changing effects are exhibited in the non-diagonality of the sfermion mass matrices. These effects can be described in terms of the mass insertion parameters

$$(\delta^q_{ij})_{MN} \equiv \frac{(M^2_{\tilde{q}})^{MN}_{ij}}{\tilde{m}^2_q}\,, \tag{2.33}$$

[§]For analytic calculation see for example [41].

where $\tilde{m}_q^2$ is a representative squark mass, ij are generation indices, and

$$(M^2_{\tilde{u,d}})^{LL} \simeq m_Q^2\,, \qquad (M^2_{\tilde{u,d}})^{RR} \simeq m_{u,d}^2\,, \qquad (M^2_{\tilde{u,d}})^{LR} \simeq A_{u,d}\, v_{u,d}\,.^{\P} \tag{2.35}$$

Consider for example the $\Delta K = 2$ process analyzed in Sec. 2.2.1 . The Wilson coefficients can now be evaluated in terms of the supersymmetric parameters, and as a result it is possible to obtain upper bounds on the mass insertions. For example if $m_{\tilde{q}} = m_{\tilde{g}} = 1$ TeV we get (using the mass insertion approximation [43]) [44]

$$(\delta^d_{12})_{LL}\,, (\delta^d_{12})_{RR} < 0.03\,, \qquad (\delta^d_{12})_{LR} < 2\times\,, 10^{-4}\,, \tag{2.36}$$

showing that also in the MSSM the flavor structures must be far from generic. Similar limits are obtained from other flavor processes, both in the quark [45] and in lepton sector [117].

However if supersymmetry breaking is mediated by a flavor blind mechanism, such as gravity or gauge interactions, the soft sector results highly simplified and the new flavor-changing effects are automatically suppressed. In the mSUGRA inspired version of the MSSM, called Constrained MSSM (CMSSM), the soft masses are

$$m_Q^2 = m_L^2 = m_u^2 = m_d^2 = m_e^2 = m_0^2\; I\,, \qquad \frac{A_u}{Y_u} = \frac{A_d}{Y_d} = \frac{A_e}{Y_e} = A_0\,, \tag{2.37}$$

in addition to the already mentioned relations

$$m^2_{H_u} = m^2_{H_d} = m_0^2\,, \qquad M_1 = M_2 = M_3 = M_{1/2}\,. \tag{2.38}$$

These relations are usually valid at the cut-off scale of the theory, to be M_{Planck} for gravity mediation (or the messengers scale M_{mess} in guage mediated models), and they are modified by the RGEs running to the electroweak scale. Interestingly at low-energy the corrections to the soft masses in Eqs. (2.37) and (2.38) result proportional to some combinations of the Yukawas and so respect the MFV assumption. Consequently the supersymmetric effects in flavor observables become under control [28], at least if the cut-off scale is not too heavy and for small $\tan\beta$.

The drawback of such constrained scenarios is that the LHC direct bounds on squarks and gluinos are very strong, as shown in Fig. 2.4. In fact the squarks are expected almost degenerate and therefore the strong limits on first two generations reflect also on the third one, making the naturalness of the theory in trouble. In the next Section we will come back to this point, showing a more natural realization of the theory in this regard.

Finally, similarly to the general case of MFV, if $\tan\beta$ is large new flavor effects can be generated. In that case threshold corrections modify the Yukawa couplings and some

¶Equivalently in the mass basis of both quarks and squarks the mass insertions can be written in terms of the mixing matrix in the gaugino couplings. For example, being W^q_M the gluino mixing to $q_M - \tilde{q}_M$, we have

$$(\delta^q_{ij})_{MM} = \frac{1}{\tilde{m}_q^2} \sum_\alpha (W^q_M)_{i\alpha} (W^q_W)^*_{j\alpha} \Delta\tilde{m}^2_{q_\alpha} \tag{2.35}$$

where $\tilde{m}_q^2$ is average squark mass-squared and $\Delta\tilde{m}^2_{q_\alpha} = \tilde{m}^2_{q_\alpha} - \tilde{m}^2_q$.

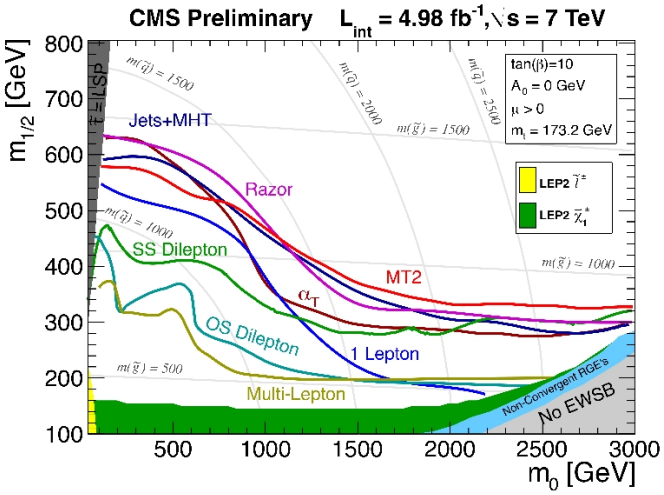

Figure 2.4: Observed limits from several 2011 CMS SUSY searches plotted in the CMSSM $m_0 - M_{1/2}$ plane.

FCNC processes become relevant, as for example $B_s \to \mu^+\mu^-$ and $B \to X_s\gamma$. Moreover if the heavy Higgs scale is not too far also the charged Higgs mediated transitions, as $B \to \tau\nu$, can receive important contributions. In Sec. 4.2 we will analyze this situation in detail.

Chapter 3

$U(2)$ and Split-Family SUSY

At the end of the previous chapter we discussed the main aspects of a SUSY theory. In particular we showed that

- A natural supersymmetric theory requires that at least the higgsino and the third generation masses should be light, and that the gluino must not be too heavy [40, 47–49].
- Flavor physics requires that the flavor structure of a low-energy SUSY must be universal or aligned with the SM [28], as for example in models satisfying the MFV hypothesis.
- The LHC direct bounds on the first generation squarks masses already exceed 1 TeV, while the third generations can be significantly lighter [50]. This seems to disfavor universal models with MFV, in which the three generations are expected almost degenerate.

A long-standing realization of SUSY that is motivated by the previous arguments is the MSSM with heavy superpartners of the first two generations, called *split-family* SUSY [51–54]. In this scenario the third generations remain lights, stabilizing the Higgs sector and, at the same time, satisfying the present LHC bounds. Moreover the tight constraints from CP and flavor violating processes are loosened in presence of a squark mass hierarchy.

In Sec. 3.1 we present a specific model compatible with the slit-family scenario, based on the $U(2)^3$ flavor symmetry [56]. Then, in Sec 3.3, we analyze a possible extension of this model to the lepton sector [1] and in Sec. 3.2 we study the behavior of the framework under the RGE evolution [2].

3.1 $U(2)^3$ model

A hierarchical spectrum is not enough to suppress flavor violation to a level consistent with experiments [55]. This is why split-family SUSY with a minimally broken $U(2)^3 = U(2)_q \times U(2)_d \times U(2)_u$ flavor symmetry, acting on the first two generations of quarks (and

squarks), has been considered in Ref. [56]. This set-up has the following advantages: i) it provides some insights about the structures of the Yukawa couplings (along the lines of $U(2)$ models proposed long ago [57–59]); ii) it ensures a sufficient protection of flavor-changing neutral currents; iii) it leads to an improved CKM fit with tiny and correlated non-standard contributions to $\Delta F = 2$ observables. Possible signatures of this framework in the $\Delta F = 1$ sector have been discussed in Ref. [60, 62] (see also Ref. [63–65], where the same symmetry with additional dynamical assumption has been considered). More general discussions about the $U(2)^3$ flavor symmetry beyond supersymmetry have recently been presented in Ref. [61, 66].

In the framework of Ref. [56] the transformation properties of the quark superfields under the $U(2)_Q \times U(2)_u \times U(2)_d$ group are:

$$Q_L \equiv (Q_{L\,1}, Q_{L\,2}) \quad \sim \quad (\bar{2}, 1, 1)\,, \tag{3.1}$$

$$u^c_R \equiv (u^c_{R1}, u^c_{R2})^T \quad \sim \quad (1, 2, 1)\,, \tag{3.2}$$

$$d^c_R \equiv (d^c_{R1}, d^c_{R2})^T \quad \sim \quad (1, 1, 2)\,, \tag{3.3}$$

while q_3, t^c, and b^c (the third generation fields) are singlets. It is also assumed a $U(1)_b$ symmetry under which only b^c is charged. In this way, in the limit of unbroken symmetry, only the top Yukawa coupling is allowed, while the small ratio m_b/m_t is generated only when $U(1)_b$ is broken, without the need of large $\tan\beta$. Subsequently three $U(2)^3$ breaking spurion fields are introduced with the transformation properties

$$V \sim (2, 1, 1)\,, \qquad \Delta Y_u \sim (2, \bar{2}, 1)\,, \qquad \Delta Y_d \sim (2, 1, \bar{2})\,. \tag{3.4}$$

3.1.1 Yukawa and soft masses

With the convention for the superpotential as in Eq. (2.20) then the Yukawas acquire the structure:

$$Y_u = y_t \left(\begin{array}{c|c} \Delta Y_u & x_t\, e^{i\phi_t} V \\ \hline 0 & 1 \end{array}\right), \qquad Y_d = y_b \left(\begin{array}{c|c} \Delta Y_d & x_b\, e^{i\phi_b} V \\ \hline 0 & 1 \end{array}\right), \tag{3.5}$$

where everything above the horizontal dashed line has two rows, and everything to the left of the vertical dashed line has two columns. $y_{t,\,b}$ are the top and bottom Yuakwa couplings, while $x_{t,\,b}$ and $\phi_{t,\,b}$ are real $O(1)$ parameters.

The flavor symmetries would allow us to parametrize each ΔY_f spurion in terms of its eigenvalues λ_{f_1}, λ_{f_2} and a complex mixing parameter $s_f\, e^{i\alpha_f}$, and the spurion V in terms of only one component:

$$V = \begin{pmatrix} 0 \\ \epsilon \end{pmatrix}, \qquad \Delta Y_u = U^\dagger_{Q_u} \Delta Y^d_u\,, \qquad \Delta Y_d = U^\dagger_{Q_u} \Delta Y^d_d \tag{3.6}$$

where

$$U_{Q_f} = \begin{pmatrix} c_f & s_f\, e^{i\alpha_f} \\ -s_f\, e^{-i\alpha_f} & c_f \end{pmatrix}, \qquad \Delta Y^d_f = \begin{pmatrix} \lambda_{f_1} & 0 \\ 0 & \lambda_{f_2} \end{pmatrix} \tag{3.7}$$

In such a basis, a fit to the CKM matrix yields:

$$s_u = \frac{|V_{ub}|}{|V_{cb}|} = 0.095 \pm 0.008 \ , \qquad s_d = \frac{|V_{td}|}{|V_{ts}|} = -0.22 \pm 0.01 \ ,$$
$$s = |V_{cb}| = 0.0411 \pm 0.0005 \ , \qquad \cos(\alpha_u - \alpha_d) = -0.13 \pm 0.2 \ , \tag{3.8}$$

where $s \propto \epsilon$. Thus, the expansion parameter value is $\epsilon \sim \lambda^2_{\rm CKM}$.

Similarly, the sfermion soft masses acquire their structure through the spurions. In the unbroken limit all mass matrices have the following structure:

$$m^2_{\tilde{f}} = \begin{pmatrix} m^2_{f_h} & 0 & 0 \\ 0 & m^2_{f_h} & 0 \\ 0 & 0 & m^2_{f_l} \end{pmatrix} \ , \tag{3.9}$$

and we assume $m^2_{f_l} << m^2_{f_h}$. Once we introduce the spurions, following the convention in Eq. (2.22), the structure of the squark masses becomes:

$$m^2_{\tilde{Q}} = \left(\begin{array}{c|c} I + c_{Qv}\, V^* V^T + c_{Qu} \Delta Y_u^* \Delta Y_u^T + c_{Qd} \Delta Y_d^* \Delta Y_d^T & x_Q\, e^{-i\phi_Q} V^* \\ \hline x_Q\, e^{i\phi_Q} V^T & m^2_{Q_l}/m^2_{Q_h} \end{array}\right) m^2_{Q_h} \tag{3.10}$$

$$m^2_{\tilde{d}} = \left(\begin{array}{c|c} I + c_{dd}\, \Delta Y_d^\dagger \Delta Y_d & x_d\, e^{-i\phi_d} \Delta Y_d^\dagger V \\ \hline x_d\, e^{i\phi_d} V^\dagger \Delta Y_d & m^2_{d_l}/m^2_{d_h} \end{array}\right) m^2_{d_h} \ , \tag{3.11}$$

$$m^2_{\tilde{u}} = \left(\begin{array}{c|c} I + c_{uu}\, \Delta Y_u^\dagger \Delta Y_u & x_u\, e^{-i\phi_u} \Delta Y_u^\dagger V \\ \hline x_u\, e^{i\phi_u} V^\dagger \Delta Y_u & m^2_{u_l}/m^2_{u_h} \end{array}\right) m^2_{u_h} \ , \tag{3.12}$$

where all c_i and x_i parameters are real, of $O(1)$. The trilinear couplings follow a structure similar to that of the Yukawas:

$$A_u = \left(\begin{array}{c|c} a^u_1 \Delta Y_u & a^u_2 V \\ \hline 0 & a^u_3 \end{array}\right) y_t\, A^0_t \, , \qquad A_d = \left(\begin{array}{c|c} a^d_1 \Delta Y_d & a^d_2 V \\ \hline 0 & a^d_3 \end{array}\right) y_b\, A^0_b \, , \tag{3.13}$$

where the a_i are complex $O(1)$ parameters.

By suitable unitary transformations one can go to the mass basis for quarks and squarks with the consequent appearance of mixing matrices in the various interaction terms; in particular the standard charged current interactions and the gaugino interactions of the down quark-squarks become

$$(\bar{u}_L \gamma_\mu V_{CKM} d_L) W_\mu \ , \quad (\bar{d}_{L,R} W^d_{L,R} \tilde{d}_{L,R}) \tilde{g} \ . \tag{3.14}$$

To a good approximation the matrices V_{CKM} and W^d_L have the following correlated forms

$$V_{\rm CKM} = \begin{pmatrix} 1 - \lambda^2/2 & \lambda & s_u s e^{-i\delta} \\ -\lambda & 1 - \lambda^2/2 & c_u s \\ -s_d s\, e^{i(\phi+\delta)} & -s c_d & 1 \end{pmatrix} , \tag{3.15}$$

$$W_L^d = \begin{pmatrix} c_d & s_d e^{-i(\delta+\phi)} & -s_d s_L e^{i\gamma} e^{-i(\delta+\phi)} \\ -s_d e^{i(\delta+\phi)} & c_d & -c_d s_L e^{i\gamma} \\ 0 & s_L e^{-i\gamma} & 1 \end{pmatrix}, \tag{3.16}$$

where

$$|s/c| = \epsilon \left(x_b e^{-i\phi_b} - x_t e^{-i\phi_t}\right), \qquad s_u c_d - c_u s_d e^{-i\phi} = \lambda e^{i\delta}, \qquad \phi = \alpha_d - \alpha_u, \tag{3.17}$$

s_L is a real parameter of order ϵ and γ is an independent CP-violating phase. At the same time the off-diagonal entries of the matrix W_R^d are negligibly small. This is an essential virtue of the model, not shared with the original $U(2)$ papers [57–59]. In fact, with a single $U(2)$ not distinguishing between left and right, a mixing matrix W_R^d is also present involving a new mixing angle ($s_L \to s_R$) and a new phase ($\gamma \to \gamma_R$). The simultaneous presence of W_L^d and W_R^d would lead to a $\Delta S = 2$ (LR) operator, which corrects by a too large amount the CP-violating ϵ_K parameter due to its chirally enhanced matrix element.

3.1.2 Implications in flavor observables

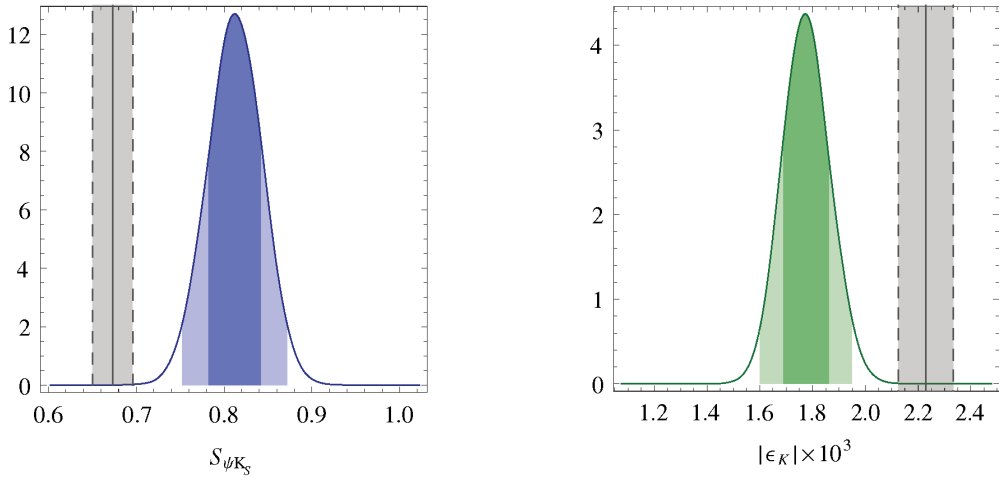

Figure 3.1: Results of two global fits of the CKM matrix using tree-level and $\Delta F = 2$ observables, excluding $S_{\psi K_S} = \sin(2\beta)$ (left) or $|\epsilon_K|$ (right). The dotted bands in correspond to 1σ errors.

The dominant supersymmetric flavor effects come from the left-handed mixing matrix W_L^d defined in Eq. (3.16). In particular the gluino-sbottom box diagrams contributing to the $i \to j$ FCNC (four fermions $(LL)^2$ operators) are governed by the combinations

$$\lambda_{i\neq j}^{(a)} = (W_L^d)_{ia} (W_L^d)_{ja}^*, \qquad \lambda_{ij}^{(1)} + \lambda_{ij}^{(2)} + \lambda_{ij}^{(3)} = 0, \tag{3.18}$$

for which we find

$$\begin{array}{rcccccc} \lambda_{ij}^{(2)} & = & c_d\kappa^* + \mathcal{O}(s_L^2\kappa^*) & [_{ij=12}], & +s_L\kappa^* e^{i\gamma} & [_{ij=13}], & +c_d s_L e^{i\gamma} \quad [_{ij=23}], \\ \lambda_{ij}^{(3)} & = & s_L^2\kappa^* c_d & [_{ij=12}], & -s_L\kappa^* e^{i\gamma} & [_{ij=13}], & -c_d s_L e^{i\gamma} \quad [_{ij=23}]. \end{array} \tag{3.19}$$

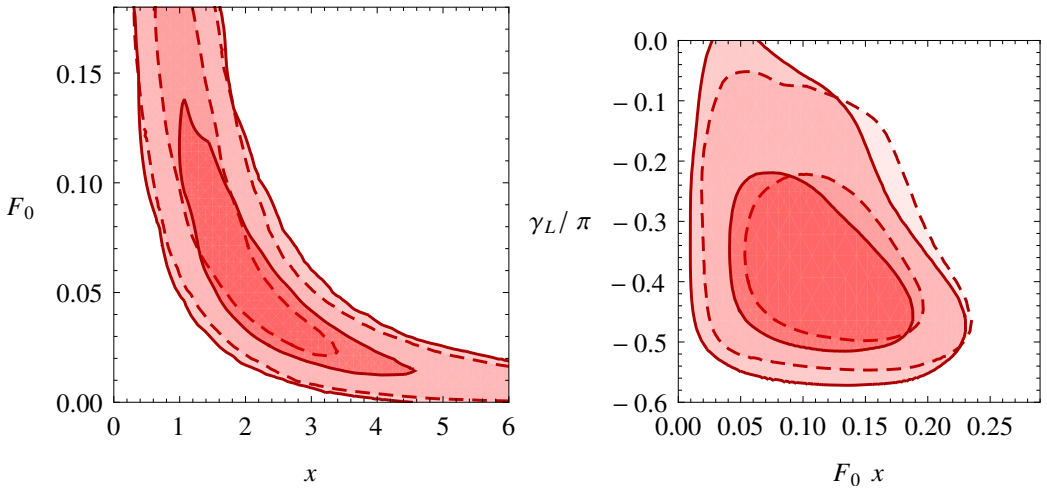

Figure 3.2: Correlations among the preferred values of $x - F_0$ (left) and $F_0\, x - \gamma_L$ (right). The dashed contours correspond to the 68% and 90% C.L. regions in the fit without $S_{\psi\phi}$, the solid contours to the fit including the new LHCb data.

From these structures we obtain tiny correlated corrections to K, B_d and B_s mixing amplitudes. In particular the modifications to B_d and B_s physics are universal and introduce a new complex parameter, while the contributions to K mixing result aligned with the SM. With hierarchical squarks the mass differences and CPV violation parameters result modified in the following way

$$\epsilon_K = \epsilon_K^{\mathrm{SM(tt)}} \times \left(1 + x^2 F_0\right) + \epsilon_K^{\mathrm{SM(tc+cc)}} \tag{3.20}$$

$$S_{\psi K_S} = \sin\left(2\beta + \arg\left(1 + x F_0 e^{2i\gamma}\right)\right) \ , \tag{3.21}$$

$$S_{\psi\phi} = \sin\left(2|\beta_s| - \arg\left(1 + x F_0 e^{2i\gamma}\right)\right) \ , \tag{3.22}$$

$$\Delta M_d = \Delta M_d^{\mathrm{SM}} \times \left|1 + x F_0 e^{2i\gamma}\right| \ , \tag{3.23}$$

$$\frac{\Delta M_d}{\Delta M_s} = \frac{\Delta M_d^{\mathrm{SM}}}{\Delta M_s^{\mathrm{SM}}} \ . \tag{3.24}$$

where $x =$ and F_0 is a loop function defined in Ref. [56].*

This pattern of effects is particularly suitable for explaining the current tension in the CKM description of CPV in ϵ_K, $S_{\phi K_S}$ and $\Delta M_d/\Delta M_s$. This tension can be seen from Fig. 3.1, where we show the fit preferred values of $S_{\psi K_S}$ and ϵ_K [56]. Note that, due to Eq. (3.22), a correlated deviation in $S_{\psi\phi}$ is also expected and it results in agreement with the recent LHCb measurement [67, 68]. The preferred values for x, γ_L and F_0 are shown in Fig. 3.2, as reported in [68].

*Note that the first two generations do not play any role (also in K physics) even if their masses are not completely decoupled, since the $1-2$ mixings have got a strong MFV suppression.

3.2 Lepton sector

In this Section we want to extend the idea of the minimally broken $U(2)^3$ flavor symmetry acting on the first two generations to the lepton sector. The extension is straightforward in the case of charged leptons, enlarging the flavor symmetry from $U(2)^3$ to $U(2)^5 = U(2)^3 \times U(2)_l \times U(2)_e$. However, the situation is more involved in the neutrino sector, whose mass matrix has a rather different flavor structure: no large hierarchies in the eigenvalues, and large mixing angles [69]. A simple ansatz to circumvent this problem is to a assume a two-step breaking in the neutrino sector: first, a leading breaking of the maximal flavor symmetry, $U(3)_l \times U(3)_e$, that includes the total Lepton Number (LN), giving rise to a fully degenerate neutrino spectrum. This would be followed by a sub-leading LN-conserving breaking with a hierarchical structure similar to the one occurring in the charged-lepton sector. As we discuss in the following, this minimal breaking structure gives rise to a phenomenologically viable neutrino mass matrix, with a few interesting predictions concerning s_{13} and the overall scale of neutrino masses. It also predicts Lepton Flavor Violation (LFV) in charged leptons compatible with present bounds and not far from the sensitivity of future experimental searches in the case of $\mu \to e\gamma$ and $\tau \to \mu\gamma$.

3.2.1 General considerations on lepton masses

We define the charged lepton Yukawa coupling (Y_e) and the effective neutrino Majorana mass matrix (m_ν) from the following effective Lagrangian, written in terms of SM fields:

$$\mathcal{L}^{\text{eff}}_{\text{mass}} = \bar{L}_{Li}(Y_e^*)_{ij} e_{Rj} H + (m_\nu)_{ij}\, \bar{\nu}^{ci}_L \nu^j_L + \text{h.c.} \tag{3.25}$$

As usual, the neutrino mass term can be interpreted as the result of an appropriate dimension-five gauge invariant operator after the spontaneous breaking of the electroweak symmetry [70], with the Higgs vacuum expectation value absorbed in the effective coupling m_ν.

By construction, $M_\nu^2 = m_\nu^\dagger m_\nu$ and $Y_e^* Y_e^T$ transform in the same way under flavor rotations of the left-handed lepton doublets, while they are invariant under rotations in the right-handed sector. The charged lepton sector exhibits a strongly hierarchical structure: with a proper basis choice for the left-handed fields, and neglecting entries of $O(m_\mu/m_\tau)$, we have

$$Y_e^* Y_e^T \approx (Y_e^* Y_e^T)^{(0)} = y_\tau^2 \ \text{diag}(0,0,1) \ , \tag{3.26}$$

where $y_\tau = \sqrt{2} m_\tau / v$ ($v \approx 246$ GeV).

In the basis where Y_e is diagonal, M_ν^2 assumes the form

$$M_\nu^2 = U_{\text{PMNS}} (m_\nu^2)^{\text{diag}} U^\dagger_{\text{PMNS}} \ , \tag{3.27}$$

where U_{PMNS} is the so-called PMNS matrix. We adopt the PDG parameterization [22], such that the mass eigenstates are ordered following a normal hierarchy ($m_{\nu_1} < m_{\nu_2} <$

m_{ν_3}) or an inverted one ($m_{\nu_3} < m_{\nu_1} < m_{\nu_2}$). To distinguish between them, one defines $\Delta m^2_{ij} = m^2_{\nu_i} - m^2_{\nu_j}$, such that $\Delta m^2_{31} = \pm \Delta m^2_{\rm atm}$ and $\Delta m^2_{21} = \Delta m^2_{\rm sol}$, where $\Delta m^2_{\rm atm,sol}$ denote the (positive) squared mass differences deduced from atmospheric and solar neutrino data. It is straightforward to deduce that the plus (minus) sign of Δm^2_{31} corresponds to the normal (inverted) hierarchy.

Experimental data on neutrino oscillations indicate the presence of (at least) two small parameters in M^2_ν,

$$\zeta = \left| \frac{\Delta m^2_{\rm sol}}{\Delta m^2_{\rm atm}} \right|^{1/2} , \qquad \zeta^{\rm exp} = 0.174 \pm 0.007 , \tag{3.28}$$

$$s_{13} = |(U_{\rm PMNS})_{13}| , \qquad s^{\rm exp}_{13} = 0.15 \pm 0.02 , \tag{3.29}$$

where the value of s_{13} has been determined from the recent result of the DayaBay experiment [71].* Expanding to lowest order in these two parameters (or in the limit $\zeta, s_{13} \to 0$) we are left with the following structure

$$(M^2_\nu)^{(0)} = m^2_{\rm light} \cdot I + \Delta m^2_{\rm atm} \cdot \Delta \tag{3.30}$$

where I is the identity matrix, $m_{\rm light}$ is the lightest neutrino mass, and

$$\Delta_{\rm [n.h.]} = \begin{pmatrix} 0 & 0 & 0 \\ 0 & s^2_{23} & s_{23}c_{23} \\ 0 & s_{23}c_{23} & c^2_{23} \end{pmatrix} \approx \frac{1}{2} \begin{pmatrix} 0 & 0 & 0 \\ 0 & 1 & 1 \\ 0 & 1 & 1 \end{pmatrix} , \tag{3.31}$$

$$\Delta_{\rm [i.h.]} = I - \Delta_{\rm [n.h.]} . \tag{3.32}$$

In order to define a starting point for the neutrino mass matrix in the limit of unbroken flavor symmetry we need to specify the hierarchy between $m^2_{\rm light}$ and $\Delta m^2_{\rm atm}$, or among the two terms in Eq. (3.30). We thus have three natural possibilities:

I. $(M^2_\nu)^{(0)} \propto I$, if $m^2_{\rm light} \gg \Delta m^2_{\rm atm}$,

II. $(M^2_\nu)^{(0)} \propto \Delta_{\rm [n.h.]}$, if $m^2_{\rm light} \ll \Delta m^2_{\rm atm}$ and $\Delta m^2_{31} > 1$,

III. $(M^2_\nu)^{(0)} \propto \Delta_{\rm [i.h.]}$, if $m^2_{\rm light} \ll \Delta m^2_{\rm atm}$ and $\Delta m^2_{31} < 1$.

3.2.2 Flavor symmetries and symmetry breaking

$\mathbf{U(2)_l \times U(2)_e}$

The $U(2)^2 = U(2)_l \times U(2)_e$ flavor symmetry, under which the lepton superfields of the first two families transform as

$$L_L \equiv (L_{L1}, L_{L2}) \sim (\bar{2}, 1) , \tag{3.33}$$

$$e^c_R \equiv (e^c_{R1}, e^c_{R2})^T \sim (1, 2) , \tag{3.34}$$

*After this analysis was completed the DayaBay results was confirmed also by RENO [72]. In this Thesis we will refer only to DayaBay but the same conclusions hold also including the subsequent experiments and fits.

offers a natural framework to justify the hierarchal structure of the charged-lepton Yukawa coupling, in close analogy to the $U(2)^3$ symmetry introduced in Ref. [56] for the quark sector and discussed in Sec 3.1. In the limit of unbroken symmetry we recover the result in Eq. (3.26). Assuming a symmetry-breaking pattern for Y_e similar to the one adopted for the quark Yukawa couplings, we get

$$Y_e = y_\tau \left(\begin{array}{c|c} \Delta Y_e & V \\ \hline 0 & 1 \end{array} \right) , \tag{3.35}$$

where we have absorbed $O(1)$ couplings in the definition of the breaking terms $V \sim (2,1)$ and $\Delta Y_e \sim (2,\bar{2})$.* Introducing the unitary matrices U_{eL} and U_{eR}, such that

$$U_{eL} Y_e U_{eR}^\dagger = \mathrm{diag}(y_e, y_\mu, y_\tau) \ , \tag{3.36}$$

and proceeding as in [56], we find that U_{eR} becomes the identity matrix in the limit $m_{e,\mu}/m_\tau \to 0$, while U_{eL} assumes the following parametric form

$$U_{eL} \approx \left(\begin{array}{ccc} c_e & s_e\, c_\tau\, e^{i\alpha_e} & -s_e\, s_\tau\, e^{i(\alpha_e+\phi_\tau)} \\ -s_e\, e^{-i\alpha_e} & c_e\, c_\tau & -c_e\, s_\tau\, e^{i\phi_\tau} \\ 0 & s_\tau\, e^{-i\phi_\tau} & c_\tau \end{array} \right) , \tag{3.37}$$

in the $U(2)_l$ basis where $V^T \propto (0,1)$. Here α_e and ϕ_τ are generic $O(1)$ phases, while $s_{e,\tau}$ are small mixing angles ($c_i^2 + s_i^2 = 1$). If the analogy with the quark sector holds, we expect s_e to be of the order of $s_d = |V_{td}|/|V_{ts}| \approx 0.22$ and s_τ of the order of $\epsilon = |V_{cb}| \approx 0.04$.

From the point of view of the $U(2)^2$ symmetry, the neutrino mass matrix can be decomposed as

$$m_\nu = \left(\begin{array}{c|c} m_3 & m_2 \\ \hline m_2^T & m_1 \end{array} \right) , \tag{3.38}$$

where $m_3 \sim (3,1)$, $m_2 \sim (2,1)$, and $m_1 \sim (1,1)$. This decomposition does not match well with any of the potential starting points identified in Eqs. (3.30)–(3.32): they can be obtained only assuming specific relations among terms with different $U(2)_l$ transformation properties. This suggests that we need to consider a larger flavor symmetry, whose breaking to $U(2)_l$ (or some of its subgroups) could explain such relations. From this point of view the degenerate case is the one that offers the most interesting prospects: on the one hand it requires a special relation only among two of the terms appearing in Eq. (3.38): $m_3 = \mathrm{diag}(m_1, m_1)$. On the other hand, it requires $m_2 \ll 1$, as expected given that m_2 transforms as the breaking spurion V of $O(\epsilon)$ appearing in the charged-lepton Yukawa coupling. As we discuss in the following, the degenerate case can easily be obtained embedding $U(2)_l$ in $U(3)_l$.

*In this Section we denote by V the analogue for the lepton sector of the left-handed vector introduced in Eq. (3.4).

$\mathbf{U(3)_l \times U(3)_e}$

The group $U(3)_l \times U(3)_e$ is the largest flavor symmetry of the lepton sector allowed by the SM gauge Lagrangian. The degenerate configuration for m_ν is achieved assuming that $U(3)_l$ and the total lepton number,

$$U(1)_{\rm LN} = U(1)_{l+e} \ , \tag{3.39}$$

are broken by a spurion $m_\nu^{(0)}$ transforming[†] as a $\mathbf{6}$ of $U(3)_l$ and leaving invariant a subgroup of $U(3)_l$ that we denote $O(3)_l$. By a proper basis choice in the $U(3)_l$ flavor space we can set

$$m_\nu^{(0)} \propto \left(\begin{array}{c:c} I & 0 \\ \hdashline 0 & 1 \end{array} \right) \ . \tag{3.40}$$

We shall also require that $U(3)_l \times U(3)_e$ is broken by $U(1)_{\rm LN}$ invariant spurions to the subgroup $U(2)_l \times U(2)_e$ relevant to the charged-lepton Yukawa coupling. However, it is essential for our construction that this (sizable) breaking does not spoil the Majorana sector, at least in first approximation. This can be achieved in a supersymmetric context introducing a new spurion $Y^{(0)} \sim (\mathbf{3}, \bar{\mathbf{3}})$ that breaks $U(3)_l \times U(3)_e$ to $U(2)_l \times U(2)_e$ leaving unbroken the $O(2)_l$ subgroup of both of $O(3)_l$ and $U(2)_l$. By means of $Y^{(0)}$ we can have a non-vanishing Yukawa coupling for the third generation in the superpotential

$$\mathbf{L}_L Y^{(0)} \mathbf{e}^c \to y_\tau^{(0)} L_3 e_3^c \ . \tag{3.41}$$

and, in first approximation, the Majorana mass matrix is unchanged. Note that supersymmetry is a key ingredient for the the latter statement to hold. Indeed, if the mass operator was not holomorphic, a Majorana term of the type $\mathbf{L}_L Y\, Y^\dagger\, m_\nu^{(0)}\, \mathbf{L}_L^T$ could also be included and this would spoil the degenerate configuration.

Summarizing, introducing the two spurions $m_\nu^{(0)}$ and $Y^{(0)}$ we recover phenomenologically viable first approximations to both the neutrino and the charged-lepton mass matrices and we are left with an exact $O(2)_l \times U(2)_e$ symmetry that leaves invariant both m_ν and Y_e. Moreover, thanks to supersymmetry, the two sectors considered separately are invariant under larger symmetries: $O(3)_l$ for the neutrinos and $U(2)_l \times U(2)_e$ for the charged leptons.

We can then proceed introducing the small $O(2)_l \times U(2)_e$ breaking terms responsible for the subleading terms in Y_e in Eq. (3.35). In order not to spoil the leading structure of the neutrino mass matrix, the spurion V in Eq. (3.35) should be regarded as a doublet of $O(2)_l$, rather than a doublet of $U(2)_l$.[‡] We can also regard it as the $O(2)_l$ component of an appropriate $\mathbf{8}$ of $U(3)_l$ with the following structure

$$X = \left(\begin{array}{c:c} \Delta_L & V \\ \hdashline V^\dagger & x \end{array} \right) \ . \tag{3.42}$$

[†] We denote in bold $U(3)$ vectors and representations.

[‡] This has no practical implications if we consider the Yukawa sector alone, where there is no preferred $O(2)$ subgroup of $U(2)_l$ in the limit $V \to 0$.

This allows to write the additional Yukawa interaction $\mathbf{L}_L X\, Y^{(0)}\, \mathbf{e}^c$ that, combined with the leading term in (3.41) and with a proper redefinition of y_τ and V implies

$$Y_e^{(1)} = y_\tau \left(\begin{array}{c|c} 0 & V \\ \hline 0 & 1 \end{array}\right) \ . \tag{3.43}$$

All the components of X do appear in the Majorana sector, via the terms $\mathbf{L}_L X\, m_\nu^{(0)}\, \mathbf{L}_L^T$ and $\mathbf{L}_L m_\nu^{(0)}\, X^T \mathbf{L}_L^T$. These imply the following structure

$$m_\nu = m_{\nu_1}^{(0)} \left[I + a \left(\begin{array}{c|c} \Delta_L & V \\ \hline \bar{V}^T & x \end{array}\right)\right] \ , \tag{3.44}$$

where a is a $O(1)$ complex coupling. Assuming that all the entries of X are at most of $O(\epsilon)$ does not spoil the degenerate configuration of m_ν in first approximation. In addition, since Δ_L could enter linearly in the sfermion mass matrices and induce sizable FCNC, we expect a small mis-alignement between Δ_L and V in the $O(2)_l$ space. Pursuing the analogy with the squark sector, we are forced to assume $(\Delta_L)_{12}$ at most of $O(\epsilon^2)$ in the basis where $V_1 = 0$. In other words, we are lead to the following assignment for the various components of X in the $O(2)_l$ basis where $V^T \propto (0, 1)$:

$$V = \left(\begin{array}{c} 0 \\ O(\epsilon) \end{array}\right), \quad \Delta_L = \left(\begin{array}{cc} 0 & O(\epsilon^2) \\ O(\epsilon^2) & O(\epsilon) \end{array}\right), \quad x = O(\epsilon). \tag{3.45}$$

In the same basis, redefining the unknown parameters, we arrive to the following parametric expression

$$m_\nu = \bar{m}_{\nu_1} \left[I + e^{i\phi_\nu} \left(\begin{array}{ccc} -\sigma\epsilon & \gamma\epsilon^2 & 0 \\ \gamma\epsilon^2 & -\delta\epsilon & r\epsilon \\ 0 & r\epsilon & 0 \end{array}\right)\right] \ , \tag{3.46}$$

where ϕ_ν, σ, δ, γ, and r are real parameters expected to be of $O(1)$.

The final step for the construction of a realistic charged-lepton Yukawa coupling is the introduction of the $U(2)_l \times U(2)_e$ bi-doublet ΔY_e. The most economical way to achieve this goal in the context of $U(3)_l \times U(3)_e$ is to introduce a bi-triplet with the following form,

$$\Delta\hat{Y}_e = \left(\begin{array}{c|c} \Delta Y_e & 0 \\ \hline 0 & 0 \end{array}\right) \ , \tag{3.47}$$

which provides the desired correction to Y_e and has no relevant impact on m_ν.

Notice that the requirement of having $Y^{(0)}$ and X acting on $O(3)$ and $O(2)$ subspaces can be naturally accomplished by demanding an exact CP symmetry acting on both spurions. The CP symmetry would be broken only by the $\Delta\hat{Y}_f$ spurions, which would provide all CP violation phases.[§]

[§]For quarks, it was shown in [56] that the CKM phase is entirely defined by the phases in the ΔY_f spurions. Thus, the conclusions for the quark sector would remain unchanged.

Our parametrical decomposition of the neutrino mass matrix is therefore the expression in Eq. (3.46). As can be seen, the latter contains only a CP-violating phase, ϕ_ν, which does not contribute to the PMNS matrix. However, this does not imply that there are no CP-violating phases in $U_{\rm PMNS}$: a non-vanishing phase arises by the diagonalization of the charged-lepton mass matrix. Indeed, to leading order in ϵ, the parametric decomposition of $M_\nu^2 = m_\nu^\dagger m_\nu$ in the basis where Y_e is diagonal is

$$M_\nu^2 = \bar{m}_{\nu_1}^2 U_{eL}^T \begin{pmatrix} 1-2\sigma\,\epsilon & & \\ 2\gamma\,\epsilon^2 & 1-2\delta\epsilon & \\ O(\epsilon^3) & 2r\,\epsilon & 1 \end{pmatrix} U_{eL}^* \ , \tag{3.48}$$

where we have redefined σ, δ, γ, and r, absorbing a $\cos(\phi_\nu)$ term and U_{eL} is given in Eq. (3.37). Despite the presence of four O(1) free parameters, the expression of M_ν^2 in Eq. (3.48) is quite constrained by the smallness of ϵ. As we discuss in the next Section, it provides a good fit to all the available neutrino data for a natural range of the free parameters and leads to a few unambiguous predictions. We finally stress that we arrived to this decomposition using essentially two main assumptions:

I. An approximate degenerate neutrino spectrum, that fits well with present data if $m^2_{\rm light} \gg \Delta m^2_{\rm atm}$.

II. A symmetry-breaking pattern with respect to a purely degenerate spectrum closely related to the minimal $U(2)^5$ symmetry breaking pattern of quark and lepton Yukawa couplings.

3.2.3 Predictions for neutrino masses and mixings

We are now ready to analyze the predictions of the M_ν^2 parameterization in Eq. (3.48). We first discuss a few simple analytic results, valid to leading order in ϵ. Given that the neutrino spectrum is almost degenerate, the ordering of the eigenvalues has no physical implications. However, for the sake of simplicity, we present analytic results only in the case of normal ordering ($m_{\nu_3} > m_{\nu_2} > m_{\nu_1}$). We then proceed with a systematic numerical scan of the four O(1) free parameters to investigate the stability of the analytic conclusions.

Mass eigenvalues

From the decomposition of M_ν^2 in Eq. (3.48) we derive the following expressions for the eigenvalues,

$$m_{\nu_1}^2 = \bar{m}_{\nu_1}^2 \,(1-2\sigma\,\epsilon) \ , \tag{3.49}$$

$$m_{\nu_2}^2 = \bar{m}_{\nu_1}^2 \left[1-\delta\,\epsilon-(\delta^2+4r^2)^{1/2}\epsilon\right] \ , \tag{3.50}$$

$$m_{\nu_3}^2 = \bar{m}_{\nu_1}^2 \left[1-\delta\,\epsilon+(\delta^2+4r^2)^{1/2}\epsilon\right] \ , \tag{3.51}$$

up to $O(\epsilon^2)$ corrections. The normal ordering of the spectrum is obtained for $\sigma > (\delta^2 + 4r^2)^{1/2}$ and in this case we find

$$\frac{\Delta m^2_{\rm atm}}{m^2_{\nu_1}} = \left[2\sigma - \delta + (\delta^2 + 4r^2)^{1/2}\right] \epsilon \ , \tag{3.52}$$

$$\zeta = \left[\frac{2\sigma - \delta - (\delta^2 + 4r^2)^{1/2}}{2\sigma - \delta + (\delta^2 + 4r^2)^{1/2}}\right]^{1/2} \ . \tag{3.53}$$

As can be seen, ϵ controls the overall scale of neutrino masses, whose natural scale is

$$O[(\Delta m^2_{\rm atm})^{1/2}\epsilon^{-1/2}] = O(0.3 \text{ eV}), \tag{3.54}$$

just below the existing bounds (see discussion at the end of this Section). Our parametric decomposition of M^2_ν does not necessarily imply $\zeta \ll 1$. However, the experimental value in Eq. (3.28) is easily obtained with a modest tuning of the free parameters, especially if δ is small. As we discuss next, the latter is a condition necessary to reproduce the maximal 2-3 mixing in the PMNS matrix.

θ_{23}

In order to determine the θ_{23} and θ_{13} mixing angles of the PMNS matrix it is sufficient to expand M^2_ν up to $O(\epsilon^2, s_e^2\epsilon)$:

$$M^2_\nu = \bar{m}_{\nu_1} \begin{pmatrix} 1 - 2\epsilon\sigma & & \\ -2s_e\epsilon(\sigma - \delta)\, e^{i\alpha_e} & 1 - 2\epsilon\delta & \\ -2\epsilon\, s_e r\, e^{i\alpha_e} & 2\epsilon r & 1 \end{pmatrix} + O(\epsilon^2, s_e^2\epsilon) \ . \tag{3.55}$$

As can be seen, at this level γ does not appear. Note also that for $s_e \to 0$ the 2-3 sector decouples. In this limit we obtain the following simple expression for the 2-3 mixing:

$$t_{23} = \frac{s_{23}}{c_{23}} = \frac{\delta \pm [\delta^2 + 4r^2]^{1/2}}{2r} \ , \tag{3.56}$$

where the sign in the numerator is chosen depending on the sign of r, such that t_{23} remains positive. As we have explicitly checked by means of the numerical scan, this result is stable with respect to the inclusion of the subleading terms of $O(s_e\epsilon)$ and $O(\epsilon^2)$.

From Eq. (3.56) it is clear that t_{23} is naturally expected to be $O(1)$, and the experimental evidence of maximal mixing, $t_{23} \approx 1$, is obtained for $\delta \to 0$.

θ_{13} and the PMNS phase

The value of θ_{13} can be obtained via the following general relation

$$\frac{(M^2_\nu)_{31}}{(M^2_\nu)_{32}} \approx \frac{s_{13}}{s_{23}}\, e^{i\delta_{\rm P}} \ , \tag{3.57}$$

that can be derived expanding M_ν^2 –in the basis where Y_e is diagonal– up to the first order in ζ and s_{13} (here $\delta_{\rm P}$ denotes the PMNS phase in the standard parameterization). Applying this result to the approximate from in Eq. (3.55) leads to

$$s_{13}e^{i\delta_P} = s_e s_{23} e^{\alpha_e+\pi} \ . \tag{3.58}$$

Assuming $s_e = s_d = |V_{td}|/|V_{ts}|$, and the experimental value of s_{23} ($s_{23}^2 = 0.52 \pm 0.06$ [73]), we predict

$$s_{13} = 0.16 \pm 0.02 \ , \tag{3.59}$$

in remarkable agreement with the recent DayaBay result in Eq. (3.29). This prediction is affected by a theoretical error (not explicitly shown) due to possible deviations from the relation $s_e = s_d$. On the other hand, as we have checked by means of the numerical scan, it is quite stable with respect to subleading corrections in the expansion of M_ν^2.

As anticipated, the PMNS phase is completely determined in terms of the CP-violating phase from the rotation of the charged-lepton Yukawa coupling: $\delta_P = \alpha_e + \pi$. However, we are not able to determine this phase even assuming $\alpha_e = \alpha_d$, where α_d is the corresponding phase appearing in the diagonalization of Y_d.* On general grounds, we expect δ_P to be a generic $O(1)$ phase.

θ_{12}

Contrary to the case of θ_{23} and θ_{13}, the determination of θ_{12} involve subleading terms in M_ν^2 and thus is more unstable.

As an illustration, consider M_ν^2 in the limit $s_e \to 0$. In this simplified case we obtain the relation

$$\tan 2\theta_{12} = \frac{2\gamma\, c_{23}}{\sigma - \delta\, c_{23}^2 - 2r\, s_{23}c_{23}}\epsilon \ , \tag{3.60}$$

that seems to imply $\theta_{12} \approx 0, \pi/2$. However, once we impose the constraints from the squared mass differences, we find a cancellation in the denominator leading to generic $O(1)$ values for θ_{12}. More explicitly, expressing s_{23} and c_{23} in terms of δ and r by means of Eq. (3.56) we find

$$\tan 2\theta_{12} = \frac{4\gamma\,\epsilon}{2\sigma - \delta - [\delta^2 + 4r^2]^{1/2}} c_{23} = O(1) \times \frac{\epsilon}{\zeta^2} \ ,$$

which is manifestly a generic O(1) number. This general conclusion remains valid when subleasing terms of $O(s_e\epsilon)$ and $O(\epsilon^2)$ are taken into account, although the explicit analytical expression for θ_{12} becomes more involved.

Parameter Scan

In order to check the stability of the above conclusions we have performed a numerical scan allowing the four free real parameters in Eq. (3.48) to vary in the range $[-2, 2]$.

*The physical phase appearing in the CKM matrix can be determined in terms of $\alpha_d - \alpha_u$ [56], but we cannot disentangle α_d and α_u without extra theoretical assumptions.

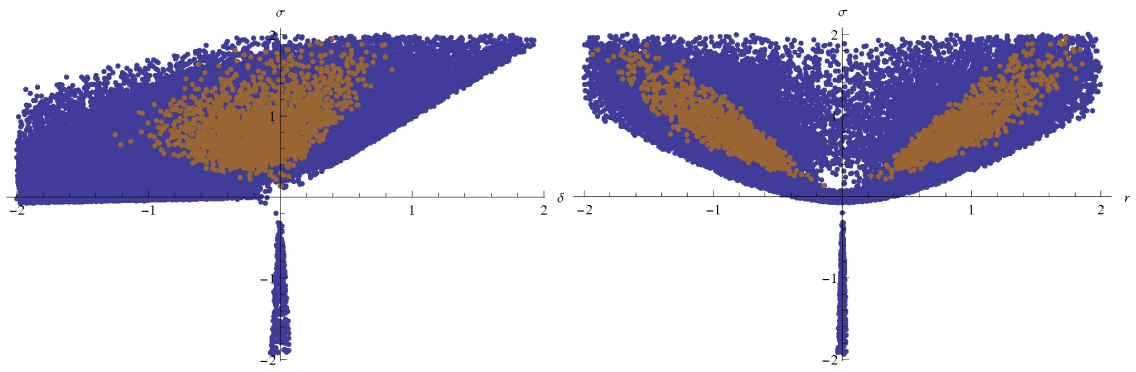

Figure 3.3: Correlation between the free parameters δ, σ, and r, after imposing the experimental constraints on the neutrino mass matrix in the case of normal hierarchy. Blue points: squared mass constraints only. Brown points: squared mass and mixing constraints imposed.

The results are summarized in Fig. 3.3–3.5. In all plots the blue points are the allowed points after imposing the squared mass constraints only, while the points in brown are those where both squared mass and mixing constraints, as resulting from the global fit in Ref. [73], are satisfied.[†]

The two plots in Fig. 3.3 illustrate the role of σ, δ, and r, in reproducing the mass spectrum. For illustrative purposes, only the points giving rise to normal hierarchy are shown: the inverted case give rise to identical distributions provided $\sigma \to -\sigma$ and $\delta \to -\delta$. As can be seen from both plots, there is a wide range of values giving rise to the correct mass spectrum and no serious tuning of the parameters is needed to explain the (modest) hierarchy between $|\Delta m_{\rm atm}|$ and $\Delta m_{\rm sol}$. The latter emerge naturally provided σ is not too small.

The results for θ_{13} and θ_{23} as a function of the corresponding most relevant free parameters are illustrated in Figure 3.4 (again only the normal hierarchy case is explicitly shown). On the top panel we show t_{23} as a function of δ/r: the two bands are those expected by the analytical expression in Eq. (3.56). As can be seen, we cannot claim to predict $t_{23} \approx 1$, but this is a value perfectly allowed by our parameterization without particular fine tuning. On the contrary, very small or very large values of t_{23} are disfavored after imposing the mass constraints. On the bottom panel we show s_{12} as a function of γ. As anticipated in the analytical discussion, s_{12} is very difficult to be predicted (any value is essentially allowed). The only clear pattern emerging is the need of a non-vanishing γ in order to reproduce the experimental value of s_{12}.

In Figure 3.5 we show the correlation of s_{13} and s_{23}, which is the only clear prediction of our decomposition, as far as the mixing angles are concerned. Also in this case we find

[†]Although the global fit of Ref. [73] does not include the recent Daya-Bay result [71], the resulting value for θ_{13} turns out to be in good agreement with the direct determination in Eq. (3.29). Similar results for all the neutrino parameters but for θ_{13} can be found also in Ref. [74].

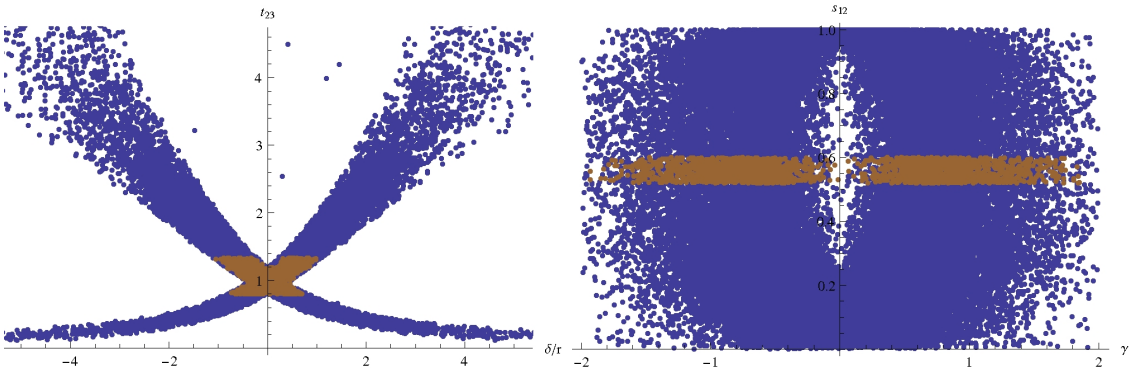

Figure 3.4: Top: t_{23} vs. δ/r. Bottom: s_{12} vs. γ. Notations as in Fig. 3.3.

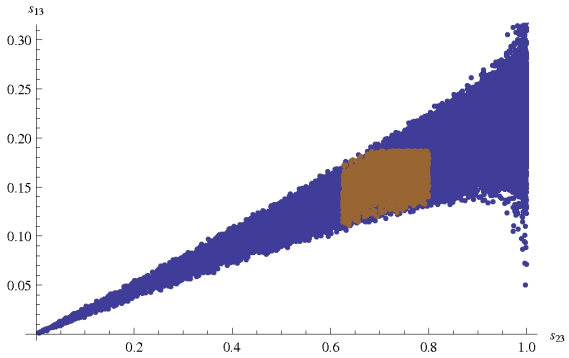

Figure 3.5: Correlation between s_{13} and s_{23} as expected in our framework. Notations as in Fig. 3.3.

a clean confirmation of what expected by means of the approximate analytical result in Eq. (3.56). The width of the band correspond to the uncertainty in the value of s_e, that we have varied in the range $[0.19,\ 0.25]$.

Finally, in Fig. 3.6 we illustrate our predictions for the absolute values of neutrino masses. We find that typical values for the sum of neutrino masses lie around $0.2 - 1$ eV, in agreement with current bounds.[‡] Interestingly, this means that neutrinoless double beta decay should be observed in the upcoming experiments, with the parameter $m_{\beta\beta}$ around $0.02 - 0.4$ eV. Current bounds for the matrix element, as well as the sensitivity of future experiments, are shown in Table 3.1.

[‡]The WMAP bound of [75] for the sum of neutrino masses varies between 1.3 eV (WMAP-only) and 0.58 (WMAP + Baryon Acoustic Oscillations + Hubble constant measurements)

Bounds			Prospects	
Experiment	Bound (eV), C.L.		Experiment	Reach (eV) [76]
KamLAND-Zen (^{136}Xe)	$< 0.3 - 0.6$, 90%	[78]	KamLAND-Zen (^{136}Xe)	0.062
CUORICINO (^{130}Te)	$< 0.19 - 0.68$, 90%	[79]	CUORE (^{130}Te)	0.062
NEMO3 (^{100}Mo)	$< 0.7 - 2.8$, 90%	[80]	NEXT (^{136}Xe)	0.071
Heidelberg-Moscow (^{76}Ge)	0.32 ± 0.03, 68%	[81]	EXO (^{136}Xe)	0.072

Table 3.1: Current bounds and prospects on $m_{\beta\beta}$. Intervals in bounds are due to uncertainty in the nuclear matrix elements. The "reach" assume reference values for $\beta\beta$ isotope masses and a 10-year data taking period.

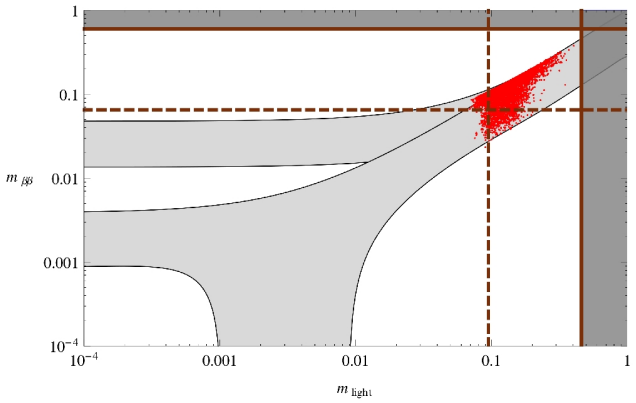

Figure 3.6: Correlation between the neutrino mass-matrix entry relevant to $0\nu\beta\beta$ experiments ($m_{\beta\beta}$) and the lightest neutrino mass (m_{light}). The gray area is the area accessible from present oscillation experiments (at 3σ), the red points denote the prediction of our framework. The solid lines indicate the current bounds [75]; the dashed lines provide an indication of the (near) future prospects [76, 77].

.

3.2.4 The slepton sector and LFV

Having identified the minimal set of spurions necessary to build the lepton Yukawa coupling and the neutrino mass matrix, we can now turn to study the consequences of this symmetry-breaking pattern in the slepton sector.

Let's start from the LL soft slepton mass matrix, which transforms as $\mathbf{8} \oplus \mathbf{1}$ under $U(3)_l$ and is invariant under $U(3)_e$. The LN conserving spurions at our disposals are $Y^{(0)}$ and $\Delta\hat{Y}_e$, both transforming as bi-triplets of $U(3)_l \times U(3)_e$, and X, transforming as an $\mathbf{8}$ of $U(3)_l$. Given the smallness of neutrino masses, we can safely neglect LN-conserving terms obtained by the contraction of two $m_\nu^{(0)}$ terms. Expanding to the first non-trivial

order in these spurions, the LL soft mass matrix assume the following form

$$\begin{aligned}
\tilde{m}^2_{\tilde{L}} &= \left(\begin{array}{c|c} (m^2_{\tilde{L}})_{\rm hh} & c_3 V^* \\ \hline c_3 V^T & (m^2_{\tilde{L}})_{33} \end{array}\right) \tilde{m}^2_{L_h} \ , \\
(m^2_{\tilde{L}})_{\rm hh} &= I + c_3 \Delta^*_L + c_4 \Delta Y^*_e \Delta Y^T_e \ , \\
(m^2_{\tilde{L}})_{33} &= 1 + c_2 |y_\tau|^2 + c_3 x \ ,
\end{aligned} \tag{3.61}$$

with all constants being real and $O(1)$. Since X is at most of $O(\epsilon)$ and ΔY_e is at most of order (y_μ/y_τ), we can approximate the above expression to

$$\tilde{m}^2_{\tilde{L}} = \left(\begin{array}{ccc} 1 & c_3'' \, \epsilon^2 & 0 \\ c_3''^* \, \epsilon^2 & 1 + c_3 \, \epsilon & c_3' \, \epsilon \\ 0 & c_3'^* \, \epsilon & 1 + c_2 |y_\tau|^2 \end{array}\right) \tilde{m}^2_{L_h} \ , \tag{3.62}$$

where we have distinguished c_3, c_3' and c_3'' due to the possibility of additional $O(1)$ factors from the spurions themselves. With this definition, c_3' and c_3'' are complex. In principle, these parameters are related to the parameters appearing in the neutrino mass matrix by

$$\mathrm{Re}(c_3') = \frac{1}{2} \frac{r}{\sigma - \delta} c_3 \ , \qquad\qquad \mathrm{Re}(c_3'') = \frac{1}{2} \frac{\gamma}{\sigma - \delta} c_3 \ . \tag{3.63}$$

However, we have explicitly checked that these relations do not provide very stringent constraints. For this reason, in the numerical analysis we have treated c_3, c_3', and c_3'' as independent free parameters.

In the sfermion sector, the main difference between the $U(3)^5$ set-up we are considering, and that based on a $U(2)^5$ symmetry, lies on the fact that in the latter case one can naturally have sfermions of the first two families considerably heavier than those of the third family [56], see Eq. (3.9). As discussed in the introduction, this possibility is attractive due to the lack of experimental signals for supersymmetry at LHC and, at the same time, the need of relatively light squarks of the third generation in order to stabilize the Higgs sector (hierarchy problem). In the $U(3)^5$ set-up we can also have third-family sfermions substantially lighter than those of the first two generations. However, this can happen only at the price of some fine-tuning of the symmetry-breaking terms. In the case of $\tilde{m}^2_{\tilde{L}}$, this happens if $1 + c_2 |y_\tau|^2 \ll 1$. However, it is worth to stress that in the slepton sector the requirement of a sizable mass splitting among the families is less motivated: the sleptons play a minor role in the hierarchy problem and there are no stringent direct experimental bounds on any of the slepton families. In Sec. 3.3.5 we will discuss the possibility that such a splitting be related with the RGEs running if the flavor symmetry is broken at M_{GUT}.

The RR soft slepton mass matrix transforms as $\mathbf{8} \oplus \mathbf{1}$ under $U(3)_e$ and is invariant under $U(3)_l$. Proceeding similarly to the LL case we find

$$\begin{aligned}
\tilde{m}^2_{\tilde{e}} &= \left(\begin{array}{c|c} (m^2_{\tilde{e}})_{\rm hh} & c_5 \Delta Y^T_e V^* y^*_\tau \\ \hline c_5 V^T \Delta Y^*_e y_\tau & (\tilde{m}^2_{\tilde{e}})_{33} \end{array}\right) \tilde{m}^2_{e_h} \ , \\
(m^2_{\tilde{e}})_{\rm hh} &= I + c_4' \Delta Y^T_e \Delta Y^*_e + c_6 \Delta Y^T_e \Delta^*_L \Delta Y^*_e \ , \\
(m^2_{\tilde{e}})_{33} &= 1 + |y_\tau|^2 (c_2' + c_7 x) \ .
\end{aligned} \tag{3.64}$$

Channel	Bound (90% C.L.)		Prospects
$\mathcal{B}(\mu \to e\gamma)$	$< 2.4 \times 10^{-12}$	[82]	10^{-13}
$\mathcal{B}(\tau \to e\gamma)$	$< 3.3 \times 10^{-8}$	[84]	10^{-9}
$\mathcal{B}(\tau \to \mu\gamma)$	$< 4.4 \times 10^{-8}$	[84]	10^{-9}

Table 3.2: Bounds and prospects for LFV searches.

Here all off-diagonal terms are heavily suppressed by the first and second generation Yukawa couplings and, to a good approximation, can be neglected.

Finally, let's consider the trilinear soft-breaking term A_e, responsible for the LR entries in the slepton mass matrices. The symmetry breaking structure of A_e is identical to that of the Yukawas, albeit with different $O(1)$ factors:

$$A_e = \left(\begin{array}{c|c} a_1 \Delta Y_e & a_2 V \\ \hline 0 & a_3 \end{array}\right) y_\tau A_0 \ . \tag{3.65}$$

Here the a_i are complex $O(1)$ parameters. When diagonalizing the charged-lepton Yukawa we find (see also Appendix A)

$$(A_e)^Y \approx \begin{pmatrix} a_1 \ell_1 & 0 & (a_2 - a_3) s_e \, e^{i\alpha_e} \epsilon \\ 0 & a_1 \ell_2 & (a_2 - a_3) c_e \epsilon \\ 0 & 0 & a_3 \end{pmatrix} y_\tau A_0 \ , \tag{3.66}$$

where $\ell_1 = (y_e/y_\tau)$ and $\ell_2 = (y_\mu/y_\tau)$. This implies a negligible LR contribution to the 1–2 sector, and suppressed contributions to the 1–2, 3 sectors.

Lepton Flavor Violation

Given the structure of the soft-breaking terms illustrated above, the leading contributions to LFV processes are induced by LL terms. Inspired by the symmetry-breaking pattern of the squark sector analyzed in Ref. [56], and also to simplify the discussion, in the following we assume the existence of an approximate cancellation in the $(3,3)$ element of the LL slepton mass matrix. Under this assumption, the leading contributions to LFV processes are dominated by the exchange of third-family sleptons.

Before analyzing the predictions of LFV rates by means of a numerical scan of the parameter space, we draw a few analytical considerations. In the limit where we assume the dominance of chargino contributions (as expected because of the larger coupling compared to neutralinos), we only need to analyze the LL mass matrix of Eq. (3.62). This is diagonalized by the analogue of Eq. (3.16):

$$W_L^e = \begin{pmatrix} c_e & s_e e^{-i\alpha_e} & -s_e s_L^e e^{i\gamma} e^{-i\alpha_e} \\ -s_e e^{i\alpha_e} & c_e & -c_e s_L^e e^{i\gamma} \\ 0 & s_L^e e^{-i\gamma} & 1 \end{pmatrix} \ , \tag{3.67}$$

where

$$s_L^e\, e^{i\gamma} = s_\tau e^{-i\phi_\tau} + c_3' = O(\epsilon)\ . \tag{3.68}$$

The relevant mixing terms are then

$$\mathcal{R}^{\tilde{\nu}}_{13} = -s_e\, s_L^e\, e^{i(\gamma-\alpha_e)}\ , \tag{3.69}$$

$$\mathcal{R}^{\tilde{\nu}}_{23} = -c_e\, s_L^e\, e^{i\gamma}\ , \tag{3.70}$$

$$\mathcal{R}^{\tilde{\nu}}_{33} = 1\ . \tag{3.71}$$

This allows us to make the approximate predictions:

$$\left(\frac{\mathcal{B}(\mu\to e\gamma)}{\mathcal{B}(\tau\to\mu\gamma)}\right)^{\chi^\pm} \approx \left(\frac{m_\mu}{m_\tau}\right)^5 \frac{\Gamma_\tau}{\Gamma_\mu}\left|\frac{\mathcal{R}^{\tilde{\nu}}_{23}\mathcal{R}^{\tilde{\nu}*}_{13}}{\mathcal{R}^{\tilde{\nu}}_{33}\mathcal{R}^{\tilde{\nu}*}_{23}}\right|^2 \approx 5.1\, s_e^2\, s_L^{e\,2}\ , \tag{3.72}$$

$$\left(\frac{\mathcal{B}(\tau\to e\gamma)}{\mathcal{B}(\tau\to\mu\gamma)}\right)^{\chi^\pm} \approx \left|\frac{\mathcal{R}^{\tilde{\nu}}_{33}\mathcal{R}^{\tilde{\nu}*}_{13}}{\mathcal{R}^{\tilde{\nu}}_{33}\mathcal{R}^{\tilde{\nu}*}_{23}}\right|^2 \approx s_e^2\ , \tag{3.73}$$

which turn out to be good approximations to the full results.

In our numerical simulation, we include both chargino- and neutralino-mediated contributions. We perform a complete diagonalization of the full 6×6 slepton mass matrix and the 3×3 sneutrino mass matrix.* We take the $(3,3)$ and $(6,6)$ elements in the range $(200\text{ GeV})^2 - (1000\text{ GeV})^2$, while we assume values between 5^2 and 100^2 times heavier for the other mass eigenvalues. The A_0 parameter is assumed to be proportional to the heavy sfermion mass with a proportionality constant in the range $[-3,3]$. The chargino soft mass is fixed to $M_2 = 500$ GeV, and we use gaugino unification arguments to set $M_1 = 0.5 M_2$. We also fix $\tan\beta = 10$, and $\mu = 600$ GeV.

The results of the numerical analysis are shown in Figure 3.7. On the upper panel we show the correlation between $\mathcal{B}(\tau\to\mu\gamma)$ and $\mathcal{B}(\mu\to e\gamma)$, while on the bottom panel we show the correlation of the former with $\mathcal{B}(\tau\to e\gamma)$. We show the current bounds for each branching ratio with solid brown lines, while the expected sensitivity of the relevant experiment (MEG for $\mu\to e\gamma$, Belle II and SuperB for $\tau\to\ell\gamma$) is shown using dashed brown lines (see Table 3.2). The contours on the left panel give an idea of the density of points, where each outer contour represents a density value one order of magnitude smaller than the respective inner contour.

The upper panel of Figure 3.7 shows that, although a small part of the parameter space is ruled out already, there exist a significant number of points that can be probed by $\mu\to e\gamma$, $\tau\to\mu\gamma$ and possibly also $\mu\to e$ conversion experiments in the near future. It is interesting to note that current and future sensitivities of $\mu\to e\gamma$ and $\tau\to\mu\gamma$ are quite comparable in constraining the model, even if the experimental sensitivity on $\tau\to\mu\gamma$ is much weaker. The fact that $\tau\to\mu\gamma$ has such an important role can easily be understood

* In the diagonalization process we discard results with tachyonic sleptons or charged LSPs. We also take into account the approximate LEP bounds on chargino, stau and sneutrino masses [83].

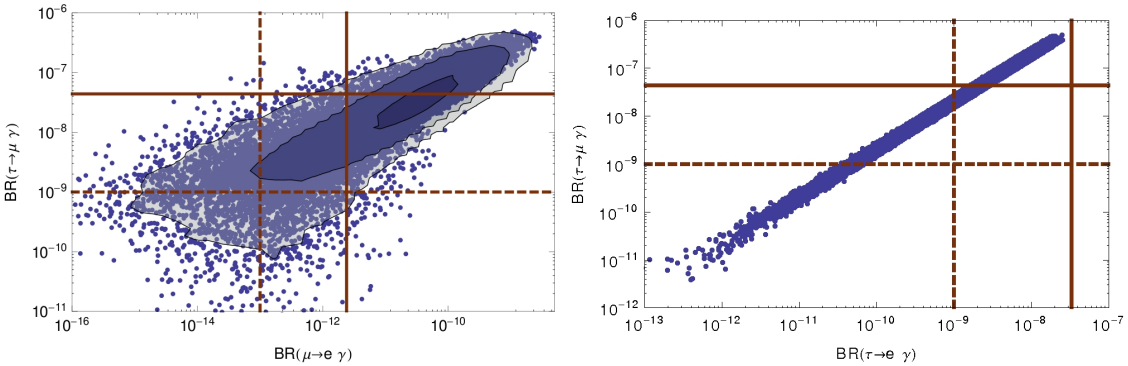

Figure 3.7: Top: Correlation between $\mathcal{B}(\tau \to \mu\gamma)$ and $\mathcal{B}(\mu \to e\gamma)$. Bottom: Correlation between $\mathcal{B}(\tau \to \mu\gamma)$ and $\mathcal{B}(\tau \to e\gamma)$. Case of hierarchical slepton mass spectrum, see text for more details.

from Eq. (3.72), where it is clear that $\mu \to e\gamma$ receives an additional suppression due to s_e^2. Similar conclusions have recently been reached also in Ref. [61]. On the other hand, the correlation between $\mu \to e\gamma$ and $\tau \to \mu\gamma$ in Figure 3.7 is quite different with respect what expected in various models of Minimal LFV [85], where there is no connections between quark and lepton flavor structures.

The lower panel of Figure 3.7 shows that $\tau \to e\gamma$ does not provide additional bounds on the model, as most points that can be probed by this decay mode are already ruled out by $\tau \to \mu\gamma$. Still, the Figure shows a very strong correlation, as expected from Eq. (3.73). This correlation could provide a very significant test of the model if it could be verified experimentally.

Finally, in order to test how these conclusions are modified if the slepton spectrum is not hierarchical, we have performed a independent scan without assuming a cancellation in the $(3,3)$ and $(6,6)$ entries of the slepton mass matrix. In particular, we vary all the diagonal entries in the range $(1000\ \text{GeV})^2 - (2000\ \text{GeV})^2$, while keeping all the other parameters (gaugino and chargino masses) fixed as in the previous scan. The result of this second numerical analysis are shown in Figure 3.8. As can be seen, in this case the correlation between $\mu \to e\gamma$ and $\tau \to \mu\gamma$ is quite different: the contribution of the sleptons of the first two families is not negligible in $\mu \to e\gamma$ and, as a consequence, the approximate relation Eq. (3.72) is no longer valid. In this framework, the recent MEG bound [82] on $\mu \to e\gamma$ provide a very severe constraint. In particular, it rules out the possibility of visible effects in the $\tau \to \mu\gamma$ case. The correlation between $\tau \to \mu\gamma$ and $\tau \to e\gamma$ is not modified with respect to Figure 3.8, but both modes are beyond the experimental reach after imposing the $\mu \to e\gamma$ bound.

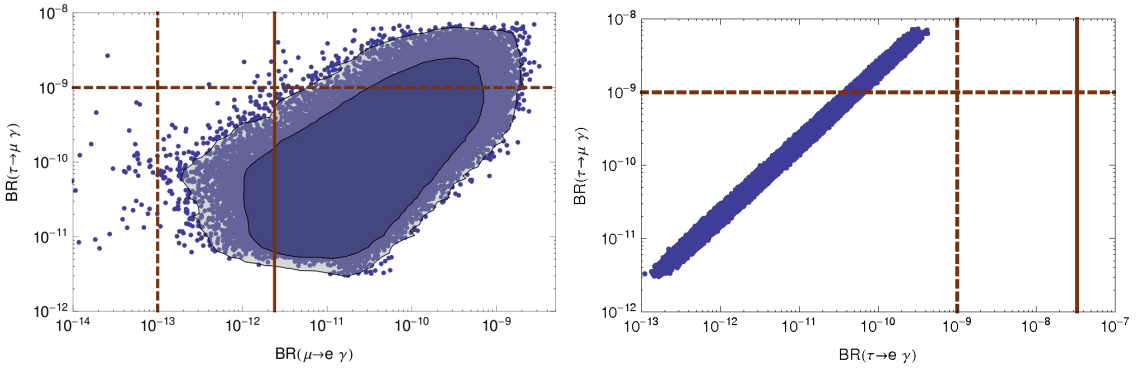

Figure 3.8: Correlation between $\mathcal{B}(\tau \to \mu\gamma)$ and $\mathcal{B}(\mu \to e\gamma)$ in the case of almost degenerate slepton mass spectrum. See text for more details.

3.2.5 Concluding remarks

We have proposed an ansatz for the neutrino mass matrix and the charged lepton Yukawa coupling based on a minimal breaking of the $U(3)^5$ flavor symmetry, consistent with the $U(2)^3$ breaking pattern of the quark Yukawa couplings discussed in Ref [56]. The key hypothesis that allows us to relate the non-hiearchical neutrino sector to the Yukawa sector is the assumption of a two-step breaking structure in the neutrino case: a leading breaking of the maximal flavor symmetry, $U(3)_l \times U(3)_e$, giving rise to a fully degenerate neutrino spectrum, followed by a sub-leading hierarchical breaking similar to the one occurring in the Yukawa sector. According to this hypothesis, the large 2-3 mixing in the neutrino sector arises as a small perturbation of an approximately degenerate spectrum. On the other hand, the ratio between θ_{13} and θ_{23} is predicted to be of the order of the Cabibbo angle, similarly to the quark sector, in good agreement with the recent DayaBay result.

As we have shown, our framework is able to reproduce all the neutrino oscillation parameters without particular tuning of the free parameters. The neutrino masses are predicted to be almost degenerate: the sum of all the eigenvalues is expected to be around $0.2 - 1$ eV, close to the present cosmological bounds, and the $0\nu\beta\beta$ parameter $m_{\beta\beta}$ is expected in the range $0.02 - 0.4$ eV, observable in next generation of experiments.

Our framework can naturally be implemented in supersymmetric extensions of the SM and, more explicitly, within the well-motivated set-up with heavy masses for the first two generations of squarks. We have analyzed the consequences of this flavor-symmetry breaking ansatz in the supersymmetric case, assuming a split family spectrum also in the slepton sector. The model can satisfy the existing constraints on LFV in charged leptons, with the most significant bounds coming from $\mu \to e\gamma$ and $\tau \to \mu\gamma$. For third-generation sleptons masses below 1 TeV both decay modes are expected to be within the reach of future experimental searches.

3.3 $U(2)^3$ and running effects

In Sec. 2.3.3 we introduced the MSSM and its constrained form, the CMSSM: we showed that, inspired by models of gravity mediated SUSY-breaking, the CMSSM has only a few additional parameters, defined at a unification scale, $M_{\rm GUT}$. In a phenomenological analysis the parameters of the model would then be evolved down to a SUSY-decoupling scale, $M_{\rm SUSY}$, through the use of renormalization group equations. One of the main consequences of this approach is that the soft SUSY-breaking terms would acquire a flavor structure compatible with the MFV ansatz [31]. However the current lack of SUSY signals at LHC have forced the theoretical community to start stepping away from this simple realization of SUSY, as for example considering models with a squark mass splitting like in the $U(2)^3$ case [56] discussed above.

Nevertheless, in most works studying the $U(2)^3$ framework [1, 56, 60–62], the flavor symmetry was considered to be directly applied at the electroweak scale, while the typical expectation is for this symmetry to be broken at a very high scale. First of all, it is unclear if the running of the MSSM parameters would preserve the virtues following from the assumption of a minimal breaking of the $U(2)^3$ symmetry, analyzed in the previous literature. Moreover, the type of initial conditions required to achieve the split scenario are not evident, especially after applying the LHC bounds on the gluino mass and trying to mitigate the naturalness problem as well as possible. In this Section, we attempt to answer these questions.

3.3.1 RGEs and masses

We are interested in the possibility that both supersymmetry and the flavor symmetries are broken at a very high scale, which we take to be $M_{\rm GUT} \sim 10^{16}$ GeV. (S)fermion mass matrices are therefore generated at M_{GUT} and they must be evolved down to M_{SUSY}, according to the MSSM RGEs.

We follow a three step procedure. In the first step, we define what our initial conditions shall be at $M_{\rm GUT}$. The fermion Yukawa couplings are determined from their electroweak values [86, 87], running them to the unification scale. For the sfermions, we assume the soft masses to follow the structures outlined in the Appendix, in particular, Eqs. (A. 2)-(A. 4). We choose a common mass for all the squarks in the first two generations, m_{heavy}, and a common mass for the third generation, m_{light}. In general, we shall refer to the splitting $\rho = (m^2_{heavy} - m^2_{light})/m^2_{heavy}$ instead of m_{light}, such that $\rho = 0$ is the totally degenerate case, while $\rho = 1$ corresponds to maximal splitting. The A-terms follow a flavor structure similar to that of the Yukawas, but the different $O(1)$s lead to a non-diagonal structure, shown in Eq. (A. 5). We assume the A-terms to be connected with the first two generations masses, so we take a universal $A_0 \sim m_{heavy}$.

Regarding the other soft parameters, we use a common value for the Higgs soft masses $m_{H_u} = m_{H_d} = m_0$, which can be different from both the light and heavy sfermion masses. We also consider a unified gaugino mass $M_{1/2}$, and, for definiteness, we fix $\tan\beta = 10$.

Thus, in our scan, the variable parameters shall be:

$$M_{1/2},\, m_{heavy},\, \rho,\, m_0,\, A_0,\, x_i,\, \gamma_i\ , \tag{3.74}$$

where x_i and γ_i represent the $O(1)$ parameters and phases shown in the Appendix. Notice that A_0 shall actually be the product of m_{heavy} and an $O(1)$ parameter.

On the second step, we run all parameters down to a common decoupling scale $M_{\rm SUSY} \sim 1$ TeV, following 2-loop MSSM RGEs [88]. As we are interested entirely in the RGE effects, we do not consider threshold corrections. At this scale, we calculate the sfermion soft masses and mixings.

Once we are at the low scale, we proceed with the third step, which is to ask several requirements to be satisfied. First, we ask the absence of color/charge-breaking minima. In fact, the third generations masses can acquire tachyonic values due to negative contributions from the running, proportional to m_0 at one loop and to m_{heavy} at two loops [89]. On the contrary, $M_{1/2}$ induces a positive contributions to the running, pushing the sfermion mass towards positive values, while the influence of the A-terms is weak. Thus, a balance between all contributions shall be required, such that no sfermion masses become tachyonic. As we shall see, the tachyon bound can forbid some scenarios with large splitting, $\rho \sim 1$*.

We also ask for correct radiative electroweak symmetry breaking (EWSB), ie we demand that at the low scale the μ parameter has a value such that the tadpole terms of the scalar potential vanish. For this to be satisfied, it is usually sufficient to have $m^2_{H_u}$ acquiring a negative value due to the running. Thus, a large m_0 shall be disfavored, as it will imply that the initial value of m_{H_u} shall be too large in order to be driven negative from the running. Moreover, a small $M_{1/2}$ is also indirectly disfavored. This is due to the negative influence of the stop masses on m_{H_u}. Larger values of $M_{1/2}$ shall give a larger positive gluino contribution to the stop masses, which in turn shall provide a larger negative contribution to $m^2_{H_u}$.

In addition, we require LHC bounds to be satisfied. In particular, we demand the light Higgs mass m_h to be compatible with the latest ATLAS and CMS measurements, that is, we take $m_h^{exp} = 125.3 \pm 0.6$ GeV [7, 8]. We calculate both m_h and its theoretical error using FeynHiggs [91–94], bounding the latter to be no larger than 3 GeV. We then ask m_h to be within the 1σ range, which in principle can allow masses as small as 123 GeV. We also check that all direct SUSY bounds are satisfied (in particular, $m_{\tilde{g}} > 1$ TeV is the most relevant limit).

Moreover, an interesting feature of the $U(2)^3$ model, in the flavor sector, is that it can improve the CKM fit with tiny and correlated new contributions to ϵ_K and $S_{\psi K_S}$ [56, 62], as shown in Eqs. (3.20) - (3.24). The size of these gluino-mediated effects depends on the

*Notice that, as we are taking a universal decoupling scale, the real edge of the tachyon bound is probably less stringent than the one shown. As shown in [90], the early decoupling of the heavy first generations can prevent some cases from becoming tachyonic.

function F_0, defined as:

$$F_0 = \frac{2}{3}\left(\frac{g_s}{g}\right)^4 \frac{m_W^2}{m_{Q_3}^2}\frac{1}{S_0(x_t)}\left[f_0\left(\frac{m_{\tilde{g}}^2}{m_{Q_3}^2}\right) + O(\frac{m_{Q_l}^2}{m_{Q_h}^2})\right] , \tag{3.75}$$

$$f_0(x) = \frac{11 + 8x - 19x^2 + 26x\log(x) + 4x^2\log(x)}{3(1-x)^3} , \tag{3.76}$$

with $S_0(x_t)$ being the typical one-loop function of the SM to $\Delta F = 2$ processes (for example, see [95]). In the updated fit of [68], it was shown that, after the inclusion of LHCb data, the $U(2)^3$ contributions could be of the correct size to solve the flavor tension if $0.01 < F_0 < 0.14$, and if the mixing was above a certain value[†]. As can be expected, the requirement on F_0 can be satisfied only if the $\tilde{g}$ and $\tilde{b}_L$ are not too heavy. We will mark this region with a special line in the following plots.

Given all these constraints, we will concentrate on the regions with a soft spectrum at $M_{\rm SUSY}$ as natural as possible. In particular, as shown in the literature [40, 47–49, 52], a natural supersymmetric theory requires that μ and the third generation masses to be light, and that the gluino must not be too heavy. Note that this represents a tension with the value of the parameters required to obtain a Higgs mass heavier than 120 GeV. Thus, we shall place ourselves in a middle ground, searching for values of $\mu < 1$ TeV, and at least one stop with mass $m_{\tilde{t}_1} < 1$ TeV.

We are also interested in understanding the type of splitting one obtains after the running. We shall be presenting our results in terms of:

$$\rho_{\tilde{t},\tilde{b}}^{\rm low} = \frac{\langle m_{sq}^2\rangle - \langle m_{\tilde{t},\tilde{b}}^2\rangle}{\langle m_{sq}^2\rangle} \tag{3.77}$$

where $\langle m_{\tilde{t},\tilde{b}}^2\rangle$ is the average mass squared for the stops or sbottoms, and $\langle m_{sq}^2\rangle$ is the average mass squared of the respective first two generations.

Spectrum

In our study we focus on two different scenarios. First, we shall take $m_{heavy} = 3$ TeV, very close to the experimental limit, such that it might be feasible to observe some signals from the first two generation squarks in the near future. On the second scenario, we use $m_{heavy} = 8$ TeV, and see what consequences this has on the spectrum.

For each value of m_{heavy}, we need to evaluate the interplay between the values of $M_{1/2}$, ρ, m_0 and A_0 required to satisfy the bounds mentioned previously. We shall explain such an interplay around the following two Benchmarks:

Benchmark 1: $M_{1/2} = 500$ GeV, $\rho = 0.5$, $m_{heavy} = 3$ TeV, $m_0 = 2.8$ TeV, $A_0 = -m_{heavy}$,

Benchmark 2: $M_{1/2} = 1.1$ TeV, $\rho = 0.97$, $m_{heavy} = 8$ TeV, $m_0 = 2.5$ TeV, $A_0 = -0.25 m_{heavy}$,

[†]This assumes $|V_{ub}| = (3.97 \pm 0.45) \times 10^{-3}$.

which, as we shall see, satisfy all our requirements. For each Benchmark, the value of A_0 has been chosen in order to maximize stop mixing without generating tachyons, such that the appropriate Higgs mass is reproduced. The choice for the other parameters shall be made clear when examining the surrounding parameter space.

In Figures 3.9 and 3.10 we show contours of μ, $\rho_{\tilde{t}}^{\text{low}}$ and $\rho_{\tilde{b}}^{\text{low}}$ on the upper, center and lower rows, and show the interplay between ρ and $M_{1/2}$, m_0 and m_{heavy} on the left, center and right columns, respectively. The dark regions correspond to points where EWSB is not achieved, and the orange regions have at least one tachyonic stop. We plot 1σ bounds on the Higgs mass as a dashed, green line, and show the region satisfying the F_0 constraint with a solid, red line.

Let us focus on the parameter space around Benchmark 1, which is shown in Figure 3.9. Here, we find a strong upper bound on ρ due to tachyons and EWSB. To avoid this bound, one can either increase $M_{1/2}$, decrease m_0 or increase m_{heavy}. However, as the Higgs and the F_0 bounds act in opposite directions, the possible variations are strongly limited. Increasing either $M_{1/2}$ or m_{heavy} shall improve the Higgs mass, but at the same time will worsen the value of F_0. This situation is even further constrained by the naturalness bound on $\mu < 1$ TeV, which fixes a lower bound on m_0. Similarly, the Higgs and F_0 constraints do not favor lower values of ρ.

Such constraints lead to values of μ around 500 GeV, and very specific splittings. In the stop sector, we find $\rho_{\tilde{t}}^{\text{low}} \sim 0.85$, which leads to an average stop mass of about 1.2 TeV. Nevertheless, as the stop mixing is large, we find the mass of the lightest stop to be lower than 500 GeV. On the other hand, in the sbottom sector, we have $\rho_{\tilde{b}}^{\text{low}} \sim 0.6$, leading to an average sbottom mass of 1.9 TeV. Notice that this setup involves a very mild splitting at the GUT scale, but can lead to a larger splitting in the stop sector. This is actually favored by the neutrino sector, which was studied in a $U(2)^5$ framework generated from the breaking of $U(3)^5$ [1]. Nevertheless, the splitting in the sbottom (and stau) sectors remains somewhat mild.

Let us turn now to Benchmark 2, shown in Figure 3.10. The motivation of this Benchmark is to study a scenario with a much stronger splitting than in Benchmark 1. However, the tachyon, Higgs and μ bounds force the value of $M_{1/2}$ to be too large to satisfy the F_0 constraint, having values about one order of magnitude lower than what is preferred from the fit in [68]. Still, we consider Benchmark 2 a useful comparison, which might become of interest if a stop signal is observed in the upcoming data, with no corresponding gluino nor squark signal.

From Figure 3.10, we find that the splitting in the stop sector remains somewhat invariant. This means that the positive RGE contribution to $m_{\tilde{t}}$ from $M_{1/2}$ cancels the large, negative RGE contribution from the y_t^2 Yukawa and the two-loop contribution from m_{heavy}. However, in the sbottom sector, the y_b^2 contribution is not as large as that for the stop sector, so the splitting is somewhat reduced. Still, we have and average stop mass of about 1.4 TeV (albeit with large mixing), an average sbottom mass close to 2 TeV, and $\mu = 600$ GeV.

One must admit that such a heavy spectrum is less natural than that in Benchmark

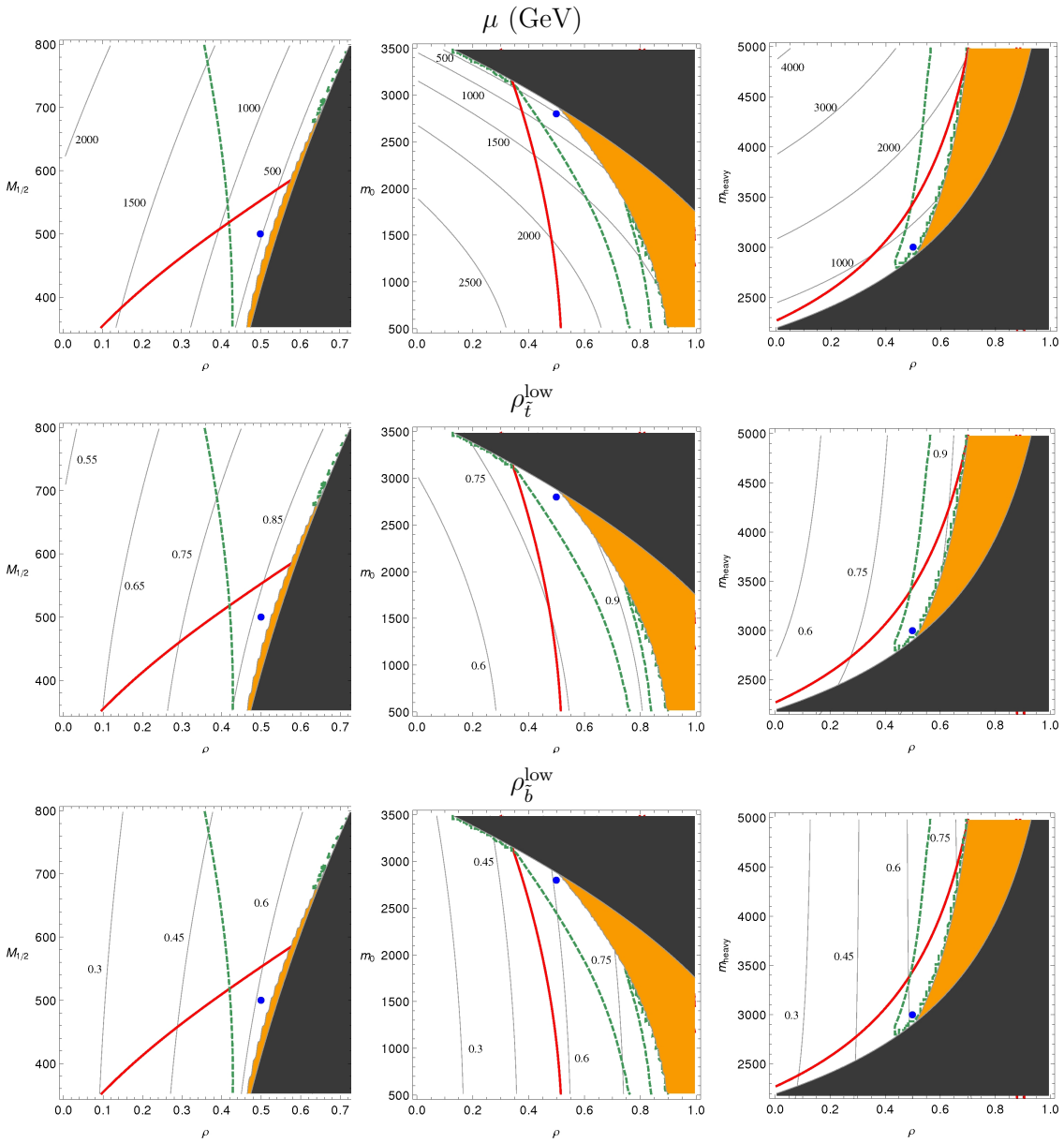

Figure 3.9: Parameter space around Benchmark 1. We show contours for μ, $\rho_{\tilde{t}}^{\text{low}}$ and $\rho_{\tilde{b}}^{\text{low}}$ on the top, center and bottom, respectively. The dark regions correspond to no EWSB, while the orange regions have a tachyonic stop. The green, dashed lines delimitate the regions within 1 sigma of the Higgs mass, and the red, solid curve indicates the regions below which the flavor tension could be solved. The blue dot represents Benchmark 1, which satisfies all constraints.

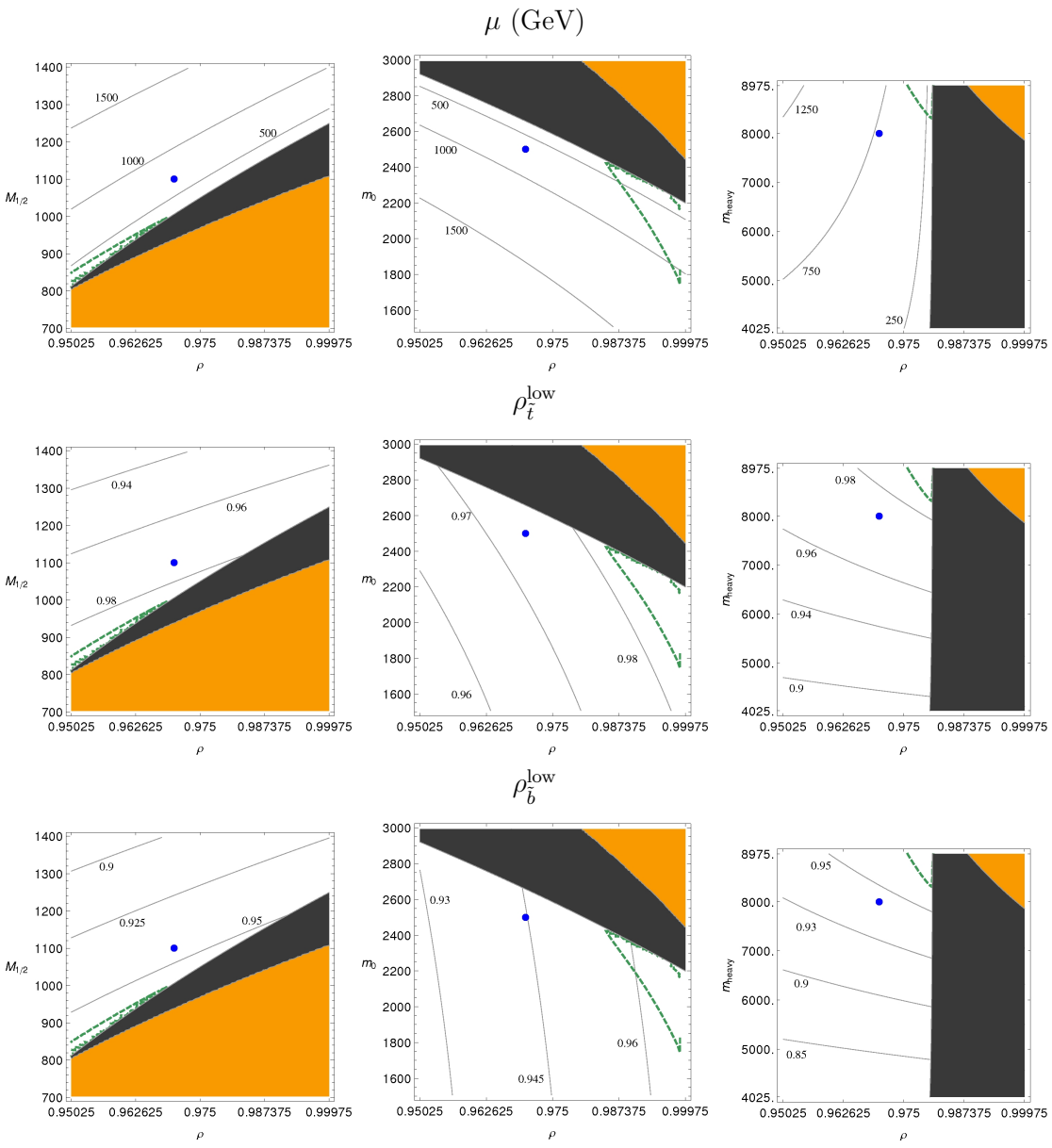

Figure 3.10: Same as Figure 3.9, but for Benchmark 2. Notice that the evaluated parameter space never satisfies the F_0 constraint. The blue dot represents Benchmark 2, which satisfies all other constraints.

1. Even though the μ parameter and the lightest stop mass are light enough, the gluino and the second stop are much heavier. Nevertheless, as this scenario reproduces the Higgs mass much easily than Benchmark 1, we still find this scenario attractive.

3.3.2 Mixings

Having found points in the parameter space leading to a split squark spectrum, we now turn to the question of what is the behavior of the mixing after the running. This is crucial in order to understand if the results given in [56, 60] are modified if we take the flavor structures at $M_{\rm GUT}$ and then evolve them to the low scale.

When evaluating the method to track the RGE evolution of the mixing, one finds several choices. First, it is possible to study the variation of the off-diagonals through the mass-insertion approximation (MIA). However, as this framework provides a non-degenerate spectrum, it is unclear if the MIA is appropriate. Second, one could track the evolution of the $O(1)$ constants shown in Eqs. (A. 2)-(A. 4), fitting the low-energy matrices into a $U(2)^3$-like structure. We find this procedure valid, but not particularly transparent nor informative. The third option is to build objects directly related to the physical observables, such that the evolution can be connected with the main results in [56,60]. As one can relate these objects with the framework parameters, we choose this approach.

As the communication between the first two and the third generations is due to a $U(2)_Q$ doublet, one would expect the main deviation from MFV to be found in $m^2_{\tilde{Q}}$. This means that, if we concentrate on $\Delta F = 2$ processes, the main supersymmetric contribution would come from $(LL)^2$ operators. Thus, we shall concentrate here on the evolution of the mixing participating in the latter operators, leaving the rest to be considered separately in Sec. 3.3.4.

From Eq. (3.18), we find that the gluino mediated contributions to $(LL)^2$ operators depend on the combination:

$$\lambda^{(a)}_{i\neq j} = (W^d_L)_{ia}(W^d_L)^*_{ja} \ , \tag{3.78}$$

where W^d_L is the diagonalization matrix of $m^2_{\tilde{Q}}$ in the basis of diagonal down quarks. In particular the supersymmetric contributions to K, B_d and B_s physics (in the limit of $\rho \to 1$) are given, respectively, by

$$\lambda^{(3)}_{12} = s^2_L \kappa^* c_d \ , \qquad \lambda^{(3)}_{13} = -s_L \kappa^* e^{i\gamma_L} \ , \qquad \lambda^{(3)}_{23} = -c_d s_L e^{i\gamma_L} \ , \tag{3.79}$$

where $s_L = x_L\,\epsilon$ and $\kappa \approx c_d V_{td}/V_{ts}$, with the remaining parameters defined in the Appendix. We see that the only parameters not fixed by the CKM matrix are s_L and γ_L, so the three objects are expected to be correlated. In Sec. 3.3.3 we shall analyze how these correlations behave under the RGE evolution, so for now it suffices to consider only the evolution of one of these objects. We shall choose $\lambda^{(3)}_{23}$.

Our procedure consists of the study of the evolution of $\lambda^{(3)}_{23}$ as a function of the renormalization scale for the two Benchmarks identified in the previous Section, similarly to [96]

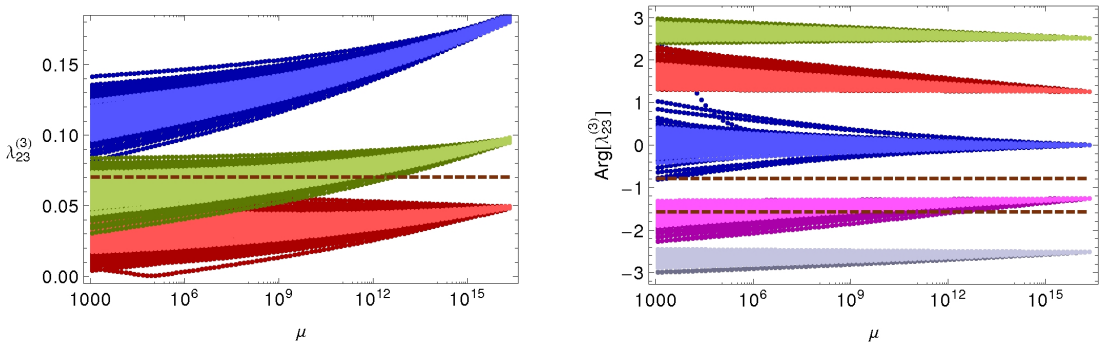

Figure 3.11: The running of $|\lambda_{23}^{(3)}|$ (left) and $\mathrm{Arg}(\lambda_{23}^{(3)})$ (right), in Benchmark 1. On the left, we show $x_L = 2$, 1, 0.5 in blue, green and red. In every region the lighter color correspond to γ_L fixed to $\pi/4$. On the right we fix $\gamma_L = (-1 + 0.4n)\pi$, with $n = 0$, 1, 2, 3, 4 in blue, red, green, gray and magenta, respectively. The lighter regions correspond to $x_L = 1$. In the first two plots the dashed brown lines mark the region where the flavor tension can be solved. On the left, the region is above the line, while on the right it is between the two lines.

for MFV. In Figure 3.11 and 3.12 we plot separately the absolute value (on the left) and the phase (on the right) of $\lambda_{23}^{(3)}$ in Benchmark 1 and 2, respectively. For the absolute values, we fix the parameter x_L that defines the mixing at M_{GUT} and we make a numerical scan of the other mixing parameters of the framework. We show with different colors three different values of x_L, as indicated in Figure 3.11. We also show with a lighter color the case in which the phase γ_L is fixed equal to $\pi/4$. On the contrary, in the plots of the phases, each color represents a different initial value for γ_L, varying all the other flavor parameters. Here, the lighter color corresponds to $x_L = 1$.

The main results are that, in general, the modulus and phase of $\lambda_{23}^{(3)}$ are relatively stable during the running. This is more true in Benchmark 2 than in Benchmark 1, where the running effects are stronger and the absolute values get a slight suppression. For the phases, we see a very mild spread in Benchmark 1. Moreover, it is interesting to see that it is possible to obtain a sizable phase even when starting from a real case at M_{GUT}. This is due mainly to the influence of phases in the trilinear parameters.

In each Figure, we also mark with a brown, dashed line the region where the mixing has got the appropriate size in order to solve the flavor tension. In the previous Section, we have outlined the region of the parameter space where the function F_0 is large enough to solve the tension. In particular, we showed that Benchmark 1 is within this region, while Benchmark 2 is not. Nevertheless, what really solves the flavor tension is the combination $x\,F_0$, where x is defined as $x = s_L^2 c_d^2/|V_{ts}|^2$, see Eq. (3.20 - 3.24). In principle, it is possible to have a very small value of F_0, but a very large value of x, and achieve the same results as with moderate values of both parameters. In contrast, it is possible to have an appropriate value of F_0 and end with a too small or too big x.

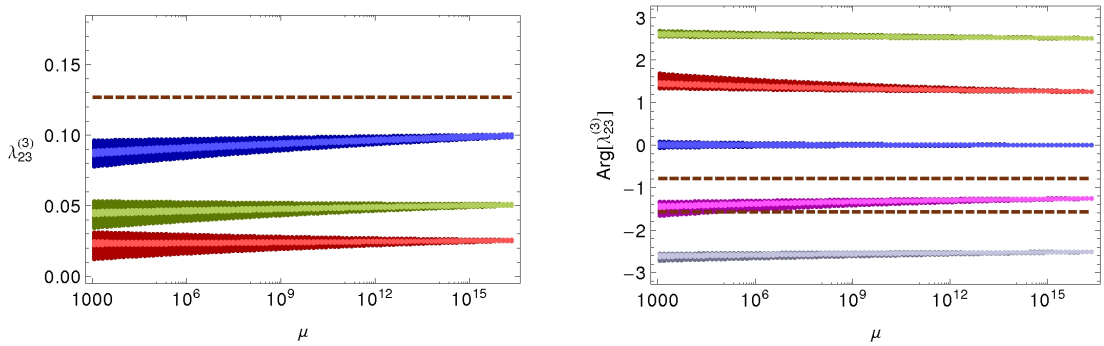

Figure 3.12: The running of $|\lambda_{23}^{(3)}|$ (left) and $\mathrm{Arg}(\lambda_{23}^{(3)})$ (right), in Benchmark 2. Notation as in Fig. 3.11.

For the absolute value, we have $x \gtrsim 3$ in Benchmark 1, while $x \gtrsim 10$ in Benchmark 2. The dashed lines on the respective Figures show this lower bound. For Benchmark 1, we find that values of x_L of $O(1)$ naturally reproduce the required mixing, as long as they are greater than unity. On the other hand, for Benchmark 2, we require the initial value of $\lambda_{23}^{(3)}$ to be somewhat large in order to obtain the minimum amount of mixing. Still, it is encouraging to note that the needed initial value is not many orders of magnitude larger, such that it could be obtained at $M_{\rm GUT}$ through an accidental enhancement.

The phase of $\lambda_{23}^{(3)}$ also needs to acquire particular values. The correct values are delimited by brown, dashed lines in the respective Figures. In both scenarios we see that, since the phase variation is not too strong, it suffices to choose $\gamma_L(M_{\rm GUT}) \sim \gamma_L(M_{\rm SUSY})$.

3.3.3 Structure

So far, we have found regions within our parameter space satisfying all our requirements, with the exception of Benchmark 2 satisfying the F_0 constraint. We have also demonstrated that the $\lambda_{23}^{(3)}$ parameter is stable during the running and, for Benchmark 1, we have found that typical values are effectively within the ballpark that can solve the flavor tension.

Nevertheless, we have not demonstrated that the $U(2)^3$ properties are maintained after the running. In principle, even if the F_0 constraint is satisfied and we have the $\lambda_{23}^{(3)}$ parameter stable, it is not evident that the full set of parameters shall evolve in a way that the correlations between their contributions to the K, B_d and B_s sector are preserved. In particular, we know that the relations in Eq. (3.79) that hold at $M_{\rm GUT}$ are one of the main features of this framework. In order to check whether these relations are followed throughout the running, we shall use the following ratios:

$$\frac{\lambda_{13}^{(3)}}{\lambda_{23}^{(3)}} = \frac{\kappa^*}{c_d}\,, \qquad\qquad \frac{\lambda_{12}^{(3)}}{|\lambda_{13}^{(3)}|^2} = \frac{c_d}{\kappa}\,, \tag{3.80}$$

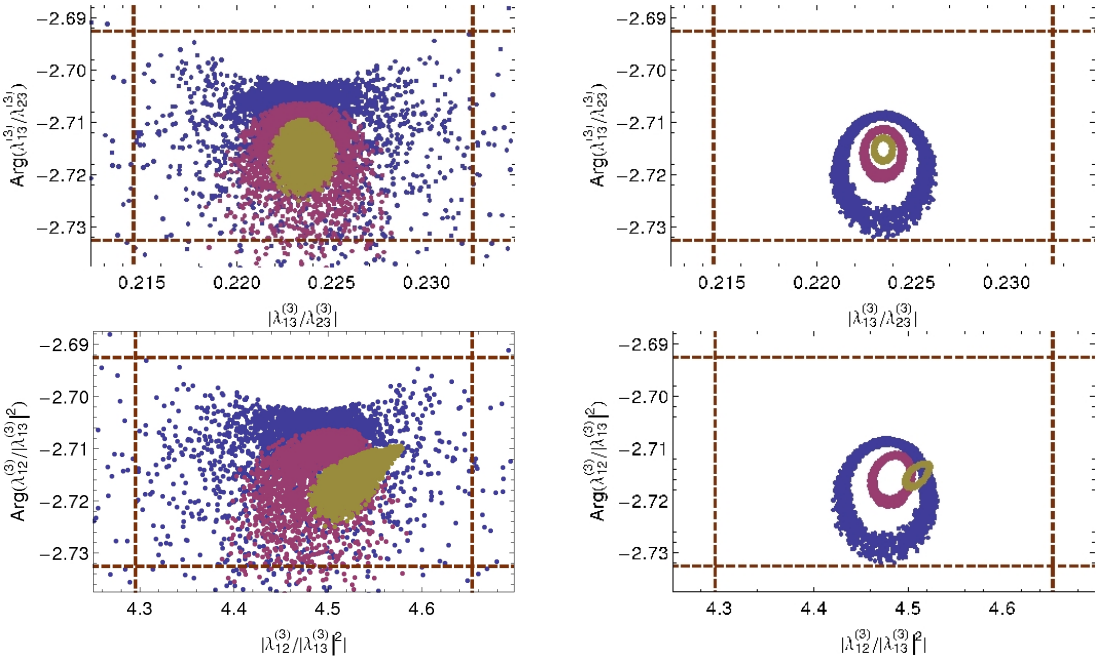

Figure 3.13: The two ratios used in order to test $U(2)^3$, evaluated at $M_{\rm SUSY}$. We show Benchmark 1 (Benchmark 2) on the left (right). The dashed lines correspond to our estimated theoretical uncertainty. We show results for $x_L = 2$, 1, 0.5 in brown, magenta and blue, respectively.

which should remain valid for any value of the scale. The first ratio tests the correlations between the B_d and B_s sectors, while the second ratio tests those between the K and B_d sectors. Thus, if we find these ratios to hold within their theoretical errors, we shall consider the $U(2)^3$ symmetry to be preserved by the running.

We need to derive an approximate theoretical error for each ratio. For the absolute value of both ratios, we have found they are held within NLO corrections dependent on the value of ρ, which can lead to an error of at most 4%. For the phase, we find a fixed correction of the order of $\varphi_c = \arg(c_u c_d + s_u s_d e^{-i\phi}) \approx 0.02$. These considerations lead us to the following requirements in order to keep the $U(2)^3$ symmetry:

$$\left|\frac{\lambda_{13}^{(3)}}{\lambda_{23}^{(3)}}\right| = \left|\frac{V_{td}}{V_{ts}}\right| (1 \pm 0.04)\ , \qquad \arg\left(\frac{\lambda_{13}^{(3)}}{\lambda_{23}^{(3)}}\right) = -\arg\left(\frac{V_{td}}{V_{ts}} e^{i\varphi_c}\right) \pm 0.02\ , \tag{3.81}$$

$$\left|\frac{\lambda_{12}^{(3)}}{|\lambda_{13}^{(3)}|^2}\right| = \left|\frac{V_{ts}}{V_{td}}\right| (1 \pm 0.04)\ , \qquad \arg\left(\frac{\lambda_{12}^{(3)}}{|\lambda_{13}^{(3)}|^2}\right) = -\arg\left(\frac{V_{td}}{V_{ts}} e^{i\varphi_c}\right) \pm 0.02\ . \tag{3.82}$$

We present our results in Figure 3.13. The left (right) column shows our results for Benchmark 1 (Benchmark 2), and the top (bottom) row shows the modulus and the phase of the $\lambda_{13}^{(3)}/\lambda_{23}^{(3)}$ ($\lambda_{12}^{(3)}/|\lambda_{13}^{(3)}|^2$) ratio. We show in brown, magenta and blue the value of each ratio at $M_{\rm SUSY}$, fixing $x_L = 2$, 1 and 0.5, respectively. The main conclusion

from all plots is that the RGE variation keeps the ratios within our estimated theoretical uncertainties, so we can expect the $U(2)^3$ symmetry correlations to be preserved at all scales. Furthermore, we expect the correlations to be better maintained the larger the value of x_L, which is compatible with the requirement of a large x_L needed to solve the flavor tension.

The distribution of points in Figure 3.13 deserves an explanation, in particular for Benchmark 2, which shows a ring-like pattern. In this case, we find the pattern to be due to fixed RGE contributions, coming from the irreducible MFV terms and off-diagonal soft terms, which are of the same order. Here, the only significant variable is the effective phase between the two contributions, which is identical in all sectors, and shapes the rings. In contrast, in Benchmark 1, we have an additional contribution from the RGEs coming from the A-Terms, which are larger than in Benchmark 2. This additional contribution involves new varying $O(1)$ parameters and new phases, which spoil the ring-like pattern.

3.3.4 Evaluation of operators leading to $\Delta F = 2$ Processes

As mentioned previously, in $U(2)^3$ supersymmetric frameworks, the main deviations from MFV happen within $m^2_{\tilde{Q}}$. This suggests that the main contribution to $\Delta F = 2$ processes should come from $(LL)^2$ operators, as other contributions would be strongly suppressed, usually by the masses of the first or second generation quarks.

In this Section, we compare the value of the different operators contributing to $\Delta F = 2$ processes after the RGE evolution, in order to make sure this is the case. We shall use the following basis for the effective operators:

$$H^F_{\text{eff}} = \sum_{i=1..5} C^F_i \, Q^F_i + \sum_{i=1..3} \tilde{C}^F_i \, \tilde{Q}^F_i \ , \tag{3.83}$$

where $F = K$, B_d, B_s and:

$$Q^F_1 = (\bar{q}^\alpha_L \gamma_\mu q'^\alpha_L)(\bar{q}^\beta_L \gamma^\mu q'^\beta_L) \ , \tag{3.84}$$

$$Q^F_2 = (\bar{q}^\alpha_R \, q'^\alpha_L)(\bar{q}^\beta_R \, q'^\beta_L) \ , \qquad Q^F_3 = (\bar{q}^\alpha_R \, q'^\beta_L)(\bar{q}^\beta_R \, q'^\alpha_L) \ , \tag{3.85}$$

$$Q^F_4 = (\bar{q}^\alpha_R \, q'^\alpha_L)(\bar{q}^\beta_L \, q'^\beta_R) \ , \qquad Q^F_5 = (\bar{q}^\alpha_R \, q'^\beta_L)(\bar{q}^\beta_L \, q'^\alpha_R) \ . \tag{3.86}$$

Here, the quarks q, q' depend on the meson F. The $\tilde{Q}^F_i$ coefficients are equal to those without a tilde, with the exchange $L \leftrightarrow R$.

The Wilson coefficients C^F_i, $\tilde{C}^F_i$ have been calculated in many works, either exactly [43, 97] or in the MIA [29, 98]. In the following, we shall calculate the coefficients from the exact expressions, but shall use the MIA to discuss our results. The $(LL)^2$ contribution corresponds to the C^F_1 coefficient. Similarly, the C^F_2 and C^F_3 coefficients correspond to the $(RL)^2$ contributions, while the C^F_4 and C^F_5 coefficients correspond to $(LL)(RR) + (LR)(RL)$ contributions. Again, these are related to $\tilde{C}^F_i$ by the exchange $L \leftrightarrow R$.

Given the vanishing value of the lower off-diagonal elements of A_d at the GUT scale, and the very small MFV contribution from the running, the $(RL)^2$ contributions are expected to be the smallest. Next in the line come the $(LR)^2$ contributions, which, although

involving non-negligible upper off-diagonal elements of A_d, also include an additional suppression proportional to m_b^2/m_{heavy}^2. This shall compete with the m_q^2/m_b^2 suppression commonly found in the $(RR)^2$ contribution, where m_q can be either the first or second generation quark mass, depending on sector involved. Finally, the $(LL)(RR)$ contribution should be the largest after the $(LL)^2$, given the relatively small suppression of the (LL) insertion. Thus, from the mixing point of view, we would expect:

$$C_2^F \sim C_3^F \ll \tilde{C}_1^F \sim \tilde{C}_2^F \sim \tilde{C}_3^F \ll C_4^F \sim C_5^F \ll C_1^F \ . \tag{3.87}$$

The results are very similar to our expectations, and are shown in Figure 3.14. Here, we show the C_i^F/C_1^F and $\tilde{C}_i^F/C_1^F$ ratios, for all possible coefficients, in the K, B_d and B_s sectors. The coefficients are calculated at $M_{\rm SUSY}$, and for transparency are not evolved to the respective meson scale. We find the hierarchies between Benchmark 1 and 2 are identical, with a smaller spread for $\tilde{C}_2^F$ and $\tilde{C}_3^F$ in Benchmark 2, due to the additional suppression in $A_0 = 0.25\, m_{heavy}$.

In the Figure, the shadowed regions indicate values where the ratios exceed 10%, meaning they should not be neglected.* Surprisingly enough, we find that in the B_s sector the C_4 coefficient can be well within this region, and can actually become as much as ten times larger than C_1, especially in Benchmark 2. This might spoil the correlation between CP violation in the B_d and B_s sectors and, more importantly, break the invariance of $\Delta M_d/\Delta M_s$ with respect to the Standard Model values.

We have found this unexpected behavior to be due to the small value of the loop functions for both Benchmarks, which can balance the suppression in the RR mixing. This can be better understood by demanding the loop function in C_1 to include an additional suppression of the $O(m_s/m_b)$ with respect to the loop function for the dominant $(LL)(RR)$ contribution in C_4. This gives:

$$\left|24x\, f_6(x) + 66\tilde{f}_6(x)\right| < (m_s/m_b)\left|504x\, f_6(x) - 72\tilde{f}_6(x)\right| \tag{3.88}$$

where $x = m_{\tilde{g}}^2/m_{\tilde{b}_L}^2$, and the loop functions $f_6(x)$ and $\tilde{f}_6(x)$ can be found, for instance, in [29]†. The region giving such a suppression is shown in Figure 3.15, where we can see that Benchmark 2 lies within it, while Benchmark 1 lies very close.

One finds that this small value in the loop function is actually due to the stringent bounds of the LHC on the gluino mass. In fact, in order to avoid the suppression, and have $C_4 < 0.1\, C_1$, one needs:

$$m_{\tilde{b}_L} > 3.2\ m_{\tilde{g}}\,, \tag{3.89}$$

apart from $O(1)$ coefficients. Considering the LHC limit of $m_{\tilde{g}} \gtrsim 1$ TeV, this bound is incompatible with a split scenario in which the third generation is relatively light. In

*In the K-system even smaller ratios should be relevant due to possible chiral enhancements, but in any case we never obtain such values.

†In the mass-insertion approximation, one should actually use $x = m_{\tilde{g}}^2/\langle m_{\tilde{d}}^2\rangle$, where $\langle m_{\tilde{d}}^2\rangle$ is the average down squark mass [100]. Nevertheless, in a split scenario this does not always give an accurate result.

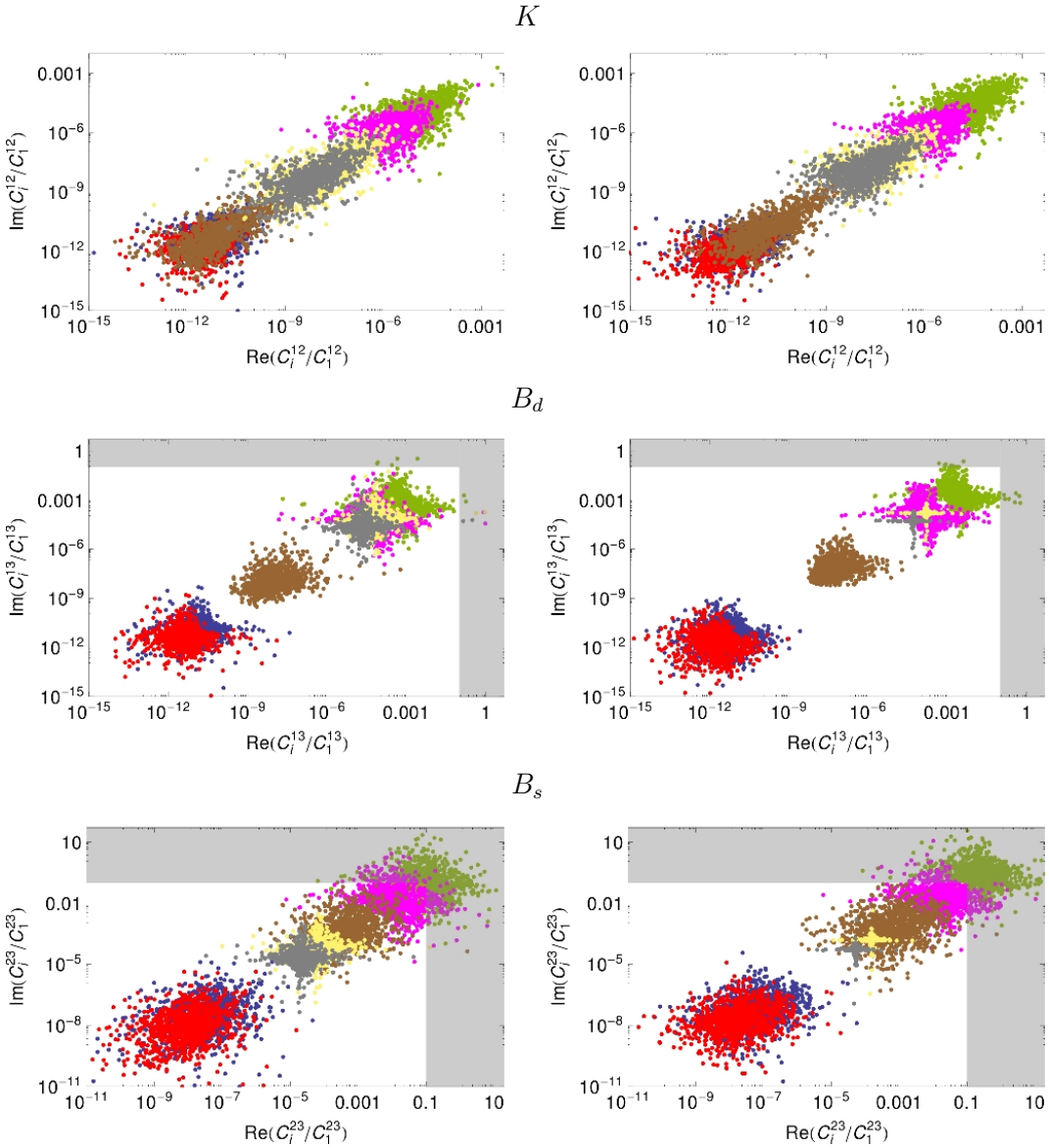

Figure 3.14: Ratios between C_i^F, $\tilde{C}_i^F$ and C_1^F coefficients. We show the ratios for the K, B_d and B_s sectors in the top, center and bottom panels, respectively. Benchmark 1 (2) is shown on the left (right) column. The C_i^F/C_1^F ratios are shown in blue, red, green and magenta, for $i = 2 \ldots 5$. The $\tilde{C}_i^F/C_1^F$ ratios are shown in brown, yellow and gray for $i = 1 \ldots 3$. The shadowed regions mark the areas where the ratios are larger than 10%.

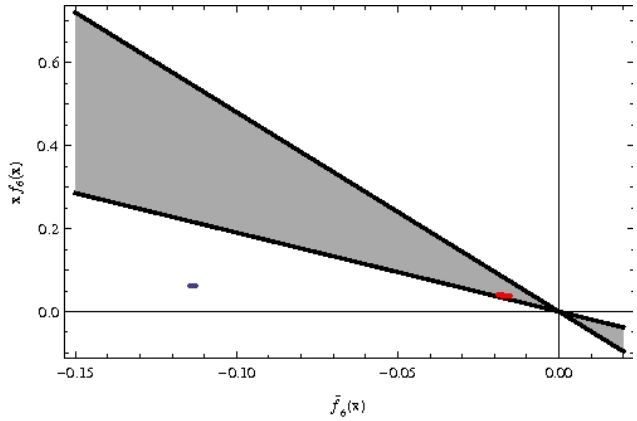

Figure 3.15: Region where loop functions provide an additional suppression of $O(m_s/m_b)$ on the $(LL)^2$ operator. Typical values of Benchmark 1 (2) are shown with the blue (red) dots.

Benchmark 2, the gluinos are heavier than in Benchmark 1, while the the sbottom are always around 2 TeV. Thus, the enhancement in C_4/C_1 is usually stronger.

However, we have checked that the regions where the $(LL)(RR)$ operators dominate are those where the $O(1)$s of the $(LL)^2$ are small. In these cases, the contributions to flavor shall always be negligible, meaning that, if this framework can solve the flavor problem, the $(LL)(RR)$ operators shall contribute at about 10% of the total SUSY contribution.

3.3.5 $U(2)^3$ as a broken subgroup of $U(3)^3$

In Ref. [1] (see also Sec. 3.2) an extension of this framework for the lepton sector has been presented. It was found that, in order to reproduce the neutrino oscillation data, it was necessary to enlarge the symmetry to $U(3)^5$, i.e. to restore MFV. A two-step breaking would then be carried out. In the first step, we would have a breaking in two directions: one preserving $O(3)_L$ in the neutrino sector, and another one preserving $U(2)^5$ in the Yukawa sector. This would be followed by a sub-leading hierarchical breaking of $U(2)^5$, leading to the Yukawa matrices studied in this paper. At the same time, this sub-leading breaking would be connected to the neutrino sector, reproducing the observed neutrino oscillation parameters.

In this case, to introduce the $U(2)_L$ doublet, the embedding in $U(3)^5$ would force the use of a spurion transforming as an **8** of $U(3)_L$. In $U(2)^5$ language, this would have the effect of having, in addition to the usual $U(2)_L$ doublet, a new spurion Δ_L, transforming with the adjoint of $U(2)_L$. Both spurions would be contained in the same representation of $U(3)_L$.

Following this breaking, we study the effects of the corresponding spurion Δ_Q, transforming as a **3** of $U(2)_Q$, in the quark sector. This modification does not alter the Yukawa structure, and affects only the $(1-2)$ block of $m^2_{\tilde{Q}}$. In particular, Eq. (3.10) is modified

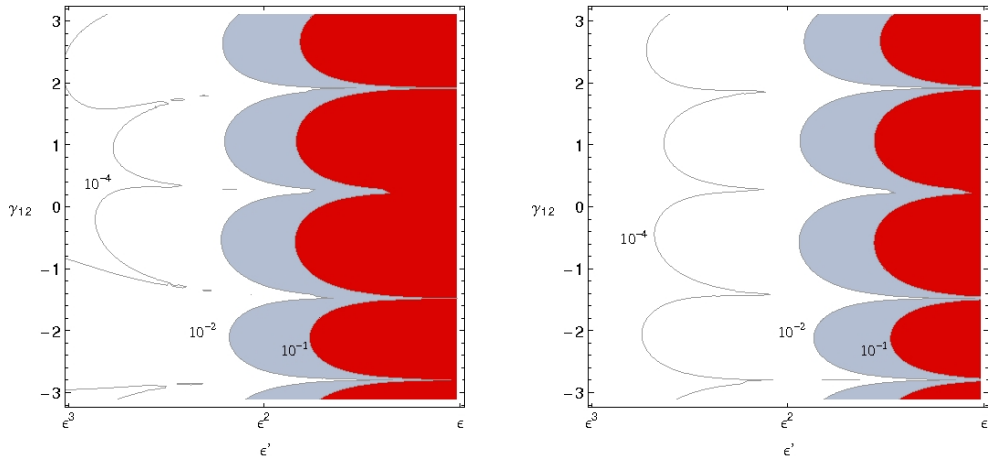

Figure 3.16: The effects of the Δ_Q spurion on K physics in Benchmark 1 (on the left) and 2 (on the right). We show the ratios $(\epsilon_K)_{12}/\epsilon_K^{exp}$ as a function of the Δ_Q elements, following Eq. (3.91). We show in red (gray) the region where $(\epsilon_K)_{12} > 0.1\,\epsilon_K^{exp}$ ($(\epsilon_K)_{12} > 0.01\,\epsilon_K^{exp}$).

to

$$m_{\tilde{Q}}^2 = \left(\begin{array}{c|c} I + c_Q\,\Delta_Q + c_{Qv}\,V^*V^T + c_{Qu}\Delta Y_u^*\Delta Y_u^T + c_{Qd}\Delta Y_d^*\Delta Y_d^T & x_Q\,e^{-i\phi_Q}V^* \\ \hline x_Q\,e^{i\phi_Q}V^T & m_{Q_l}^2/m_{Q_h}^2 \end{array}\right) m_{Q_h}^2\ . \tag{3.90}$$

Note that, even without considering the leptonic case, it is of general interest to study if other non-minimal breakings of $U(2)^3$ can be compatible with low-energy data. In this case, the addition of the new spurion affects only the soft sector, and would be a further deviation from MFV with new physics effects in the K sector. This is particularly relevant if the first two generations of squarks are not too heavy.

The most important constraints in K sector come from ϵ_K and ΔM_K, which can get an additional contribution from gluino-mediated processes involving only the first two generation squarks. This contribution is negligible in the minimal $U(2)^3$ breaking, since the 1-2 mixing has got a strong MFV suppression. On the contrary it can be sizable with the Δ_Q spurion, for example in Benchmark 1, where $m_{heavy} \simeq 3$ TeV. In the following, we shall refer to the SUSY contribution to ϵ_K coming exclusively from the Δ_Q spurion as $(\epsilon_K)_{12}$.*

For simplicity we first assume that all the elements of Δ_Q are of the same size

$$\Delta_Q = \epsilon' \begin{pmatrix} 1 & e^{i\gamma_{12}} \\ e^{-i\gamma_{12}} & 1 \end{pmatrix}\ , \tag{3.91}$$

neglecting the contributions of the other spurions to the $(1-2)$ block.

*For a detailed analysis of the full contribution to ϵ_K in natural SUSY, see [99].

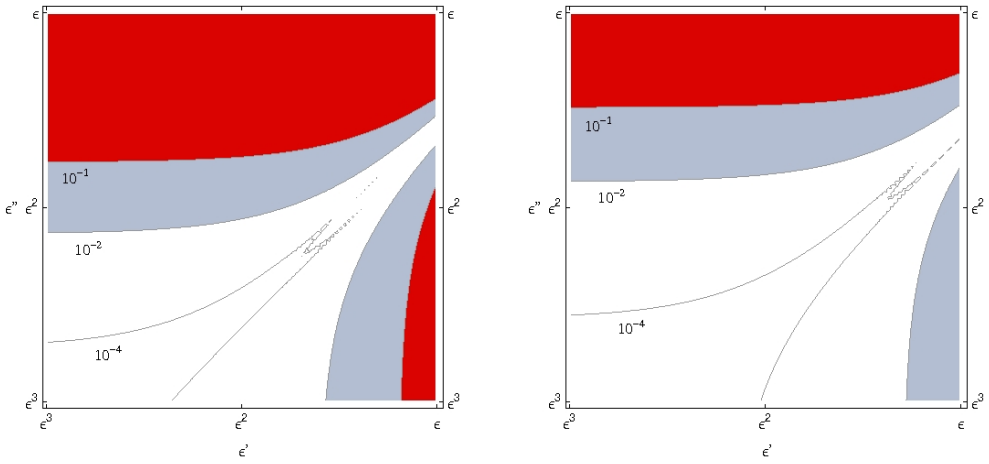

Figure 3.17: The effects of the Δ_Q spurion on K physics in Benchmark 1 (on the left) and 2 (on the right).We show the ratios $\epsilon_K/\epsilon_K^{exp}$ in function of the Δ_Q elements as explained in Eq. (3.92). In red the region where $\epsilon_K > 0.1\,\epsilon_K^{exp}$.

In Figure 3.16 we show the contours for the ratio of $(\epsilon_K)_{12}$ on the experimental values, as a function of ϵ' and γ_{12} in Benchmark 1 (on the left) and 2 (on the right). We show in red the region where the new contribution is bigger than 10% of the experimental value. This would mean that, given a similar error in the SM prediction [101], the new effect cannot be neglected. The gray regions, on the other hand, provide a contribution larger that 1%, and although not dangerous, could be important in the solution of the flavor tension. We do not show the contributions to ΔM_K, which are always very small and provide no constraint.

The main result is that, if we want the new contributions to be smaller than 1%, we need $\epsilon' \lesssim \epsilon^2$ (barring fine-tuning of the phase). As expected in the Benchmark 2, where the first two generations are heavier, Δ_Q can take somewhat larger values.

Another interesting case to consider is the one with the elements of Δ_Q being of different sizes. For example, we take the case:

$$\Delta_Q = \begin{pmatrix} 0 & \epsilon''\, e^{i\gamma_{12}} \\ \epsilon''\, e^{-i\gamma_{12}} & \epsilon' \end{pmatrix} , \tag{3.92}$$

which is precisely the form of the spurion introduced in [1] (see Eq. (3.45)). For simplicity, we fix the phase $\gamma_{12} = \pi/4$ and again show the ratio of $(\epsilon_K)_{12}$ over ϵ_K^{exp} as a function of ϵ' and ϵ'' in Figure 3.17. As expected, the ratio is very small when both ϵ' and ϵ'' are small, and increases accordingly with them. The impact of ϵ' on $(\epsilon_K)_{12}$ is much smaller, as it enters with an additional suppression proportional to s_d. For Benchmark 1, $\epsilon'' \lesssim \epsilon^2$ and $\epsilon' \lesssim \epsilon/5$ ensure that the contribution to ϵ_K shall be lower than $\sim 1\%$, while for Benchmark 2 the bounds again are much milder. Notice, however, there exists a region where the ϵ'' contribution cancels the ϵ' contribution. This interference depends on the values of γ_{12}

and α_d. Moreover, we note that the RGEs effects on 1-2 sector are very weak, and the values of Δ_Q do not change significantly during the running.

3.3.6 Concluding remarks

We have studied the running behavior of a split-family SUSY framework based on a $U(2)^3$ family symmetry. As already mentioned, such a framework is motivated by the current lack of experimental evidence for SUSY at the early runs of the LHC, and by the existence of a small flavor tension between the K and B_d sectors. Nevertheless, it was not evident if the several low-scale analyses of this framework were valid if the symmetry was actually broken at a large scale.

In this work, we studied the $U(2)^3$ framework through a CMSSM-like parameter space, and understood the consequences on the low-energy spectrum. This was made clear through the use of two benchmark scenarios, the first one having the heavy squarks slightly beyond the current reach of the LHC, and the second one having them considerably heavier.

Theoretical consistency, along with the requirement of reproducing the Higgs mass and solving the flavor tension at the low scale, forced Benchmark 1 to have a very specific spectrum, with a very light stop and somewhat heavier sbottoms. Here, we found that the evolution of the mixing parameters was very mild, and required the relevant $O(1)$ constants to be slightly larger than unity in order to successfully solve the flavor tension. The correlations between the $(LL)^2$ SUSY contributions to K, B_d and B_s physics were found to be preserved, but it was found necessary to check explicitly the magnitude of the $(LL)(RR)$ contributions to B_s mixing, as it could easily become of the same order of the $(LL)^2$.

For heavier first generations masses, as in Benchmark 2, we found that in order to avoid tachyons while keeping at least one stop light, it was necessary to use large gluino masses. This spoils the solution of the flavor tension, unless considerably large $O(1)$ parameters were used in the mixing. Although this scenario preserved better the relations between the $(LL)^2$ SUSY contributions to $\Delta F = 2$ observables, we found the $(LL)(RR)$ contribution for B_s to be even larger than in the previous benchmark.

The main conclusion for $U(2)^3$ is that it does work as a flavor framework starting at a high scale, preserving most of its virtues without any critical assumptions. From the perspective of solving the flavor tension, this situation changes as the masses of the first two generations are pushed beyond 3 TeV, as the tachyon bound requires heavier gluinos, which in turn spoil the solution of the tension, and give the $(LL)(RR)$ operators further importance.

Finally, we also considered a deviation from minimal $U(2)^3$ breaking, motivated by the need to reproduce neutrino oscillation data. This deviation could induce large contributions to observables in the K sector, spoiling again the correlations. We found that, for both Benchmarks, as long as the deviation was kept of order $\sim \epsilon^2$, the new contributions could be generally considered negligible.

Chapter 4

Non-minimal Higgs sector

As anticipated in the Introduction the LHC experiments have claimed the discovery of a new particle compatible with the Higgs boson with mass of $m_h \simeq 125$ GeV [7,8]. However we are still far from being able to assert that it is exactly the SM Higgs. Indeed, many alternative scenarios of electroweak symmetry breaking are themselves compatible with the LHC signal at 125 GeV and a more accurate study of the Higgs properties is in order for discriminating among the various models. Fortunately 125 GeV is a very favorable mass region because it opens many decay channels ($\bar{b}b$, $\tau^+\tau^-$, $\gamma\gamma$, W^+W^-, ZZ and gg) to be measured at LHC and to be compared with the SM Higgs expectations [102–104].

In this Chapter we concentrate on the study of the phenomenology of models with a non-standard Higgs sector, on the flavor physics playground. In particular in Sec 4.1 we analyze possible Higgs mediated FCNC to be measured at LHC [3], while in Sec. 4.2 and 4.3 we concentrate on the study of the flavor phenomenology of the 2 Higgs Doublets Model (2HDM) in a generic case with MFV [4] and in supersymmetry [5], respectively.

4.1 Flavor-changing decays of a 125 GeV Higgs-like particle

The LHC phenomenology of a SM-like Higgs boson, with mass around 125 GeV, is characterized in the first place by six effective couplings: the couplings of h to $\bar{b}b$, $\tau^+\tau^-$, $\gamma\gamma$, W^+W^-, ZZ and gg. ATLAS and CMS are indeed searching for possible decays of any new neutral particle in these flavor-conserving final states (except for gg, whose coupling to h is accessible only through the production mechanism). Within the SM, flavor-changing decays of h are expected to be strongly suppressed and well beyond the LHC reach. However, there are alternatives to the SM Higgs interpretation of the 125 GeV hint, and in some of these cases relatively large flavor-changing couplings become a significant possibility. This is the case, for example, of the pseudo-dilaton Higgs boson look-alike discussed in [105], which is quite compatible with the hint observed by ATLAS and CMS. Flavor-changing decays of h are expected also in the case of a composite Higgs [106] in models where the Yukawa couplings are functions of the Higgs field [107] and in several

other extensions of the SM with more than one Higgs field (see, e.g., Ref. [108] and references therein). It is therefore important to explore the possible existence and the allowed magnitudes of flavor-changing couplings of a neutral 125 GeV scalar particle h, looking for possible deviations from SM predictions.

In this analysis we adopt a phenomenological bottom-up approach, studying the flavor-changing couplings of the hypothetical h particle allowed by low-energy data. Several previous studies of this type have been presented in the recent literature, see, e.g., [108–113]. However, a systematic analysis of both the quark and lepton sectors and their implications for the h decays was still missing. As we will show, the available experimental constraints on FCNC interactions provide strong bounds on many possible quark- and lepton-flavor-changing couplings. However, there are instances where relatively large flavor-changing h couplings are still allowed by present data, cases in point being the $h\bar{\tau}\mu$ and $h\bar{\tau}e$ couplings (as already noticed in [112,113]). Specifically, we find that current experimental upper limits on lepton-flavor-violating processes allow the branching ratio $\mathcal{B}(h \to \tau\bar{\mu} + \bar{\mu}\tau) = \mathcal{O}(10\%)$, and that this can be obtained without particular tuning of the effective couplings. It is also possible that $\mathcal{B}(h \to \tau\bar{e} + \bar{e}\tau) = \mathcal{O}(10\%)$, though this possibility could be realized only at the expense of some fine-tuning of the corresponding couplings and, if realized, would forbid a large $\mathcal{B}(h \to \tau\bar{\mu} + \bar{\mu}\tau)$. The bound on the μe modes are substantially stronger, implying $\mathcal{B}(h \to \bar{\mu}e + \bar{e}\mu) = O(10^{-9})$ in the absence of fine-tuned cancellations.

We note that CMS currently reports a 68% CL range of $0.8^{+1.2}_{-1.3}$ for a possible $h \to \tau^+\tau^-$ signal relative to its SM value [114], and that in the SM $\mathcal{B}(h \to \tau^+\tau^-) \sim 6.5\%$ for an Higgs boson weighing 125 GeV. It therefore seems that dedicated searches in the LHC experiments might already be able to explore flavor-changing leptonic beyond the limits imposed by searches for lepton-flavor-violating processes.

On the other hand, the indirect upper bounds on possible quark-flavor-violating couplings of a scalar with mass 125 GeV are much stronger, and the detection of hadronic flavor-changing decays are much more challenging, so these offer poorer prospects for direct detection at the LHC.

4.1.1 Effective Lagrangian

We employ here a strictly phenomenological approach, considering the following effective Lagrangian to describe the possible flavor-changing couplings of a possible neutral scalar boson h to SM quarks and leptons:

$$\mathcal{L}_{\text{eff}} = \sum_{i,j=d,s,b \ (i\neq j)} c_{ij}\ \bar{d}^i_L d^j_R h + \sum_{i,j=u,c,t \ (i\neq j)} c_{ij}\ \bar{u}^i_L u^j_R h + \sum_{i,j=e,\mu,\tau \ (i\neq j)} c_{ij}\ \bar{\ell}^i_L \ell^j_R h + \text{h.c.} \qquad (4.1)$$

The field h can be identified with the physical Higgs boson of the SM or, more generally, with a mass eigenstate resulting from the mixing of other scalar fields present in the underlying theory with the SM Higgs (if it exists). Therefore, the operators in (4.1) are not necessarily $SU(2)_L \times U(1)_Y$ invariant. However, they may be regarded as resulting

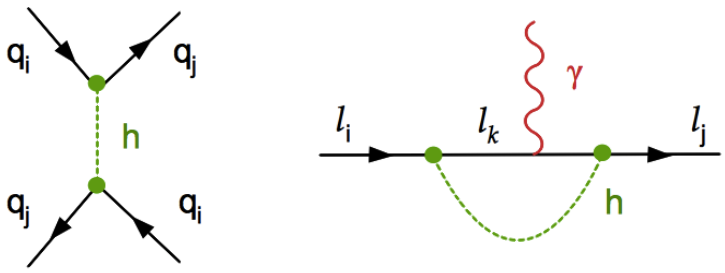

Figure 4.1: Left: Tree-level diagram contributing to $\Delta F = 2$ amplitudes. Right: One-loop diagram contributing to anomalous magnetic moments and electric dipole moments of charged leptons ($i = j$), or radiative LFV decay modes ($i \neq j$).

from higher-order $SU(2)_L \times U(1)_Y$-invariant operators after the spontaneous breaking of $SU(2)_L \times U(1)_Y$.

By construction, the effective couplings described by (4.1) are momentum-independent. In principle, higher-order operators with derivative couplings could also appear, leading to momentum-dependent terms, or effective form factors for the flavor-changing vertices. We assume here that any such effects are subleading, though it is clear that direct observation of h decays would, in general, provide much more stringent constraints on such momentum dependence than could be provided by the indirect low-energy constraints considered below.

4.1.2 Bounds in the quark sector

Operator	Eff. couplings	95% C.L. Bound		Observables
		$\lvert c_{\text{eff}}\rvert$	$\lvert\text{Im}(c_{\text{eff}})\rvert$	
$(\bar{s}_R\, d_L)(\bar{s}_L d_R)$	$c_{sd}\ c_{ds}^*$	1.1×10^{-10}	4.1×10^{-13}	Δm_K; ϵ_K
$(\bar{s}_R\, d_L)^2,\ (\bar{s}_L d_R)^2$	$c_{ds}^2,\ c_{sd}^2$	2.2×10^{-10}	0.8×10^{-12}	
$(\bar{c}_R\, u_L)(\bar{c}_L u_R)$	$c_{cu}\ c_{uc}^*$	0.9×10^{-9}	1.7×10^{-10}	Δm_D; $\lvert q/p\rvert, \phi_D$
$(\bar{c}_R\, u_L)^2,\ (\bar{c}_L u_R)^2$	$c_{uc}^2,\ c_{cu}^2$	1.4×10^{-9}	2.5×10^{-10}	
$(\bar{b}_R\, d_L)(\bar{b}_L d_R)$	$c_{bd}\ c_{db}^*$	0.9×10^{-8}	2.7×10^{-9}	Δm_{B_d}; $S_{B_d \to \psi K}$
$(\bar{b}_R\, d_L)^2,\ (\bar{b}_L d_R)^2$	$c_{db}^2,\ c_{bd}^2$	1.0×10^{-8}	3.0×10^{-9}	
$(\bar{b}_R\, s_L)(\bar{b}_L s_R)$	$c_{bs}\ c_{sb}^*$	2.0×10^{-7}	2.0×10^{-7}	Δm_{B_s}
$(\bar{b}_R\, s_L)^2,\ (\bar{b}_L s_R)^2$	$c_{sb}^2,\ c_{bs}^2$	2.2×10^{-7}	2.2×10^{-7}	

Table 4.1: Bounds on combinations of the flavor-changing h couplings defined in (4.1) obtained from $\Delta F = 2$ processes [28], assuming that $m_h = 125$ GeV.

In the quark sector, strong bounds on all the effective couplings in (4.1) involving light quarks (i.e., excluding the top) can be derived from the tree-level contributions to meson-

Eff. couplings	Bound	Constraint
$\lvert c_{sb}\rvert^2,\ \lvert c_{bs}\rvert^2$	2.9×10^{-5} [*]	$\mathcal{B}(B_s \to \mu^+\mu^-) < 1.4 \times 10^{-8}$
$\lvert c_{db}\rvert^2,\ \lvert c_{bd}\rvert^2$	1.3×10^{-5} [*]	$\mathcal{B}(B_d \to \mu^+\mu^-) < 3.2 \times 10^{-9}$

Table 4.2: Bounds on combinations of the flavor-changing h couplings defined in (4.1) obtained from experimental constraints on rare B decays [115], assuming that $m_h = 125$ GeV. (Here and in subsequent Tables, the [*] denotes bounds obtained under the assumption that the flavor-diagonal couplings of h are the same as the corresponding SM Yukawa couplings.)

antimeson mixing induced by diagrams of the type shown in the left panel of Fig. 4.1. Using the bounds on dimension-six $\Delta F = 2$ operators reported in [28], we derive the indirect limits on different combinations of c_{ij} couplings reported in Table 4.1. As we discuss in Sec. 4.1.3, these bounds forbid any flavor-changing decay of the h into a pair of quarks with a branching ratio exceeding 10^{-3}.

The $\Delta F = 1$ bounds on the c_{ij} also prevent sizable Higgs-mediated contributions in $\Delta F = 1$ amplitudes, *if* the flavor-diagonal couplings of the h are the same as the SM Yukawa couplings. In Table 4.2 we report the bounds on the c_{ij} couplings obtained from $B_{s,d} \to \mu^+\mu^-$ obtained under this assumption, namely setting $c_{\mu\mu} = \sqrt{2}m_\mu/v$ with $v \approx 246$ GeV [*]. As can be seen, these $\Delta F = 1$ bounds are weaker than those in Table 4.1. This would not be true if the flavor-diagonal couplings of h were enhanced with respect to the SM Yukawa couplings, or if there were some extra contribution cancelling h-exchange in the $\Delta F = 2$ amplitudes. The latter happens, for instance, in some two-Higgs doublet models, because of the destructive interference of scalar and pseudo-scalar exchange amplitudes: see, e.g., [108, 116].

4.1.3 Bounds in the lepton sector

In the lepton sector we do not have an analogous of the $\Delta F = 2$ constraints, leaving more room for sizeable non-standard contributions.

We start by analyzing the tree-level contributions of h to the lepton-flavor violating decays of charged leptons and $\mu \to e$ conversion in nuclei. In most cases bounds on the effective couplings in (4.1) can be derived only with an Ansatz about the flavor-diagonal couplings. Here we assume again that the flavor-diagonal couplings are the SM Yukawas,

$$c_{\ell\ell} = y_\ell \equiv \frac{\sqrt{2}m_\ell}{v} \ . \tag{4.2}$$

This leads to the bounds reported in Table 4.3, where we have used the limits of the corresponding dimension-six operators reported in [117], updating the results on various τ

[*] This assumption is not true in general. For example, in the pseudo-dilaton scenario of [105] the flavor-diagonal h couplings are in general suppressed by a universal factor $c < 1$, in which case the bounds in Table 4.2 would be weakened by a factor $1/c > 1$.

Operator	Eff. couplings	Bound	Constraint
$(\bar{\mu}_R\, e_L)(\bar{q}_L q_R),\ \ (\bar{\mu}_L\, e_R)(\bar{q}_L q_R)$	$\lvert c_{\mu e}\rvert^2,\ \ \lvert c_{e\mu}\rvert^2$	3.0×10^{-8} [*]	$\mathcal{B}_{\mu\to e}(\mathrm{Ti}) < 4.3 \times 10^{-12}$
$(\bar{\tau}_R\, \mu_L)(\bar{\mu}_L \mu_R),\ \ (\bar{\tau}_L\, \mu_R)(\bar{\mu}_L \mu_R)$	$\lvert c_{\tau\mu}\rvert^2,\ \ \lvert c_{\mu\tau}\rvert^2$	2.0×10^{-1} [*]	$\Gamma(\tau \to \mu\bar{\mu}\mu) < 2.1 \times 10^{-8}$
$(\bar{\tau}_R\, e_L)(\bar{\mu}_L \mu_R),\ \ (\bar{\tau}_L\, e_R)(\bar{\mu}_L \mu_R)$	$\lvert c_{\tau e}\rvert^2,\ \ \lvert c_{e\tau}\rvert^2$	4.8×10^{-1} [*]	$\Gamma(\tau \to e\bar{\mu}\mu) < 2.7 \times 10^{-8}$
$(\bar{\tau}_R\, e_L)(\bar{\mu}_L e_R),\ \ (\bar{\tau}_L\, e_R)(\bar{\mu}_L e_R)$	$\lvert c_{\mu e} c^*_{e\tau}\rvert,\ \ \lvert c_{\mu e} c_{\tau e}\rvert$	0.9×10^{-4}	$\Gamma(\tau \to \bar{\mu}ee) < 1.5 \times 10^{-8}$
$(\bar{\tau}_R\, e_L)(\bar{\mu}_R e_L),\ \ (\bar{\tau}_L\, e_R)(\bar{\mu}_R e_L)$	$\lvert c^*_{e\mu} c^*_{e\tau}\rvert,\ \ \lvert c^*_{e\mu} c_{\tau e}\rvert$		
$(\bar{\tau}_R\, \mu_L)(\bar{e}_L \mu_R),\ \ (\bar{\tau}_L\, \mu_R)(\bar{e}_L \mu_R)$	$\lvert c_{e\mu} c^*_{\mu\tau}\rvert,\ \ \lvert c_{e\mu} c_{\tau\mu}\rvert$	1.0×10^{-4}	$\Gamma(\tau \to \bar{e}\mu\mu) < 1.7 \times 10^{-8}$
$(\bar{\tau}_R\, \mu_L)(\bar{e}_R \mu_L),\ \ (\bar{\tau}_L\, \mu_R)(\bar{e}_R \mu_L)$	$\lvert c^*_{\mu e} c^*_{\mu\tau}\rvert,\ \ \lvert c^*_{\mu e} c_{\tau\mu}\rvert$		

Table 4.3: Bounds on combinations of the flavor-changing h couplings defined in (4.1) obtained from charged-lepton-flavor-violating decays, assuming that $m_h = 125$ GeV.

decay modes from Ref. [22]. As can be seen, all the bounds except that derived from $\mu \to e$ conversion* are quite weak.† Note in particular that if we impose $c_{\mu e}, c_{e\mu} < y_\mu \approx 6 \times 10^{-4}$ we have essentially no bounds on the flavor-violating couplings involving the τ lepton. Note also that we cannot profit from the strong experimental bound on $\Gamma(\mu \to e\bar{e}e)$, since the corresponding amplitude is strongly suppressed by the electron Yukawa coupling.

Next we proceed to analyze one-loop-induced amplitudes. At the one loop level the flavor-violating couplings in (4.1) induce: (i) logarithmically-divergent corrections to the lepton masses; (ii) finite contributions to the anomalous magnetic moments and the electric-dipole moments of charged leptons; and (iii) finite contributions to radiative LFV decays of the type $l_i \to l_j \gamma$ (see the right panel of Fig. 4.1).

As far as the mass corrections are concerned, in the leading-logarithmic approximation we find‡

$$\delta m_\ell = \frac{1}{(4\pi)^2} \sum_{j \neq \ell} c_{\ell j} c_{j\ell} m_j \log\left(\frac{m_h^2}{\Lambda^2}\right) \ . \tag{4.3}$$

In absence of fine-tuning we expect $|\delta m_\ell| < m_\ell$ for each of the two possible contributions in the sum. The most significant bounds thus derived, setting $\Lambda = 1$ TeV, are reported in Table 4.4. Note that in this case no assumption on the flavor-diagonal couplings is needed.

More stringent (and more physical) bounds on the same combinations of couplings are derived from the contributions to the anomalous magnetic moments, $a_\ell = (g_\ell - 2)/2$ and

* The bound from $\mu \to e$ conversion has been derived following the recent analysis of Ref. [118]: the dominant constraint follows from $\mathcal{B}_{\mu\to e}(\mathrm{Ti})$ and, in order to derive a conservative bound, we have set $y = 2\langle N|\bar{s}s|N\rangle / \langle N|\bar{d}d + \bar{u}u|N\rangle = 0.03$.

† As commented previously, in the scenario of Ref. [105] the flavor-diagonal h couplings are in general suppressed by a universal factor $c < 1$, in which case the first three bounds in Table 4.3 would be weakened by a factor $1/c > 1$.

‡ The complex mass correction δm_ℓ is defined by $m_\ell \bar{\ell}\ell \longrightarrow \bar{\ell}\,[m_\ell + \mathrm{Re}(\delta m_\ell) + i\mathrm{Im}(\delta m_\ell)\gamma_5]\,\ell$.

Eff. couplings	Bound	Constraint
$\lvert c_{e\tau}c_{\tau e}\rvert \quad (\lvert c_{e\mu}c_{\mu e}\rvert)$	$1.1\times10^{-2} \quad (1.8\times10^{-1})$	$\lvert\delta m_e\rvert < m_e$
$\lvert\mathrm{Re}(c_{e\tau}c_{\tau e})\rvert \quad (\lvert\mathrm{Re}(c_{e\mu}c_{\mu e})\rvert)$	$0.6\times10^{-3} \quad (0.6\times10^{-2})$	$\lvert\delta a_e\rvert < 6\times10^{-12}$
$\lvert\mathrm{Im}(c_{e\tau}c_{\tau e})\rvert \quad (\lvert\mathrm{Im}(c_{e\mu}c_{\mu e})\rvert)$	$0.8\times10^{-8} \quad (0.8\times10^{-7})$	$\lvert d_e\rvert < 1.6\times10^{-27}\ e$cm
$\lvert c_{\mu\tau}c_{\tau\mu}\rvert$	2	$\lvert\delta m_\mu\rvert < m_\mu$
$\lvert\mathrm{Re}(c_{\mu\tau}c_{\tau\mu})\rvert$	2×10^{-3}	$\lvert\delta a_\mu\rvert < 4\times10^{-9}$
$\lvert\mathrm{Im}(c_{\mu\tau}c_{\tau\mu})\rvert$	0.6	$\lvert d_\mu\rvert < 1.2\times10^{-19}\ e$cm
$\lvert c_{e\tau}c_{\tau\mu}\rvert,\ \lvert c_{\tau e}c_{\mu\tau}\rvert$	1.7×10^{-7}	$\mathcal{B}(\mu\to e\gamma) < 2.4\times10^{-12}$
$\lvert c_{\mu\tau}\rvert^2,\ \lvert c_{\tau\mu}\rvert^2$	0.9×10^{-2} [*]	$\mathcal{B}(\tau\to\mu\gamma) < 4.4\times10^{-8}$
$\lvert c_{e\tau}\rvert^2,\ \lvert c_{\tau e}\rvert^2$	0.6×10^{-2} [*]	$\mathcal{B}(\tau\to e\gamma) < 3.3\times10^{-8}$

Table 4.4: Bounds on combinations of the flavor-changing h couplings defined in (4.1) obtained from the naturalness requirement $|\delta m_\ell| < m_\ell$ (assuming $\Lambda = 1$ TeV), from the contributions to a_ℓ and d_ℓ ($\ell = e, \mu$), and from radiative LFV decays (in all cases we set $m_h = 125$ GeV.

the EDMs of the electron and the muon. The corresponding one-loop amplitudes are

$$|\delta a_\ell| = \frac{4m_\ell^2}{m_h^2}\frac{1}{(4\pi)^2}\sum_{j\neq\ell}\mathrm{Re}(c_{\ell j}c_{j\ell})\frac{m_j}{m_\ell}\left(\log\frac{m_h^2}{m_\tau^2}-\frac{3}{2}\right)\ , \tag{4.4}$$

$$|d_\ell| = \frac{2m_\ell}{m_h^2}\frac{e}{(4\pi)^2}\sum_{j\neq\ell}\mathrm{Im}(c_{\ell j}c_{j\ell})\frac{m_j}{m_\ell}\left(\log\frac{m_h^2}{m_\tau^2}-\frac{3}{2}\right)\ , \tag{4.5}$$

from which we derive the bounds reported in Table 4.4.[§] We do not report the corresponding bounds from a_τ and d_τ since they are much weaker. As can be seen, with the exception of the bound from the electron EDM, which can easily be evaded assuming real couplings, the bounds are still rather weak.

The radiative LFV decay rates generated at one loop level can be written as

$$\Gamma(l_i\to l_j\gamma) = m_i^3\frac{e^2}{16\pi}(|A_{ij}^L|^2+|A_{ij}^R|^2) \tag{4.6}$$

with coefficients

$$|A_{\mu e}^R| = \frac{1}{(4\pi)^2}|c_{e\tau}c_{\tau\mu}|\frac{m_\tau}{m_h^2}\left(\log\frac{m_h^2}{m_\tau^2}-\frac{3}{2}\right),\quad |A_{\mu e}^L| = \frac{1}{(4\pi)^2}|c_{\tau e}c_{\mu\tau}|\frac{m_\tau}{m_h^2}\left(\log\frac{m_h^2}{m_\tau^2}-\frac{3}{2}\right) \tag{4.7}$$

$$|A_{\tau\ell}^R| = \frac{1}{(4\pi)^2}|c_{\ell\tau}|y_\tau\frac{m_\tau}{m_h^2}\left(\log\frac{m_h^2}{m_\tau^2}-\frac{4}{3}\right),\quad |A_{\tau\ell}^L| = \frac{1}{(4\pi)^2}|c_{\tau\ell}|y_\tau\frac{m_\tau}{m_h^2}\left(\log\frac{m_h^2}{m_\tau^2}-\frac{4}{3}\right), \tag{4.8}$$

and corresponding bounds reported in Table 4.4. Here it should be noted the strong and model-independent bound from $\mu\to e\gamma$ [120] which prevents the $h\bar{\tau}\mu$ ($h\bar{\mu}\tau$) and $h\bar{\tau}e$ ($h\bar{e}\tau$) couplings to be both large at the same time.

[§] As usual, we define a_ℓ and d_ℓ in terms of the couplings of the corresponding dipole operators as follows: $(ea_\ell/4m_\ell)\bar{\ell}\sigma_{\mu\nu}\ell F^{\mu\nu}$, $i(d_\ell/2)\bar{\ell}\sigma_{\mu\nu}\gamma_5\ell F^{\mu\nu}$. The error on δa_e reported in Table 4.4 is the theoretical error in predicting $(g-2)_e$ using independent determinations of $\alpha_{\rm em}$ [119].

Eff. couplings	Bound	Constraint
$\lvert c_{e\mu}\rvert^2,\ \lvert c_{\mu e}\rvert^2$	1×10^{-11} [*]	$\mathcal{B}(\mu \to e\gamma) < 2.4 \times 10^{-12}$
$\lvert c_{\mu\tau}\rvert^2,\ \lvert c_{\tau\mu}\rvert^2$	5×10^{-4} [*]	$\mathcal{B}(\tau \to \mu\gamma) < 4.4 \times 10^{-8}$
$\lvert c_{e\tau}\rvert^2,\ \lvert c_{\tau e}\rvert^2$	3×10^{-4} [*]	$\mathcal{B}(\tau \to e\gamma) < 3.3 \times 10^{-8}$

Table 4.5: Bounds from two-loop Barr-Zee diagrams [121] contributing to LFV decays.

Finally we consider the bounds coming from two loop diagrams of Barr-Zee type [121], with a top-quark loop, whose relevance in constraining Higgs LFV couplings has been stressed recently in [112, 113]. Despite being suppressed by an extra $1/(16\pi^2)$ factor, these amplitudes are proportional to a single lepton Yukawa coupling and cannot be neglected. The resulting bounds, shown in Table 4.5, are obtained under the assumption that the coupling of h to the top quark is the same as in the SM ($c_{yy} = y_t \equiv \sqrt{2}m_t/v$). These bounds are consistent with those reported in Ref. [113].

4.1.4 Higgs decays

Normalizing the flavor-violating h decays to the $h \to \tau\bar{\tau}$ mode, which we assume to be SM-like, we can write

$$\frac{\mathcal{B}(h \to f_i \bar{f}_j)}{\mathcal{B}(h \to \tau\bar{\tau})} \approx N_f \times \frac{|c_{ij}|^2 + |c_{ji}|^2}{2y_\tau^2} = 0.48 \times 10^4 \times N_f \left(|c_{ij}|^2 + |c_{ji}|^2\right) \ , \tag{4.9}$$

where $N_q = 3$ and $N_\ell = 1$, and we have neglected tiny $m_{f_{i,j}}/m_h$ corrections. Assuming $\mathcal{B}(h \to \tau\bar{\tau}) \approx 6.5\%$, as expected for a SM Higgs boson with $m_h = 125$ GeV, we get

$$\mathcal{B}(h \to f_i \bar{f}_j) \approx 3.1 \times 10^2 \times N_f \left(|c_{ij}|^2 + |c_{ji}|^2\right) \ . \tag{4.10}$$

In the quark sector, in the most favourable case we get $\mathcal{B}(h \to b\bar{s},\ \bar{s}b) < 4 \times 10^{-4}$, which is beyond the reach of the LHC, also in view of the difficult experimental signature. However, the situation is much more favourable in the lepton sector. From the compilation of bounds in the previous Section we derive the following conclusions:

- $\mathcal{B}(h \to \tau\bar{\mu} + \bar{\mu}\tau) = \mathcal{O}(10\%)$ does not contradict any experimental bound and does not require off-diagonal couplings larger than the corresponding diagonal ones ($|c_{\mu\tau}|, |c_{\tau\mu}| \lesssim y_\tau$). It can be obtained even assuming $\mathcal{O}(1)$ CP-violating phases for the $c_{\mu\tau(\tau\mu)}$ couplings, provided $|c_{e\tau(\tau e)}/c_{\mu\tau(\tau\mu)}| < 10^{-2}$ in order to satisfy the $\mu \to e\gamma$ bound.

- $\mathcal{B}(h \to \tau\bar{e} + \bar{e}\tau)$ can also reach $\mathcal{O}(10\%)$ values, but only at the price of some tuning of the corresponding effective couplings. In particular, negligible CP-violating phases are needed in order to satisfy the tight constraint provided by the electron EDM shown in Tab. 4.4. Moreover, $|c_{\mu\tau(\tau\mu)}/c_{e\tau(\tau e)}| < 10^{-2}$ in order to satisfy the $\mu \to e\gamma$ bound.

- The $\mu \to e\gamma$ bound implies that only one of $\mathcal{B}(h \to \tau\bar{\mu} + \bar{\mu}\tau)$ or $\mathcal{B}(h \to \tau\bar{e} + \bar{e}\tau)$ could be $\mathcal{O}(10\%)$.

- The bounds from $\mu \to e$ conversion in nuclei and from $\mu \to e\gamma$ forbid large branching ratios for the clean μe modes. Specifically, we find $\mathcal{B}(h \to \bar{\mu}e + e\bar{\mu}) < 3 \times 10^{-9}$, several orders of magnitude below the flavor-conserving $\mathcal{B}(h \to \mu\bar{\mu}) \approx 2.3 \times 10^{-4}$ expected for a 125 GeV SM Higgs. However, we recall that this strong bound holds under the hypothesis of SM-like flavor-diagonal couplings for h.

4.1.5 Concluding remarks

The possible observation of a new particle h with mass around 125 GeV raises the important question of its possible nature: is it a SM-like Higgs boson, or not? Key answers to this question will be provided by measurements of the h couplings, and ATLAS and CMS have already provided valuable information [7, 8] on its flavor-diagonal couplings. Further information could be provided by searches for (and measurements of) its flavor-changing couplings. In this study we have analyzed the indirect upper bounds on these couplings that are provided by constraints on flavor-changing and other interactions in both the quark and lepton sectors.

We have found that in the quark sector the indirect constraints are so strong, and the experimental possibilities at the LHC so challenging, that quark flavor-changing decays of the h are unlikely to be observable.

However, the situation is very different in the lepton sector. Here the indirect constraints are typically much weaker, and the experimental possibilities much less challenging. Specifically, we find that either $\mathcal{B}(h \to \tau\bar{\mu} + \bar{\mu}\tau)$ or $\mathcal{B}(h \to \tau\bar{e} + \bar{e}\tau)$ of order 10% is a possibility allowed by the available LFV constraints. These large partial decay rates are the combined result not only of relatively weak bounds on Higgs-mediated LFV amplitudes involving the τ lepton, but also of the smallness of the total h decay width for $m_h \approx 125$ GeV. Interestingly, these potentially large LFV rates are comparable to the expected branching ratio for $h \to \tau^+\tau^-$ in the SM, which is already close to the sensitivity of the CMS experiment [114]. Therefore the LHC experiments may soon be able to provide complementary information on the LFV couplings of the h particle with mass 125 GeV. The decays $h \to \bar{\mu}e, \bar{e}\mu$ are constrained to have very small branching ratios, but their experimental signatures are so clean that here also the LHC may soon be able to provide interesting information.

We therefore urge our experimental colleagues to make dedicated searches for these interesting flavor-violating decays of the possible h particle with mass 125 GeV.

4.2 $B \to \tau\nu$ in Two Higgs doublet models with MFV

The 2HDM is one of the simplest extensions of the SM, in which two Higgs doublets are introduced instead of one*. It was first considered by Lee [123] with the aim of achieving spontaneous CP violation in the SM when only two families of fermions were known. The 2HDM is realized in many NP models, among which the most popular is the MSSM, where, due to the holomorphy of the superpotential, different Higgs doublets couple separately to up and down fermions. After the electroweak symmetry breaking five physical Higgs bosons are generated, dubbed as h, A, H and $H^\pm$ (see Sec 2.3.2). Even if it is usually assumed that only one of them becomes light (mimicking the SM Higgs) and the others remain heavy, the flavor phenomenology can be very rich and different from the SM. In fact in general:

- Each fermion-type can couple to both the Higgs doublets (see Eq. (4.14) later on) with different interaction matrices, that therefore can not be simultaneously diagonalized in the mass basis. This generates large tree level FCNC that, as discussed in the previous Section, are not allowed by the data. A common solution to this problem is given by the *natural flavor conservation* hypothesis [125], in which only one Higgs doublet can couple to a given fermion species, for example due to an additional $U(1)_{PQ}$ symmetry. Alternatively it is possible to consider the MFV assumption, as discussed in the following.

- If the ratio between the vevs of two Higgs doublets is large, the b and τ Yukawa couplings can be $O(1)$ similarly to the t one. In this case additional down-type Yukawa combinations can become important in the MFV expansion. Moreover the effects of the heavy Higgs particles can be enhanced, making possible to observe deviations in some rare processes, as shown in the following for $H^\pm$ in $B \to \tau\nu$. In addiction the Yukawas can get sizable threshold corrections.

- New sources of CPV can be present in the Higgs sector that must be taken into account [126].

In this analysis we concentrate on the study of the 2HDM with MFV. As recently discussed in [35, 127], the MFV hypothesis applied to two-Higgs doublet models not only provides a sufficient protection of FCNC, it can also provide an explanation of the existing tensions in $\Delta F = 2$ observables. More explicitly, it has been show that 2HDM respecting the MFV hypothesis with the inclusion of flavor-blind CP-violating (CPV) phases (dubbed $2\text{HDM}_{\overline{\text{MFV}}}$ framework), can accommodate a large CPV phase in B_s mixing softening in a correlated manner the observed anomaly in the relation between ε_K and $S_{\psi K_S}$ [127]. In this analysis we study the $2\text{HDM}_{\overline{\text{MFV}}}$ framework respect to the latest experimental data on the decay $B \to \tau\nu$.†

*For a recent review see [124].

† Recent analyses of $B \to \tau\nu$ in different models with an extended Higss sector can be found in Ref. [128–130].

In fact the processes $B \to \ell\nu$ are particularly interesting probes of the Higgs sector and, particularly, of the Yukawa interaction. On the one hand they are theoretically very clean: all hadronic uncertainties are confined to the B meson decay constant (f_B), which can be computed reliably using Lattice QCD. On the other hand, the strong helicity suppression makes them particularly sensitive probes of possible deviations from the Standard Model Yukawa interaction. The τ channel is the only decay mode of this type observed so far. The experimental world average [131],[‡]

$$\mathcal{B}(B \to \tau\nu)^{\rm exp} = (1.64 \pm 0.34) \times 10^{-4} \ , \tag{4.11}$$

has to be compared with the SM prediction

$$\mathcal{B}(B \to \tau\nu)^{\rm SM} = \frac{G_F^2 m_B m_\tau^2}{8\pi} \left(1 - \frac{m_\tau^2}{m_B^2}\right)^2 f_B^2 |V_{ub}|^2 \tau_B \ , \tag{4.12}$$

whose uncertainty is mainly due to the determination of $|V_{ub}|$ and f_B. Using the best fit values of $|V_{ub}|$ from global CKM fits, the UTfit [25,132] and CKMfitter [26] collaborations quote

$$\begin{aligned} \mathcal{B}(B \to \tau\nu)^{\rm SM} &= (0.79 \pm 0.07) \times 10^{-4} \ \text{[UTfit]} \ , \\ \mathcal{B}(B \to \tau\nu)^{\rm SM} &= (0.76 \, ^{+\ 0.10}_{-\ 0.06}) \times 10^{-4} \ \text{[CKMfit]} \ . \end{aligned}$$

These low values correspond to a 2.5(2.8) σ deviation from the experimental result in Eq. (4.11).[§]

In models with two Higgs doublets coupled separately to up- and down-type quarks (2HDM-II models), ie taking the natural flavor conservation assumption introduced before, the $B \to \tau\nu$ amplitude receives an additional tree-level contribution from the heavy charged-Higgs exchange, leading to [134]

$$\frac{\mathcal{B}^{\rm 2HDM-II}(B \to \tau\nu)}{\mathcal{B}^{\rm SM}(B \to \tau\nu)} = \left[1 - \frac{m_B^2 \tan^2\beta}{m_H^2}\right]^2 \ , \tag{4.13}$$

where $\tan\beta = v_2/v_1$ is the ratio of the two Higgs vacuum expectation values and m_H is the charged-Higgs boson mass. For large $\tan\beta$ values the ratio in (4.13) can be substantially different from one. However, within this simple framework the interference sign of SM and non-standard amplitudes is fixed. Taking into account the constraints on m_H from other processes, this sign implies a suppression of $\mathcal{B}(B \to \tau\nu)$ in the 2HDM-II compared to the SM, worsening the comparison with the experimental result in Eq. (4.11). Anyway, in the 2HDM$_{\overline{\rm MFV}}$ the relation in Eq. (4.13) can be sizably modified and an enhancement in the $B \to \tau\nu$ rate becomes possible, as we will show in the following.

[‡]After this analysis was completed the Belle collaboration measured a smaller value for $\mathcal{B}(B \to \tau\nu)$ (see Sec 4.3), lowering the tension with the SM. However a slight enhancement is still preferred by the data, as studied in this analysis.

[§]This deviation decreases to about 2σ if $|V_{ub}|$ is calculated directly from semileptonic B decays (see e.g. Ref. [133]) and is not extracted from global CKM fits.

4.2.1 The 2HDM$_{\overline{\text{MFV}}}$ framework

We consider a model with two Higgs fields, $H_{1,2}$, with opposite hypercharge ($Y = \pm 1/2$). The generic form of the Yukawa interaction for such a Higgs sector is

$$\begin{aligned} -\mathcal{L}_Y^{\text{gen}} &= \bar{Q}_L X_{d1} D_R H_1 + \bar{Q}_L X_{u1} U_R H_1^c \\ &+ \bar{Q}_L X_{d2} D_R H_2^c + \bar{Q}_L X_{u2} U_R H_2 + \text{h.c.} \,, \end{aligned} \tag{4.14}$$

where $H_{1(2)}^c = -i\tau_2 H_{1(2)}^*$. The two real vacuum expectation values (vevs) are defined as $\langle H_{1(2)}^\dagger H_{1(2)} \rangle = v_{1(2)}^2/2$, with $v^2 = v_1^2 + v_2^2 \approx (246\ \text{GeV})^2$, and, as anticipated, $\tan\beta = v_2/v_1$.

The X_i are 3×3 matrices in flavor space. The general structure implied by the MFV hypothesis for these matrices is a polynomial expansion in terms of the two (left-handed) spurions $Y_u Y_u^\dagger$ and $Y_d Y_d^\dagger$ [31, 127]:

$$\begin{aligned} X_{d1} &\equiv Y_d \,, \\ X_{d2} &= \epsilon_0 Y_d + \epsilon_1 Y_d Y_d^\dagger Y_d + \epsilon_2 Y_u Y_u^\dagger Y_d + \dots \,, \\ X_{u2} &\equiv Y_u \,, \\ X_{u1} &= \epsilon_0' Y_u + \epsilon_1' Y_d Y_d^\dagger Y_u + \epsilon_2' Y_u Y_u^\dagger Y_u + \dots \,, \end{aligned} \tag{4.15}$$

where the $\epsilon_i^{(\prime)}$ are complex parameters. We work under the assumption $\epsilon_i^{(\prime)} \ll 1$, as expected by an approximate $U(1)_{\text{PQ}}$ symmetry that forbids non-vanishing $X_{u1,d2}$ at the tree level, and we assume $\tan\beta = t_\beta = s_\beta/c_\beta \gg 1$. For simplicity, we also restrict the attention to terms with at most three Yukawa couplings in this expansion (namely we consider only the terms explicitly shown above) and we assume real $\epsilon_i^{(\prime)}$ since we are interested only in CP-conserving observables. Finally, we assume negligible violations of the $U(1)_{\text{PQ}}$ symmetry in the lepton Yukawa couplings.

After diagonalizing quark mass terms and rotating the Higgs fields such that only one doublet has a non-vanishing vev, the interaction of down-type quarks with the neutral Higgs fields assumes the form

$$\mathcal{L}_{\text{n.c.}}^d = -\frac{\sqrt{2}}{v} \bar{d}_L M_d d_R \phi_v^0 - \frac{1}{s_\beta} \bar{d}_L Z^d \lambda_d d_R \phi_H^0 + \text{h.c.} \,, \tag{4.16}$$

where ϕ_v (ϕ_H) is the linear combination of $H_{1,2}$ with non-vanishing (vanishing) vev $\langle \phi_v^0 \rangle = v/\sqrt{2}$ ($\langle \phi_H^0 \rangle = 0$). The flavor structure of the Z^d couplings is

$$Z_{ij}^d = \bar{a}\delta_{ij} + \left[a_0 V^\dagger \lambda_u^2 V + a_1 V^\dagger \lambda_u^2 V \Delta + a_2 \Delta V^\dagger \lambda_u^2 V \right]_{ij} \,,$$

where V is the physical CKM matrix, $\Delta \equiv \text{diag}(0,0,1)$, $\lambda_{u,d}$ are the diagonal Yukawa couplings in the limit of unbroken $U(1)_{\text{PQ}}$ symmetry, and the a_i are flavor-blind coefficients (see [31, 127] for notations). Similarly, the interaction of the quarks with the physical charged Higgs is described by the following flavor-changing effective Lagrangian [31]

$$\mathcal{L}_{\text{H}^+} = \left[\bar{U}_L C_R^{H^+} \lambda_d D_R + \frac{1}{t_\beta} \bar{U}_R \lambda_u C_L^{H^+} D_L \right] H^+ + \text{h.c.}, \tag{4.17}$$

where the flavor structure of $C_{L,R}^{H^+}$ is

$$C_R^{H^+} = (b_0 V + b_1 V\Delta + b_2 \Delta V + b_3 \Delta) \ , \tag{4.18}$$
$$C_L^{H^+} = (b_0' V + b_1' V\Delta + b_2' \Delta V + b_3' \Delta) \ , \tag{4.19}$$

and the $b_i^{(\prime)}$ are flavor-blind coefficients. As explicitly given in [31, 127], the a_i and $b_i^{(\prime)}$ depend on the $\epsilon_i^{(\prime)}$, on $\tan\beta$, and on the overall normalization of the Yukawa couplings. Even if $\epsilon_i^{(\prime)} \ll 1$, the a_i and b_i can reach values of $\mathcal{O}(1)$ at large $\tan\beta$ and can be complex, since we allow flavor-blind phases in the model.

$\mathcal{B}(B \to \tau\nu)$ and other observables

We present here the theoretical expressions of $\mathcal{B}(B \to \tau\nu)$ and a series of other flavor-violating observables, necessary to set bounds on the parameter space, in the 2HDM$_{\overline{\text{MFV}}}$ framework.

In order to simplify the notations, we absorb terms proportional to the top and bottom Yukawa coupling into the definition of $\epsilon_{1,2}^{(\prime)}$. More explicitly, we redefine $\epsilon_{1,2}^{(\prime)}$ as follows:

$$\epsilon_1^{(\prime)} y_b^2 \to \epsilon_1^{(\prime)} \ , \qquad \epsilon_2^{(\prime)} y_t^2 \to \epsilon_2^{(\prime)} \ . \tag{4.20}$$

With such a notation, the $b_R \to u_L$ and $s_R \to u_L$ interactions with the physical charged Higgs are

$$\begin{aligned} \mathcal{L}^{b,s\to u} &= \frac{m_b \tan\beta}{v} V_{ub} \frac{1}{1+(\epsilon_0+\epsilon_1)\tan\beta} \bar{u}_L b_R H^+ \\ &+ \frac{m_s \tan\beta}{v} V_{us} \frac{1}{1+\epsilon_0 \tan\beta} \bar{u}_L s_R H^+ + \text{h.c.} \end{aligned} \tag{4.21}$$

This allows us to derive the following expression for the modification of $\mathcal{B}(B \to \tau\nu)$, relative to the SM, within this framework:

$$\begin{aligned} R_{B\tau\nu} &= \frac{\mathcal{B}(B\to\tau\nu)}{\mathcal{B}^{\text{SM}}(B\to\tau\nu)} \\ &= \left[1 - \frac{m_B^2}{m_H^2} \frac{\tan^2\beta}{1+(\epsilon_0+\epsilon_1)\tan\beta}\right]^2 \ , \end{aligned} \tag{4.22}$$

A closely related observable which provides a significant constraint on the parameter space is $\mathcal{B}(K \to \mu\nu)$. In this case from (4.21) we find

$$\begin{aligned} R_{K\mu\nu} &= \frac{\mathcal{B}(K\to\mu\nu)}{\mathcal{B}^{\text{SM}}(K\to\mu\nu)} \\ &= \left[1 - \frac{m_K^2}{m_H^2} \frac{\tan^2\beta}{1+\epsilon_0\tan\beta}\right]^2 \ . \end{aligned} \tag{4.23}$$

Beside semileptonic charged currents, stringent constraints on the 2HDM$_{\overline{\text{MFV}}}$ parameter space are provided also by the flavor-changing neutral-current (FCNC) transitions

$B \to X_s\gamma$ and $B_s \to \mu^+\mu^-$. In principle, also the B_s–$\bar{B}_s$ mixing amplitude could be used to constrain the parameter space of the model; however, as we will discuss below, it turns out that B_s–$\bar{B}_s$ constraints are automatically satisfied after imposing the bounds from $B_s \to \mu^+\mu^-$. In order to implement these bounds, we introduce the FCNC Hamiltonian

$$\mathcal{L}^{b\to s} = -\frac{G_{\rm F}\alpha_{\rm em}}{2\sqrt{2}\pi\sin^2\theta_{\rm W}} V_{tb}^* V_{ts} \sum_n C_n \mathcal{Q}_n \;+\; \text{h.c.}\,, \tag{4.24}$$

where

$$\mathcal{Q}_7 \;=\; \frac{e}{g^2} m_b\, \bar{s}\sigma_{\mu\nu}(1+\gamma_5)\, b\, F_{\mu\nu}\,, \tag{4.25}$$

$$\mathcal{Q}_S^\mu \;=\; \bar{s}\,(1+\gamma_5)\, b\;\bar{\mu}\,(1-\gamma_5)\,\mu\,, \tag{4.26}$$

and the complete list of effective operators can be found in [135]. Following Ref. [135], the experimental constraints on $B \to X_s\gamma$ and $B_s \to \mu^+\mu^-$ can effectively be encoded into constraints on C_7 and C_S^μ. More precisely, we can translate the experimental data into bounds on $\delta C_7 = C_7(M_W^2) - C_7^{\rm SM}(M_W^2)$ and $\delta C_S^\mu = C_S^\mu(M_W^2) - C_S^{\mu\,\rm SM}(M_W^2)$.

Working under the hypothesis that the only relevant non-standard contributions are those associated to the heavy Higgs fields, the dominant contributions to δC_7 are the one-loop contributions from both charged and neutral Higgs exchange. Adopting to our notations the results of Ref. [31] we have

$$\begin{aligned}\delta C_7 \;&=\; \frac{1}{D_{012}}\left[1 + (\epsilon_0' + \epsilon_2')\tan\beta - \frac{\epsilon_2\epsilon_1'\tan^2\beta}{D_{01}}\right] F_7(x_{tH}^2) \\ &-\; \frac{\epsilon_2\tan^3\beta}{D_{012}^2 D_{01}}\frac{x_{bH}^2}{36}\end{aligned} \tag{4.27}$$

where $x_{qH} = m_q/m_H$,

$$\begin{aligned} D_{012} \;&=\; 1 + (\epsilon_0 + \epsilon_1 + \epsilon_2)\tan\beta\,, \\ D_{01} \;&=\; 1 + (\epsilon_0 + \epsilon_1)\tan\beta\,, \end{aligned} \tag{4.28}$$

and $F_7(x)$ is defined as in [31].

The effective coupling of $\mathcal{Q}_S^\mu$ receives contributions from the FCNC component of (4.16) already at the tree-level:

$$\delta C_S^\mu = \frac{m_b m_\mu}{m_H^2}\frac{2\pi\sin^2\theta_W}{\alpha_{\rm em}}\frac{\epsilon_2\tan^3\beta}{D_{01}D_{012}}\,. \tag{4.29}$$

4.2.2 Phenomenological analysis

We are now ready to analyse the parameter space of the model, searching for regions where $\mathcal{B}(B \to \tau\nu)$ is enhanced over its SM prediction and the other low-energy constraints are satisfied. Since the main observables used in CKM fits receive tiny corrections from the extended Higgs sector, we assume that the standard CKM determination remains valid.

The low-energy phenomenological constraints used in our analysis are

$$\begin{aligned} R_{K\mu\nu} &\in (0.98, 1.02) \ , \\ \delta C_7 &\in (-0.14, 0.06) \ , \\ \delta C_S^\mu &\in (-0.03, 0.005) \ . \end{aligned} \tag{4.30}$$

The first input follows from the analysis of semileptonic K decays in [136] (see also [137]), while the range of δC_7 and δC_S^μ follows from the analysis of $B \to X_s\gamma$ and $B_s \to \mu^+\mu^-$ performed in [135], updated with the latest LHCb results. Moreover, since we are interested in substantial enhancements of $\mathcal{B}(B \to \tau\nu)$, we impose

$$R_{B\tau\nu} > 1.2 \ . \tag{4.31}$$

On the other hand, given the condition $\epsilon_i^{(\prime)} \ll 1$ expected from an approximate $U(1)_{\rm PQ}$ symmetry, we will restrict the free parameters of the model to vary in the following interval:

$$\begin{aligned} \tan\beta &\in (40, 60) \ , \\ m_H[\text{GeV}] &\in (150, 1000) \ , \\ \epsilon_i^{(\prime)} \tan\beta &\in (-2, 2) \ . \end{aligned} \tag{4.32}$$

Analytical considerations

In principle the model has enough parameters that allow us to to satisfy the three conditions in Eqs. (4.30) and, at the same time, get the desired enhancement in $B \to \tau\nu$, provided we properly tunes the values of $\epsilon_i^{(\prime)} \times \tan\beta$. However, we are not interested in fine-tuned solutions. In particular, while it is natural setting to zero some of the $\epsilon_i^{(\prime)}$, which are symmetry breaking terms, we consider not natural fine-tuned solutions corresponding to large values of $\epsilon_i^{(\prime)} \tan\beta$. In this perspective, taking into account the theoretical expressions for the observables presented in the previous Section, we find that:

i. Since $\delta C_S^\mu \propto \epsilon_2$, the bound from $B_s \to \mu^+\mu^-$ can easily be satisfied assuming $\epsilon_2 \approx 0$. This "natural" tuning (according to the discussion above) allow us to decouple charged-Higgs and neutral-Higgs flavor-changing amplitudes. Incidentally, this is why we do not get additional significant constraints from B_s–$\bar{B}_s$ mixing.

ii. Contrary to $B_s \to \mu^+\mu^-$, we cannot get rid of the $B \to X_s\gamma$ bound without some amount of fine tuning. In particular, setting $\epsilon_2 \approx 0$, the charged-Higgs contribution to $B \to X_s\gamma$ vanishes completely only under the fine-tuned condition

$$(\epsilon_0' + \epsilon_2') \tan\beta = -1 \ . \tag{4.33}$$

Before analysing how far from the fine-tuned condition in Eq. (4.33) we can move, it is worth discussing the correlation between $B \to \tau\nu$ and $K \to \mu\nu$ ignoring all other constraints.

In the case of $K \to \mu\nu$, the Higgs-mediated amplitude is always much smaller that the SM one. Imposing $R_{K\mu\nu} \in [0.98, 1.02]$ implies

$$|\epsilon_0 \tan\beta + 1| > 0.9 \times r \tag{4.34}$$

where $r = m_B^2 \tan^2\beta / m_H^2$. For the chosen range of $\tan\beta$ and m_H we have $0.04 < r < 4.3$. For small values of r the above condition is very natural: we only exlude a narrow region around the (unnatural) point $\epsilon_0 \tan\beta = -1$. On the other hand, for growing values of r we are pushed toward a fine tuned configuration. We thus conclude that the $K \to \mu\nu$ bound points toward small values of r.

Two solutions are possible to generate an enhancement of $\mathcal{B}(B \to \tau\nu)$: a destructive interference of SM and charged-Higgs amplitudes, if the latter is more than twice the SM one in size; a constructive interference of SM and charged-Higgs amplitudes, independently from the size of the charged-Higgs amplitude. Requiring $R_{B\tau\nu} > 1.2$ implies

$$-(1 + \epsilon_0 \tan\beta) < \epsilon_1 \tan\beta < -(1 + \epsilon_0 \tan\beta) + 0.5 \times r \tag{4.35}$$

for the case of destructive interference, and

$$(1 + \epsilon_0 \tan\beta) < -\epsilon_1 \tan\beta < (1 + \epsilon_0 \tan\beta) + 10 \times r \tag{4.36}$$

for the case of constructive interference. It is clear from the above equations that the constructive case allow a larger region of the parameter space. This is particularly true for small values of r, as suggested by the $K \to \mu\nu$ bound. As we will discuss in the following, this conclusion remains true and is even reinforced once we take into account also the $B \to X_s\gamma$ bound. Finally, a destructive interference of scalar and SM amplitudes in $b \to c\tau\nu$, able to increase $\mathcal{B}(B \to \tau\nu)$, is strongly disfavored by $B \to D\tau\nu$ data [138] and the lower bounds on m_H from direct searches at the LHC (see discussion below).

We finally comment on previous analyses about the possiblity to enhance $\mathcal{B}(B \to \tau\nu)$ in 2HDMs. A general analysis in the context of the Higgs sector of the minimal supersymmetric extension of the SM (MSSM) has been presented in Ref. [130]. In that framework the ϵ_i are not free parameters. As a result, their analysis is less general than the one presented here, at least as Higgs-mediated amplitudes are concerned. In particular, the constructive interference solution, occurring for $1 + (\epsilon_0 + \epsilon_1)\tan\beta < 0$ has not been considered in Ref. [130]. The importance of the latter has been pointed out first in Ref. [139]. However, in the latter work the correlation with the other observables we are considering has not been analyzed.

Numerical analysis

In order to analyze all the constraints at the same time, trying to avoid fine-tuned configurations, we have randomly generated values for the relevant $\epsilon_i^{(\prime)} \tan\beta$ using (uncorrelated) Gaussian distributions centered in zero –corresponding to the limit of exact $U(1)_{\rm PQ}$ symmetry– and with $\sigma = 0.5$. The values of m_H and $\tan\beta$ are extracted with uniform distributions in the ranges specified in Eq. (4.32).

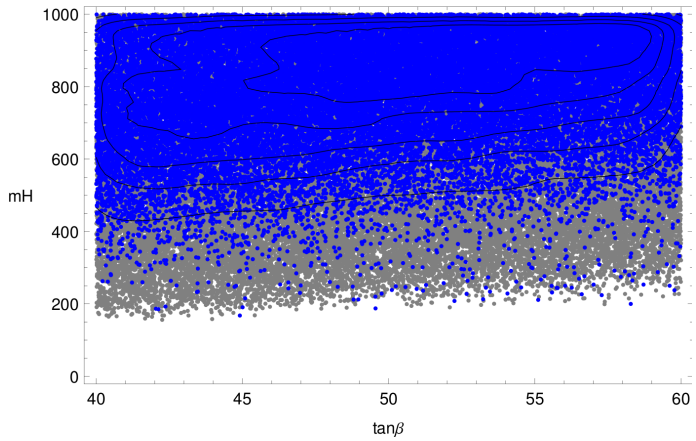

Figure 4.2: Allowed regions in the $\tan\beta$–m_H plane. The grey points correspond to regions of the parameter space that can be reached only in the fine-tuned configuration where $\epsilon_2 = 0$ and $\epsilon'_{0,2}$ are fixed to satisfy the condition (4.33). The black contours mark equally-populated areas resulting from the the global sampling (without fine-tuned conditions): the three most inner contours include 50% of the points.

The results of this numerical analysis are shown in Fig. 4.2–4.5. In Fig. 4.2 and Fig. 4.3 we show the points satisfying all constraints in Eqs. (4.30)–(4.31). To better quantify the role of the $B \to X_s\gamma$ and $B_s \to \mu^+\mu^-$ bounds, we have plotted with a different color (grey point) the region of parameter space that can be reached only in the fine-tuned configuration where $\epsilon_2 = 0$ and ϵ'_0 and ϵ'_2 are fixed to satisfy the condition (4.33). As can be seen from Fig. 4.2, in general there is no significant constraint on m_H and $\tan\beta$; however, low values of m_H can be obtained only in the in the fine-tuned configuration.

At this point it is worth to comment on the bounds in the m_H–$\tan\beta$ plane by direct searches for heavy Higgs bosons at the LHC [114]. A direct implementation of these constraints in our frameworks is not possible, given the former are obtained in the limit limit $\epsilon_i^{(\prime)} = 0$. Still, it is worth to note that in this limit direct searches set the approximate bound $m_H \gtrsim 420\ \text{GeV} + 6 \times (\tan\beta - 40)$ [114], which does not represent a problem for most of the points in Fig. 4.2. Only the fine-tuned (gray) points are potentially affected by this constraint, which thus provide a further argument against the tuned configuration with low m_H.

In Fig. 4.3 we show the points satisfying all constraints in the ϵ_0–ϵ_1 plane. We also show the line $1 + (\epsilon_0 + \epsilon_1)\tan\beta = 0$, separating the region of destructive interference (above the line) and constructive interference (below the line) in $B \to \tau\nu$. As can be seen, the region of destructive interference is reached essentially only in the fine-tuned configuration where ϵ_2 and $\epsilon'_{0,2}$ are fixed to eliminate any non-standard contribution to $B \to X_s\gamma$ and $B_s \to \mu^+\mu^-$. Indeed in this region we need large values of m_H, that would get in conflict with $B \to X_s\gamma$ and $B_s \to \mu^+\mu^-$ for generic values of ϵ_2 and $\epsilon'_{0,2}$.

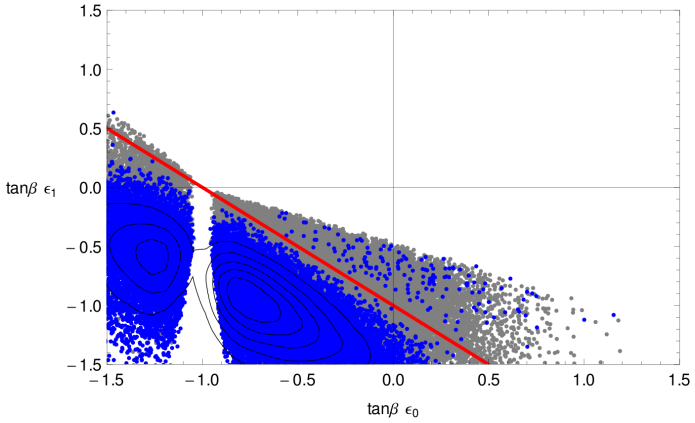

Figure 4.3: Allowed regions in the ϵ_0–ϵ_1 plane. Notations as in Fig. 4.2.

On the other hand, the region of constructive interference is densely populated even in absence of a fine-tuning on ϵ_2 and $\epsilon'_{0,2}$. As anticipated in the analytical discussion, the absence of points for $\epsilon_0 \tan\beta$ close to -1 is a consequence of the $K \to \mu\nu$ bound. Last but not least, we stress the absence of points near the $U(1)_{\rm PQ}$ symmetric point $\epsilon_0 = \epsilon_1 = 0$. This is a simple consequence of combining the $K \to \mu\nu$ and $B \to \mu\nu$ constraints in Eqs. (4.34)–(4.36).

In Fig. 4.4 and 4.5 we show the correlation of $R_{B\tau\nu}$ with the two most significant constraints, namely $\mathcal{B}(K \to \mu\nu)$ and δC_7 (or $B \to X_s\gamma$) (in these two figures we do not plot with different colors the fine-tuned points). As can be seen from Fig. 4.5, the interference between SM and charged-Higgs amplitudes is necessarily destructive in $B \to X_s\gamma$ (we recall that $C_7^{\rm SM} < 0$). On the other hand, both positive and negative interferences in $K \to \mu\nu$ are possible, depending on the sign of $1 + \epsilon_0 \tan\beta$. As illustrated in Fig. 4.4, if the maximal deviation from the SM in $\mathcal{B}(K \to \mu\nu)$ could be reduced to 1%, the parameter space leading to an enhancement of $\mathcal{B}(B \to \tau\nu)$ would be strongly reduced. This also implies that if the precision on $\mathcal{B}(K \to \mu\nu)$ will improve, there are realistic chances to see a deviation from the SM in this mode within this framework. On the contrary, we have checked that for $R_{B\tau\nu} < 2$ the deviations from the SM predictions in $\mathcal{B}(B \to D\tau\nu)$ do not exceed the 20% level, well within the present theoretical and experimental uncertainties [138].

As a final check of the stability of our findings, we have performed scan of the parameter space allowing arbitrary complex phases for the $\epsilon_i^{(\prime)}$. As expected, no significant deviations in Fig. 4.2, 4.4 , and 4.5 has been observed. Fig. 4.3 is unaffected provided we interpret it as the $\mathrm{Re}(\epsilon_0)$–$\mathrm{Re}(\epsilon_1)$ plane.

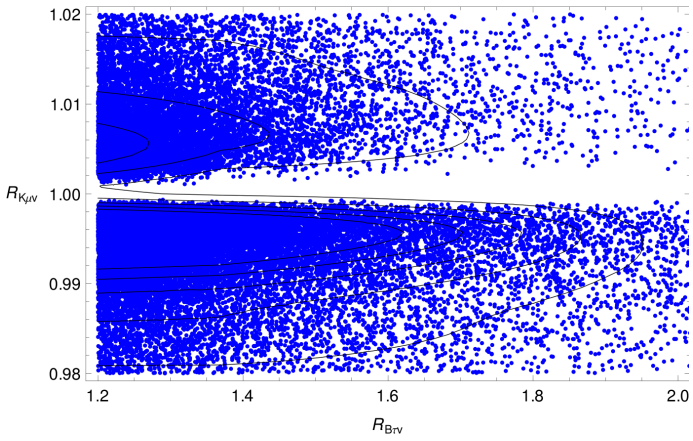

Figure 4.4: Allowed regions in the $R_{B\tau\nu}$–$R_{K\mu\nu}$ plane.

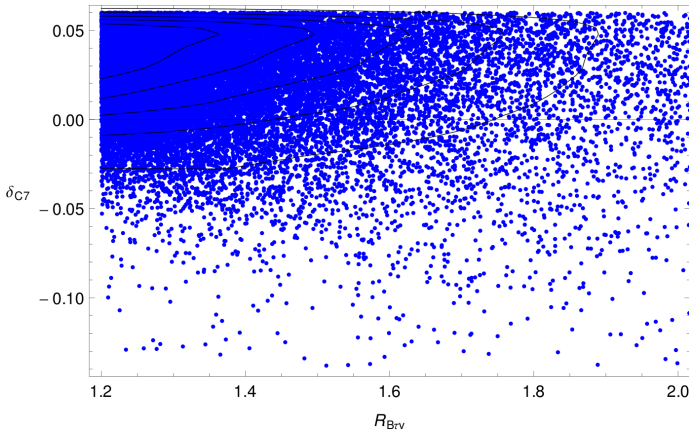

Figure 4.5: Allowed regions in the $R_{B\tau\nu}$–δC_7 plane.

4.2.3 Recent results on $B \to D^{(*)}\tau\nu$

After this analysis was completed, the Babar collaboration has reported improved measurements of the $B \to D^{(*)}\tau\nu$ rates, normalized to the corresponding decays with a light charged lepton ($\ell = e, \mu$) [142]. In both cases an excess around $\approx 30\%$ over the SM predictions is observed, with a significance of about 2σ in the D mode and 2.7σ in the D^* mode (see Ref. [143] for an updated discussion). The excess in the $B \to D^{(*)}\tau\nu$ rate cannot be explained in terms of scalar amplitudes, at least in the context of MFV models [143, 144]. On the other hand, an excess in $B \to D\tau\nu$ can be generated by the $b \to c$ component of Eq. (4.17),

$$\mathcal{L}^{b\to c} = \frac{m_b \tan\beta}{v} V_{cb} \frac{1}{1 + (\epsilon_0 + \epsilon_1)\tan\beta} \bar{c}_L b_R H^+ + \text{h.c.} \,,$$

that leads to a $B \to D\tau\nu$ scalar amplitude with the same parametric dependence of the charged-Higgs contribution to $B \to \tau\nu$. As pointed out in [143], the central value of the $B \to D\tau\nu$ rate points toward the same central value of the scalar amplitude necessary to reproduce the $B \to \tau\nu$ rate under the hypothesis of *constructive interference* between scalar and SM amplitudes. The recent $B \to D\tau\nu$ result in [142] therefore proved further support for the scenario analyzed in this work.

4.2.4 Concluding remarks

Our analysis shows that is possible to accommodate sizable enhancements of $\mathcal{B}(B \to \tau\nu)$ in the $2\text{HDM}_{\overline{\text{MFV}}}$ framework, despite the tight constraints of other low-energy observables. This is clearly illustrated by the plots discussed in the previous Section. However, it must be stressed that this enhancement occurs under a few specific circumstances:

i. At least some of the $\epsilon_i \tan\beta$ must of order one, i.e. sizable deviations from the exact 2HDM-II limit, or from the limit of unbroken $U(1)_{\text{PQ}}$ symmetry in the Yukawa sector, are necessary. As shown in Fig. 4.3, almost no solution survive for $|\epsilon_i \tan\beta| < 0.5$. This conclusion holds independenlty of the simplifying assumptions on the ϵ_i adopted in the present analysis.

ii. If we assume $\epsilon_i \ll 1$, as realised in several explicit models where the $U(1)_{\text{PQ}}$ symmetry in the Yukawa sector is broken only by radiative corrections, the need for large $\epsilon_i \tan\beta$ necessarily imply large $\tan\beta$ values.

iii. In addition of being sizable, the $U(1)_{\text{PQ}}$ breaking terms ϵ_0 and ϵ_1 should conspire to suppress the combination $1 + (\epsilon_0 + \epsilon_1)\tan\beta$ appearing in the denominator of the $B \to \tau\nu$ amplitude. The more m_H is large, the more fine tuning on $1+(\epsilon_0+\epsilon_1)\tan\beta$ is needed in order to keep the charged-Higgs amplitude at the level of the SM one.

iv. The most likely possibility to enhance $B \to \tau\nu$, especially if m_H is above 200 GeV, occurs in the case of constructive interference between SM and charged Higgs amplitudes in $B \to \tau\nu$. This requires values of the ϵ_i which cannot be obtained in simplified MSSM scenarios, such as the one considered in Ref. [130], but can be obtained in less standard supersymmetric frameworks, such as the "up-lifted" scenario considered in Ref. [140].

If the above conditions are satisfied, a large enhancement of $\mathcal{B}(B \to \tau\nu)$ is compatible with the existing constraints. In absence of fine tuning, this implies non-negligible and potentially visible deviations from the SM in $B \to X_s\gamma$ and $K \to \mu\nu$. The most interesting effects are expected in $\mathcal{B}(K \to \mu\nu)$, as illustrated in Fig. 4.4. To this purpose, we stress that $\mathcal{B}(K \to \mu\nu)$ is presently measured with a 0.27% relative error [141]. If future lattice determinations of the kaon form factors could allow us to reduce the theoretical error on $\mathcal{B}(K \to \mu\nu)$ at the same level, the $\mathcal{B}(B \to \tau\nu)$–$\mathcal{B}(K \to \mu\nu)$ correlation would provide a useful tool to test this framework.

4.3 MSSM at large $\tan\beta$ and future prospects

Very recently the LCHb collaboration has presented the first evidence for the rare decay $B_s \to \mu\mu$ [145]

$$\mathcal{B}(B_s \to \mu\mu)^{\rm exp} = (3.2^{+1.5}_{-1.2}) \times 10^{-9} \,, \tag{4.37}$$

that results compatible with the SM expectation [146]

$$\mathcal{B}(B_s \to \mu\mu)^{\rm exp} = (3.23 \pm 0.27) \times 10^{-9} \,. \tag{4.38}$$

Even if this measurement is still dominated by large errors, it is a very important test for several NP models. For instance it is very sensible to non-standard effects from heavy Higgs exchanges in the 2HDM with large $\tan\beta$, putting strong constraints on its parameter space.

On the other hand the decay $B \to \tau\nu$ is also sensitive to heavy (charged) Higgs contributions that can be sizable for large $\tan\beta$ (see Sec. 4.2). This process can be hardly measured at LCHb, due to the high missing energy produced, but is one of the golden channels for a superB machine [150,151]. The current experimental and theoretical situation is*

$$\mathcal{B}(B \to \tau\nu)^{\rm exp} = (1.16 \pm 0.22) \times 10^{-4} \tag{4.39}$$

$$\mathcal{B}(B \to \tau\nu)^{\rm SM} = (0.97 \pm 0.22) \times 10^{-4} \tag{4.40}$$

In this analysis we study the interplays between these two processes in relation to future experimental sensitivities and to the other flavor observables.† We will consider the two cases of 2HDM-II (i.e. the 2HDM with the natural flavor conservation assumption) and the MSSM with MFV, dubbed as MSSM$_{\overline{\rm MFV}}$. In particular usually the $\tan\beta$ enhancement is stronger in $B_s \to \mu\mu$, while the corrections to $B \to \tau\nu$ arise already at tree level. For this reason a quantitative estimate of the discovery potential of the LCHb and the superB measurements is very important. In particular we explore the hypothetical case in which, with the estimated luminosity of 5 fb^{-1} (reached before the possible upgrade in 2017), LHCb would have measured $B_s \to \mu\mu$ at the SM value with the estimated error [152]

$$\frac{\delta\mathcal{B}(B_s \to \mu\mu)}{\mathcal{B}(B_s \to \mu\mu)} \sim 20\% \,, \tag{4.41}$$

In this situation we check which is the parameter space that can be probed with a superB measurement of $B \to \tau\nu$ at level [150, 151]

$$\frac{\delta\mathcal{B}(B \to \tau\nu)}{\mathcal{B}(B \to \tau\nu)} \sim 5\% \,, \tag{4.42}$$

estimated with the luminosity of 50-75 ab^{-1} (after few years of running).

*We have updated the values in Eqs. (4.11) and (4.13) with the inclusion of recent Belle results [147] and we have chosen the more conservative value for the SM prediction given in [148].

†See also [149] for a similar analysis.

4.3.1 $B_s \to \mu\mu$ and $B \to \tau\nu$ in comparison

In the 2HDM-II the FCNC can be forbidden by an exact $U(1)_{PQ}$ symmetry [125]. In this case $B \to \tau\nu$ receives tree level corrections from the charged Higgs exchange, while $B_s \to \mu\mu$ is corrected at one-loop order, giving [134, 153]

$$R^{\rm 2HDM-II}_{B\tau\nu} = \frac{\mathcal{B}^{\rm 2HDM-II}(B\to\tau\nu)}{\mathcal{B}^{\rm SM}(B\to\tau\nu)} = \left[1 - \frac{m_B^2 \tan^2\beta}{m_H^2}\right]^2 , \tag{4.43}$$

$$R^{\rm 2HDM-II}_{B\mu\mu} = \frac{\mathcal{B}^{\rm 2HDM-II}(B\to\mu\mu)}{\mathcal{B}^{\rm SM}(B\to\mu\mu)} = (1+\delta_S)^2 + \left(1 - \frac{4m_\mu^2}{m_B^2}\right)\delta_S^2 , \tag{4.44}$$

where

$$\delta_S = -\frac{m_B^2 \, \log\left(M_H^2/m_t^2\right)}{8\, M_W^2 \left(M_H^2/m_t^2 - 1\right)} \tan^2\beta \tag{4.45}$$

As already discussed in the previous Section, in this case only a suppression in the $B \to \tau\nu$ rate is possible and both the effects are of order $\propto \tan^4\beta$.

The 2HDM with MFV as been already presented in Sec 4.2. Here we want to focus on its supersymmetric version, the MSSM$_{\overline{\rm MFV}}$. In this case the $U(1)_{PQ}$ breaking parameters $\epsilon^{(\prime)}$ defined in Eq. (4.15) become fixed functions of the supersymmetric spectrum. In fact, the $U(1)_{PQ}$ symmetry must be explicitly broken in the scalar potential in order avoid the presence of undesired goldstone bosons and, in the MSSM, this breaking is given by the μ-term in the superpotential and by the b-soft-term. This generates at one-loop level the non-holomorphic interactions with the "wrong-type" Higgs (see Eq. (4.15)), where the $\epsilon^{(\prime)}$ are calculated for example in [31]. In particular following the notation in [4] we obtain

$$\epsilon_0 = -\frac{2\,\alpha_s\,\mu}{3\pi\, m_{\tilde g}} H_2\left(\frac{m_{\tilde Q}^2}{m_{\tilde g}^2}, \frac{m_{\tilde d}^2}{m_{\tilde g}^2}\right) , \quad \epsilon_2 = -\frac{A\,\mu}{16\pi^2 m_{\tilde Q}^2} H_2\left(\frac{\mu^2}{m_{\tilde Q}^2}, \frac{m_{\tilde u}^2}{m_{\tilde Q}^2}\right) , \quad \epsilon_1 = \epsilon_3 = \epsilon_4 = 0 \tag{4.46}$$

where H_2 is defined in [31]. Similar relations hold also for the ϵ' parameters. At leading order in $\tan\beta$ and neglecting the other supersymmetric effects, that within MFV and large $\tan\beta$ are subdominant, the decay rates result modified as [31, 139]

$$R^{\rm MSSM_{\overline{MFV}}}_{B\tau\nu} = \left[1 - \frac{m_B^2}{m_H^2}\frac{\tan^2\beta}{1+\epsilon_0\tan\beta}\right]^2 , \tag{4.47}$$

$$R^{\rm MSSM_{\overline{MFV}}}_{B\mu\mu} = (1+\delta_S)^2 + \left(1 - \frac{4m_\mu^2}{m_B^2}\right)\delta_S^2 , \tag{4.48}$$

where now

$$\delta_S = \frac{\pi \sin^2\theta_W M_B^2}{\alpha M_H^2 \left(1+\epsilon_0\tan\beta\right)^2}\epsilon_2 \, \tan^3\beta \tag{4.49}$$

Note that we are neglecting any possible $U(1)_{PQ}$ breaking effect in the lepton sector and we are assuming a common mass for all the heavy Higgs particles. From the previous equations it is clear that, given the $O(\tan^6\beta)$ enhancement in $B_s \to \mu\mu$, a SM measurement of this process with an error of 20% would severely constrain the allowed parameter

space. However the loop nature of this transition in the $\text{MSSM}_{\overline{\text{MFV}}}$ causes that it would vanish in the limit of $\epsilon_2 \to 0$, that is obtained for small μ and A-term, and for large squark masses. All these three cases are possible but are limited by other requirements: the chargino mass limit requires that μ should be non-zero; the light Higgs mass value prefers a large A-term; in a natural theory the squark can not be too heavy. The interplay between all these requirements are quantitatively analyzed in the next Section.

Similarly other two flavor transitions that are relevant in the 2HDM for large $\tan\beta$ are $K \to \mu\nu$ and $B \to X_s\gamma$. For the first one we find

$$R_{K\mu\nu}^{\text{MSSM}_{\overline{\text{MFV}}}} = \left[1 - \frac{m_K^2}{m_H^2}\frac{\tan^2\beta}{1+\epsilon_0\tan\beta}\right]^2 . \tag{4.50}$$

The second one receives corrections from the heavy Higgs penguin diagrams contributing to the chromomagnetic operator. Following the notation in [4] we obtain [31]

$$\begin{aligned}\delta C_7^{\text{MSSM}_{\overline{\text{MFV}}}} &= \frac{1}{1+(\epsilon_0+\epsilon_2)\tan\beta}\left[1+\epsilon_0'\tan\beta - \frac{\epsilon_2\epsilon_1'\tan^2\beta}{1+\epsilon_0\tan\beta}\right] F_7\left(\frac{m_t^2}{m_H^2}\right) \\ &- \frac{\epsilon_2\tan^3\beta}{(1+(\epsilon_0+\epsilon_2)\tan\beta)^2(1+\epsilon_1\tan\beta)}\frac{m_b^2}{36\,m_H^2}\end{aligned} \tag{4.51}$$

where δC_7 is the deviation from the SM Wilson coefficient of the chromomagnetic operator. The respective contributions in the 2HDM-II are identical to Eqs. (4.50) and (4.51) with all the $\epsilon^{(\prime)} = 0$

4.3.2 Numerical analysis

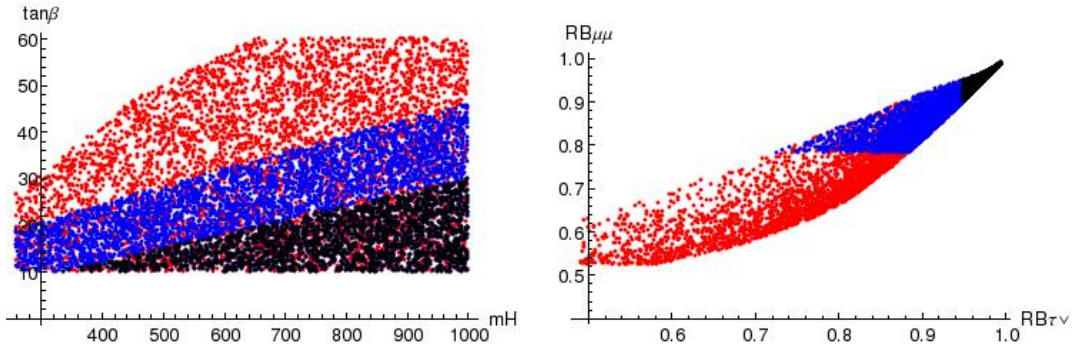

Figure 4.6: 2HDM-II case. Left: allowed $m_H - \tan\beta$ parameter space given the current experimental bounds (red), after measuring $B_s \to \mu\mu$ with a 20% error (blue) and after measuring $B \to \tau\nu$ at 5% level. No deviations from the SM are always assumed. Right: correlation between the non-standard effects in $B \to \tau\nu$ and $B_s \to \mu\mu$.

As already anticipated we are interested in the present and future (in case of no

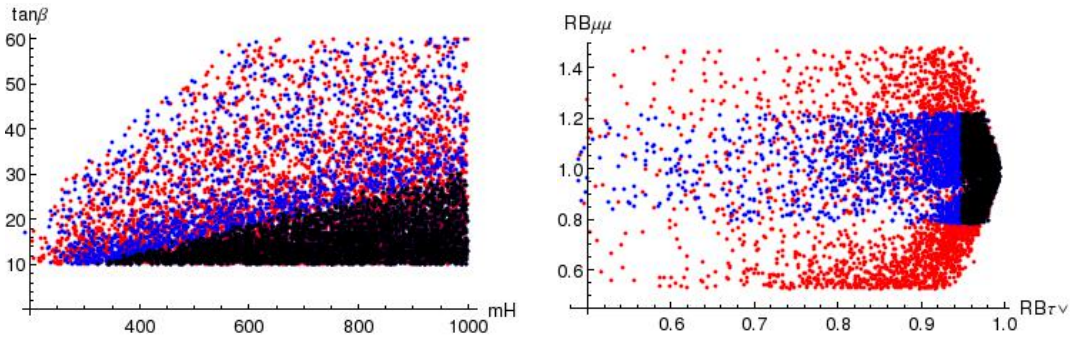

Figure 4.7: MSSM with MFV case. Notation as in Fig. 4.6.

deviations from the SM) sensitivity on $B_s \to \mu\mu$, that at 1σ gives

$$\delta_S^p \in [-1.2, -0.61] \oplus [-0.39, 0.20] \quad \text{(LHCb today [145])} \tag{4.52}$$

$$\delta_S^f \in [-1.1, -0.88] \oplus [-0.12, 0.099] \quad \text{(LHCb 5 fb}^{-1}\text{ [152])} \tag{4.53}$$

Given the theoretical discrepancy in the value of V_{ub} obtained from exclusive or inclusive semileptonic B decays and the not very clear experimental situation, we take for $B \to \tau\nu$ the 2 σ range [148]

$$R_{B\tau\nu}^{exp} \in [0.48, 1.9] \tag{4.54}$$

After a superB measurement the previous quantity will be measured at 5% level [150]. We consider also the bounds from $K \to \mu\nu$ [136] and $B \to X_s\gamma$ [135]

$$R_{K\mu\nu}^{exp} \in [0.98, 1.02] \tag{4.55}$$

$$\delta C_7 \in [-0.14, 0.06]\,. \tag{4.56}$$

With the previous four processes it is already possible to investigate the 2HDM-II case. In Fig. 4.6 we show the region allowed by current data (red) and the region allowed considering the future LCHb prospects in Eq. (4.41) (blue). In black we show also the points the will remain unconstrained also after a future measurements of $B \to \tau\nu$ in a superB. We vary $\tan\beta$ and the mass of the heavy Higgs in the range: $\tan\beta \in [10, 60]$ and $m_H \in [200, 1000]$. The main result is that in this scenario only a suppression in $B \to \tau\nu$ is possible and, after the hypothetical future LHCb confirmation of the SM, the deviation in $B \to \tau\nu$ can be still of order $\lesssim 30\%$.

As far as the MSSM$_{\overline{\text{MFV}}}$ is concerned other requirements are in order. First we ask that the light Higgs mass must be compatible at 1 σ with the experimental data $m_h^{exp} = 125.3 \pm 0.6$ GeV [7, 8], including the theoretical error. Then we consider the direct search bounds, that we take conservatively from [154]

$$m_S > 800\,\text{GeV} \tag{4.57}$$

$$m_{\tilde{g}} > 600\,\text{GeV} \tag{4.58}$$

$$m_{\tilde{\chi}_1^\pm} > 92\,\text{GeV} \tag{4.59}$$

$$\tag{4.60}$$

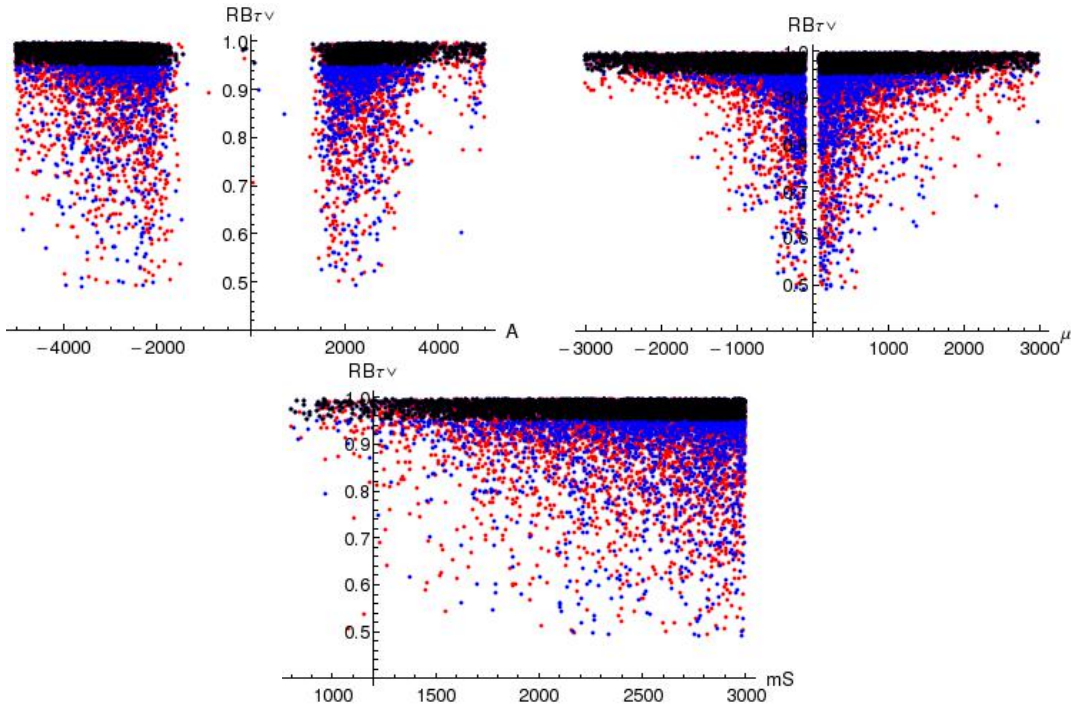

Figure 4.8: Allowed parameter space for A, μ and m_S in the MSSM with MFV as function of $R_{B\tau\nu}$. Notation as in Fig. 4.6.

where m_S is a common squark mass, $m_{\tilde{g}}$ is the gluino mass and $m_{\tilde{\chi}_1^\pm}$ is the lightest charghino. We chose 3 TeV as the upper bound for all the soft terms but A that we vary uniformly between -5 and 5 TeV. We consider the case in which all the squarks have the same mass m_S.

In Fig. 4.7 we show the allowed regions in the $\tan\beta - m_H$ plane in the various experimental situations, where we follow the same color notation as in the 2HDM-II case. In the same figure we show also the direct comparison between $B \to \tau\nu$ and $B_s \to \mu\mu$. Note that, unlike the general 2HDM$_{\overline{\text{MFV}}}$ studied in [4], in the supersymmetric version only a suppression in $B \to \tau\nu$ is possible. This possibility seems to be disfavored by the B-factories data, showing a possible enahncement in the $B \to \tau\nu$ decay rate compared to the SM. However the experimental situation is not very clear and after the recent Belle data [147] this anomaly is reduced. The supersymmetric parameter space is given in Fig. 4.8. As you can see in this simple realization of the MSSM the light Higgs mass bound strongly disfavor low A-term values, that would suppress the $B_s \to \mu\mu$ decay. On the other hand the chargino mass limit is quite weak and the low μ region can only be constrained after a $B \to \tau\nu$ measurement. Similarly also for the large squark region.

Finally, as already discussed in the first chapters, we consider the very precise muon $g-2$ measurement, which presents a 3.5 σ discrepancy with the SM expectation (see for example the recent analysis in [155]). In the MSSM$_{\overline{\text{MFV}}}$ this effect can be easily explained

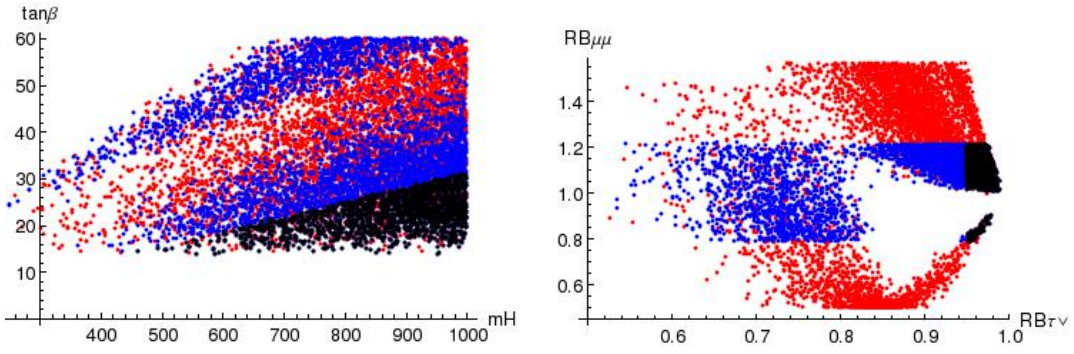

Figure 4.9: MSSM with MFV case adding the $g-2$ constraint to be satisfied at 2σ. Notation as in Fig. 4.6.

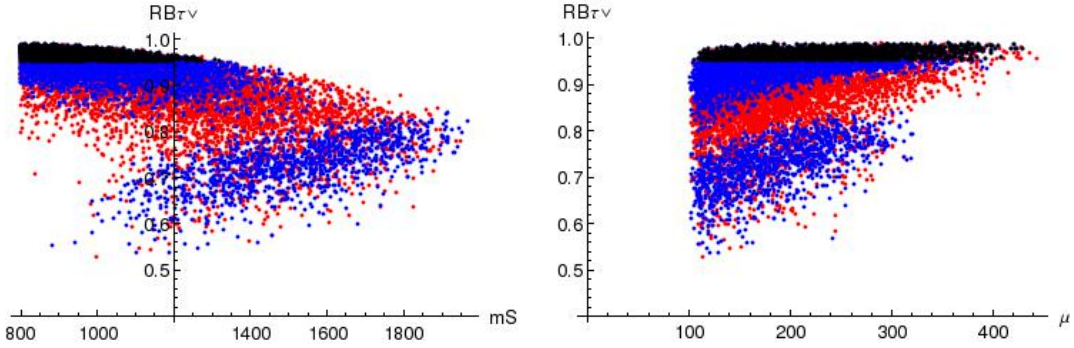

Figure 4.10: Allowed parameter space for m_S and μ as function of $R_{B\tau\nu}$ in the MSSM with MFV considering also $g-2$. Notation as in Fig. 4.6.

for large tan β. With our approximations the leading Wino contributions are [156]

$$\Delta a_\mu^{\text{MSSM}_{\overline{\text{MFV}}}} = \frac{\alpha_2}{4\,\pi} m_\mu^2 \frac{\mu\, M_2\, \tan\beta}{m_S^4} f_4\left(\frac{M_2^2}{m_S^2}, \frac{\mu^2}{m_S^2}\right) \tag{4.61}$$

where f_4 is given in [156]. We consider the conservative 2 σ bound

$$\Delta a_\mu^{exp} \in [0.95, 4, 15] \times 10^{-9}\,.$$

In this case, barring the finetuned solution with $\delta_S \simeq -1$ (the blue band at large tan β and low m_H in Fig. 4.9 on the left), the measurement of $B_s \to \mu\mu$ at 20% would highly constrain the parameter space, as show in Fig. 4.9, and the deviations in $B \to \tau\nu$ can hardly reach the 20% level. However for $\mu < 400$ GeV, $m_S < 1.4$ TeV and $m_{\tilde{g}} < 1.1$ TeV we find viable solutions that can be probed with $B \to \tau\nu$, as shown in Fig. 4.10.

4.3.3 Preliminary conclusions

In this preliminary analysis we compare the $B \to \tau\nu$ and $B_s \to \mu\mu$ processes in respect of their NP discovery potential. We analyze the case in which $B_s \to \mu\mu$ would be measured with a 20% error and compatible with the SM prediction, as can be expected before the LHCb upgrade with 5 fb^{-1} collected. In this case we study the remaining allowed parameter space that could be probed by a 5% measurement of $B \to \tau\nu$ by a superB machine. These regions will be tested also at LHC. The main results are that in the 2HDM-II a $B_s \to \mu\mu$ measurement would forbid part of the $\tan\beta - m_H$ plane, but $B \to \tau\nu$ turns out to be more efficient, mostly in the large m_H region. Moreover in the 2HDM$_{\overline{\text{MFV}}}$ the $\tan\beta$ dependence in $B_s \to \mu\mu$ is stronger then in $B \to \tau\nu$, but there are specific regions of the parameter space in which $B_s \to \mu\mu$ can be highly suppressed due to its loop nature.

This analysis has already been presented at the 4^{th} superB general meeting [5], but several improvement are in progress. First recently an excess from the SM prediction has been measured in the decays $B \to D^{(*)}\tau\nu$ [142]. This data can not be explained in the 2HDM assuming MFV [143, 144] and so different models need to be studied. Second the subleading correction in $\tan\beta$ can become sizable in the region where a cancellation in the leading $\tan\beta$ term appears in order to suppress the contribution to $B_s \to \mu\mu$, that we already know to be small. In this case pure supersymmetric effects, for example from squark non-degeneracy or non-alignement, must be considered. Third we showed that only a suppression in $B \to \tau\nu$ is possible in the models that we considered. Currently the experiments still prefer an enhancement compared to the SM value and we plan to study more models in which this is possible. Finally we also need to consider the present and future constraints from the Higgs decay in $\tau\tau$ from ATLAS and CMS.

Chapter 5

Final Remarks

The aim of this Thesis is to investigate the physics beyond the SM through flavor-changing processes of quarks and leptons.

In the first part we focused on supersymmetry and in particular on scenarios in which the first two squark generations are heavier than the third one, so as to explain in a natural way the absence of any SUSY signal at LHC. For what concern the flavor sector, interesting results can be achieved introducing $U(2)^5$ flavor symmetry acting on the first two generations. We analyze the lepton sector in this framework, showing that neutrino masses and lepton flavor violation in charged leptons can be described with a minimal ansatz about the breaking of the $U(2)^5$ flavor symmetry, consistent with the $U(2)^3$ breaking pattern of quark Yukawa couplings [1]. Neutrino masses are expected to be almost degenerate, close to present bounds from cosmology and $0\nu\beta\beta$ experiments. We also predict $s_{13} \approx s_{23}|V_{td}|/|V_{ts}| \approx 0.16$, in perfect agreement with the recent oscillation result. For slepton masses below 1 TeV, barring accidental cancellations, we expect $\mathcal{B}(\mu \to e\gamma) > 10^{-13}$ and $\mathcal{B}(\tau \to \mu\gamma) > 10^{-9}$, within the reach of future experimental searches.

We consider also the case in which this flavor symmetry is broken at a very high scale and we study the consequences at low energies through its RGE evolution [2]. Initial conditions compatible with a split scenario are found, and the preservation of correlations from minimal $U(2)^3$ breaking are checked. The various chiral operators in $\Delta F = 2$ processes are analyzed, and we show that, due to LHC gluino bounds, the $(LL)(RR)$ operators can not always be neglected. Finally, we also study a possible extension of the $U(2)^3$ model compatible with the lepton sector.

In the second part of the Thesis we focused on the phenomenology of non-minimal Higgs sectors. Given the ATLAS and CMS observation of a signal compatible with the SM Higgs boson we study the possibility of constraining and measuring its couplings in order to better understand the real nature of this particle [3]. We analyze the indirect constraints on flavor-changing Higgs decays that are provided by limits on low-energy flavor-changing interactions. We find that indirect limits in the quark sector impose such strong constraints that flavor-changing Higgs decays to quark-antiquark pairs are unlikely to be observable at the LHC. On the other hand, the upper limits on lepton-

flavor-changing decays are weaker, and the experimental signatures less challenging. In particular, we find that either $\mathcal{B}(h \to \tau\bar{\mu} + \bar{\mu}\tau)$ or $\mathcal{B}(h \to \tau\bar{e} + \bar{e}\tau)$ could be $\mathcal{O}(10)\%$, i.e., comparable to $\mathcal{B}(h \to \tau^+\tau^-)$ and potentially observable at the LHC.

We also consider the Two Higgs Doublets Model framework. In particular we analyze the $B \to \tau\nu$ decay in a generic case satisfying the MFV hypothesis [4]. We show under which conditions $\mathcal{B}(B \to \tau\nu)$ can be substantially enhanced over its SM value, taking into account the constraints of $K \to \mu\nu$, $B \to X_s\gamma$, and $B_s \to \mu^+\mu^-$. We find that for large $\tan\beta$ values and Peccei-Quinn symmetry breaking terms of $\mathcal{O}(1/\tan\beta)$ a sizable ($\sim 50\%$) enhancement of $\mathcal{B}(B \to \tau\nu)$ is possible, even for $m_H \sim 1$ TeV. We also study in detail the discovery potential of the $B \to \tau\nu$ and $B_s \to \mu\mu$ processes, in respect of the future experimental prospects [5].

Appendix A

Soft masses in SCKM basis

In the $U(3)^3$ framework of [56], both the Yukawa matrices and the soft masses are constructed through the addition of three spurions ΔY_u, ΔY_d and V, transforming adequately under the flavor symmetries. In the basis in which the Yukawas assume the form as in Eq (3.5), the squark mass and the trilinear couplings are given by Eqs (3.10 - 3.13). When the Yukawas are diagonalized, the soft matrices are rotated. We are interested in these matrices in the basis where Y_d is diagonal. Such change of basis involves a rotation in the $(2-3)$ block, followed by a further rotation in the $(1-2)$ block. For transparency, we shall write the structure of the soft masses after the first rotation, to leading order in ϵ:

$$\left(\frac{m^2_{\tilde{Q}}}{m^2_{Q_h}}\right)_{R_{23}} = I - \begin{pmatrix} 0 & 0 & 0 \\ 0 & x_{22}\,\epsilon^2 & -x_L\,\epsilon\,e^{i\gamma_L} \\ 0 & -x_L\,\epsilon\,e^{-i\gamma_L} & \rho_Q - x_{33}\epsilon^2 \end{pmatrix}, \tag{A. 1}$$

$$\left(\frac{m^2_{\tilde{d}}}{m^2_{d_h}}\right)_{R_{23}} = I - \begin{pmatrix} 0 & 0 & 0 \\ 0 & 0 & -x_D\,\lambda_{d_2}\,\epsilon\,e^{-i\gamma_D} \\ 0 & -x_D\,\lambda_{d_2}\,\epsilon\,e^{i\gamma_D} & \rho_d \end{pmatrix}, \tag{A. 2}$$

$$\left(\frac{m^2_{\tilde{u}}}{m^2_{u_h}}\right)_{R_{23}} = I - \begin{pmatrix} 0 & 0 & 0 \\ 0 & 0 & -x_U\,\lambda_{u_2}\,\epsilon\,e^{-i\gamma_U} \\ 0 & -x_U\,\lambda_{u_2}\,\epsilon\,e^{i\gamma_U} & \rho_u \end{pmatrix}. \tag{A. 3}$$

where $\rho_f = (m^2_{f_h} - m^2_{f_l})/m^2_{f_h}$, x_i are real parameters of $O(1)$ and λ_i are the ratios between the first two and the third Yukawa eigenvalues, defined in Eq (3.7). These shall be the parameters relevant for phenomenology. Notice that the off-diagonals in $m^2_{\tilde{d}}$ and $m^2_{\tilde{u}}$ are suppressed by the second generation quark masses.

Finally, we can apply the rotation in the $(1-2)$ sector, including any further rephasings:

$$\left(\frac{m^2_{\tilde{Q}}}{m^2_{Q_h}}\right)_{Y_d} = \begin{pmatrix} c_d\,e^{-i(\delta-\alpha_u)} & s_d\,e^{-i(\delta+\alpha_d-\alpha_u)} & 0 \\ -s_d\,e^{i\alpha_d} & c_d & 0 \\ 0 & 0 & 1 \end{pmatrix} \cdot \left(\frac{m^2_{\tilde{Q}}}{m^2_{Q_h}}\right)_{R_{23}} \cdot \begin{pmatrix} c_d\,e^{i(\delta-\alpha_u)} & -s_d\,e^{-i\alpha_d} & 0 \\ s_d\,e^{i(\delta+\alpha_d-\alpha_u)} & c_d & 0 \\ 0 & 0 & 1 \end{pmatrix}, \tag{A. 4}$$

with a negligible modification of $m^2_{\tilde{u}}$ and $m^2_{\tilde{d}}$.

The trilinear couplings follow a structure similar to that of the Yukawas. Their leading structure in the SCKM basis is:

$$A_u = V_{CKM}^T \cdot \begin{pmatrix} a_1^u \lambda_{u_1} & 0 & (a_2^u - a_3^u) s_u \, e^{i\alpha_u} \epsilon \\ 0 & a_1^u \lambda_{u_2} & (a_2^u - a_3^u) c_u \epsilon \\ 0 & 0 & a_3^u \end{pmatrix} y_t A_t^0 \,, \tag{A. 5}$$

$$A_d = \begin{pmatrix} a_1^d \lambda_{d_1} & 0 & (a_2^d - a_3^d) s_d \, e^{i\alpha_d} \epsilon \\ 0 & a_1^d \lambda_{d_2} & (a_2^d - a_3^d) c_d \epsilon \\ 0 & 0 & a_3^u \end{pmatrix} y_b A_b^0 \,. \tag{A. 6}$$

Similarly in the charged lepton sector, we obtain $m_{\tilde{L}}^2 \sim m_{\tilde{Q}}^2$, $m_{\tilde{e}}^2 \sim m_{\tilde{d}}^2$ and $A_e \sim A_d$, in the Y_e diagonal basis.

Bibliography

[1] G. Blankenburg, G. Isidori and J. Jones-Perez, Eur. Phys. J. C **72** (2012) 2126 [arXiv:1204.0688 [hep-ph]].

[2] G. Blankenburg and J. Jones-Perez, arXiv:1210.4561 [hep-ph].

[3] G. Blankenburg, J. Ellis and G. Isidori, Phys. Lett. B **712**, 386 (2012) [arXiv:1202.5704 [hep-ph]].

[4] G. Blankenburg and G. Isidori, Eur. Phys. J. Plus **127**, 85 (2012) [arXiv:1107.1216 [hep-ph]].

[5] G. Blankenburg (in collaboration with M. Ciuchini), 4^{th} SuperB Collaboration Meeting
http://agenda.infn.it/conferenceDisplay.py?confId=4880
work in progress

[6] LEP Electroweak Working Group, status of March 2012, http://lepewwg.web.cern.ch/LEPEWWG/;

[7] S. Chatrchyan *et al.* [CMS Collaboration], Phys. Lett. B **716**, 30 (2012) [arXiv:1207.7235 [hep-ex]].

[8] G. Aad *et al.* [ATLAS Collaboration], Phys. Lett. B **716**, 1 (2012) [arXiv:1207.7214 [hep-ex]].

[9] [KamLAND-Zen Collaboration], Phys. Rev. C **85**, 045504 (2012) [arXiv:1201.4664 [hep-ex]].

[10] J. J. Gomez-Cadenas, J. Martin-Albo, M. Sorel, P. Ferrario, F. Monrabal, J. Munoz-Vidal, P. Novella and A. Poves, JCAP **1106**, 007 (2011) [arXiv:1010.5112 [hep-ex]].

[11] C. D. Froggatt and H. B. Nielsen, Nucl. Phys. B **147**, 277 (1979).

[12] L. Randall and R. Sundrum, Phys. Rev. Lett. **83**, 3370 (1999) [hep-ph/9905221].

[13] N. Haba and H. Murayama, Phys. Rev. D **63**, 053010 (2001) [hep-ph/0009174].

[14] G. Altarelli and F. Feruglio, Rev. Mod. Phys. **82**, 2701 (2010) [arXiv:1002.0211 [hep-ph]].

[15] A. Osipowicz *et al.* [KATRIN Collaboration], hep-ex/0109033.

[16] S. Plaszczynski, PoS IDM **2010**, 066 (2011) [arXiv:1012.2215 [astro-ph.CO]].

[17] A. J. Buras, hep-ph/9806471.

[18] Y. Nir, hep-ph/9911321. Y. Nir, CERN Yellow Report CERN-2010-001, 279-314 [arXiv:1010.2666 [hep-ph]].

[19] A. Pich, arXiv:1112.4094 [hep-ph].

[20] S. P. Martin, In *Kane, G.L. (ed.): Perspectives on supersymmetry II* 1-153 [hep-ph/9709356].

[21] I. J. R. Aitchison, hep-ph/0505105.

[22] K. Nakamura *et al.* [PDG Collaboration], J. Phys. G **37** (2010) 075021.

[23] R. Aaij *et al.* [LHCb Collaboration], Phys. Rev. Lett. **108**, 111602 (2012) [arXiv:1112.0938 [hep-ex]].

[24] M. Dine, hep-ph/0011376.

[25] A. J. Bevan *et al.* [UTfit Collaboration], PoS ICHEP **2010**, 270 (2010) [arXiv:1010.5089 [hep-ph]].

[26] J. Charles, O. Deschamps, S. Descotes-Genon, R. Itoh, H. Lacker, A. Menzel, S. Monteil and V. Niess *et al.*, Phys. Rev. D **84**, 033005 (2011) [arXiv:1106.4041 [hep-ph]].

[27] A. J. Buras and J. Girrbach, Acta Phys. Polon. B **43**, 1427 (2012) [arXiv:1204.5064 [hep-ph]].

[28] G. Isidori, Y. Nir and G. Perez, Ann. Rev. Nucl. Part. Sci. **60**, 355 (2010) [arXiv:1002.0900 [hep-ph]].

[29] M. Ciuchini, V. Lubicz, L. Conti, A. Vladikas, A. Donini, E. Franco, G. Martinelli and I. Scimemi *et al.*, JHEP **9810**, 008 (1998) [hep-ph/9808328].

[30] M. Bona *et al.* [UTfit Collaboration], JHEP **0803**, 049 (2008) [arXiv:0707.0636 [hep-ph]].

[31] G. D'Ambrosio, G. F. Giudice, G. Isidori and A. Strumia, Nucl. Phys. B **645**, 155 (2002) [hep-ph/0207036].

[32] R. S. Chivukula and H. Georgi, Phys. Lett. B **188** (1987) 99.

[33] A. J. Buras, P. Gambino, M. Gorbahn, S. Jager and L. Silvestrini, Phys. Lett. B **500** (2001) 161 [arXiv:hep-ph/0007085].

[34] A. L. Kagan, G. Perez, T. Volansky, J. Zupan, Phys. Rev. **D80** (2009) 076002. [arXiv:0903.1794 [hep-ph]].

[35] A. J. Buras, G. Isidori and P. Paradisi, Phys. Lett. B **694**, 402 (2011) [arXiv:1007.5291 [hep-ph]].

[36] P. Paradisi and D. M. Straub, Phys. Lett. B **684**, 147 (2010) [arXiv:0906.4551 [hep-ph]].

[37] A. J. Buras, Acta Phys. Polon. B **34**, 5615 (2003) [hep-ph/0310208].

[38] E. Nikolidakis and C. Smith, Phys. Rev. D **77**, 015021 (2008) [arXiv:0710.3129 [hep-ph]].

[39] G. Arcadi, L. Di Luzio and M. Nardecchia, JHEP **1205**, 048 (2012) [arXiv:1111.3941 [hep-ph]].

[40] M. Papucci, J. T. Ruderman and A. Weiler, JHEP **1209**, 035 (2012) [arXiv:1110.6926 [hep-ph]].

[41] M. S. Carena, M. Quiros and C. E. M. Wagner, Nucl. Phys. B **461**, 407 (1996) [hep-ph/9508343].

[42] A. Arbey, M. Battaglia, A. Djouadi, F. Mahmoudi and J. Quevillon, Phys. Lett. B **708**, 162 (2012) [arXiv:1112.3028 [hep-ph]].

[43] J. S. Hagelin, S. Kelley and T. Tanaka, Nucl. Phys. B **415**, 293 (1994).

[44] A. Masiero, S. K. Vempati and O. Vives, arXiv:0711.2903 [hep-ph].

[45] M. Artuso, D. M. Asner, P. Ball, E. Baracchini, G. Bell, M. Beneke, J. Berryhill and A. Bevan *et al.*, Eur. Phys. J. C **57**, 309 (2008) [arXiv:0801.1833 [hep-ph]].

[46] M. Raidal, A. van der Schaaf, I. Bigi, M. L. Mangano, Y. K. Semertzidis, S. Abel, S. Albino and S. Antusch *et al.*, Eur. Phys. J. C **57**, 13 (2008) [arXiv:0801.1826 [hep-ph]].

[47] H. Baer, S. Kraml, A. Lessa, S. Sekmen and X. Tata, JHEP **1010**, 018 (2010) [arXiv:1007.3897 [hep-ph]].

[48] H. Baer, V. Barger, P. Huang and X. Tata, JHEP **1205**, 109 (2012) [arXiv:1203.5539 [hep-ph]].

[49] B. C. Allanach and B. Gripaios, arXiv:1202.6616.

[50] G. Aad *et al.* [ATLAS Collaboration], arXiv:1209.4186 [hep-ex].

[51] M. Dine, R. G. Leigh and A. Kagan, Phys. Rev. D **48** (1993) 4269 [hep-ph/9304299].

[52] S. Dimopoulos and G. F. Giudice, Phys. Lett. B **357** (1995) 573 [hep-ph/9507282].

[53] A. G. Cohen, D. B. Kaplan and A. E. Nelson, Phys. Lett. B **388** (1996) 588 [hep-ph/9607394].

[54] R. Barbieri, E. Bertuzzo, M. Farina, P. Lodone and D. Pappadopulo, JHEP **1008** (2010) 024 [arXiv:1004.2256 [hep-ph]].

[55] G. F. Giudice, M. Nardecchia and A. Romanino, Nucl. Phys. B **813** (2009) 156 [arXiv:0812.3610 [hep-ph]].

[56] R. Barbieri, G. Isidori, J. Jones-Perez, P. Lodone and D. M. Straub, Eur. Phys. J. C **71** (2011) 1725 [arXiv:1105.2296 [hep-ph]].

[57] A. Pomarol and D. Tommasini, Nucl. Phys. B **466** (1996) 3 [hep-ph/9507462];

[58] R. Barbieri, G. R. Dvali and L. J. Hall, Phys. Lett. B **377** (1996) 76 [hep-ph/9512388];

[59] R. Barbieri, L. J. Hall and A. Romanino, Phys. Lett. B **401** (1997) 47 [hep-ph/9702315].

[60] R. Barbieri, P. Campli, G. Isidori, F. Sala and D. M. Straub, Eur. Phys. J. C **71** (2011) 1812 [arXiv:1108.5125 [hep-ph]].

[61] R. Barbieri, D. Buttazzo, F. Sala and D. M. Straub, JHEP **1207** (2012) 181 [arXiv:1203.4218 [hep-ph]].

[62] A. J. Buras and J. Girrbach, arXiv:1206.3878 [hep-ph].

[63] A. Crivellin, L. Hofer and U. Nierste, PoS EPS **-HEP2011**, 145 (2011) [arXiv:1111.0246 [hep-ph]].

[64] T. Feldmann and T. Mannel, Phys. Rev. Lett. **100** (2008) 171601 [arXiv:0801.1802 [hep-ph]].

[65] R. T. D'Agnolo and D. M. Straub, JHEP **1205**, 034 (2012) [arXiv:1202.4759 [hep-ph]].

[66] R. Barbieri, D. Buttazzo, F. Sala and D. M. Straub, arXiv:1206.1327 [hep-ph].

[67] LHCb Collaboration. LHCb-CONF-2011-056

[68] D. M. Straub, PoS EPS **-HEP2011**, 146 (2011) [arXiv:1110.6391 [hep-ph]].

[69] S. L. Glashow, arXiv:1106.3319.

[70] S. Weinberg, Phys. Rev. Lett. **43** (1979) 1566.

[71] F. P. An *et al.* [DAYA-BAY Collaboration], arXiv:1203.1669.

[72] J. K. Ahn *et al.* [RENO Collaboration], Phys. Rev. Lett. **108**, 191802 (2012) [arXiv:1204.0626 [hep-ex]].

[73] T. Schwetz, M. Tortola and J. W. F. Valle, New J. Phys. **13** (2011) 109401 [arXiv:1108.1376].

[74] G. L. Fogli, E. Lisi, A. Marrone, A. Palazzo and A. M. Rotunno, Phys. Rev. D **84** (2011) 053007 [arXiv:1106.6028].

[75] E. Komatsu *et al.* [WMAP Collaboration], Astrophys. J. Suppl. **192** (2011) 18 [arXiv:1001.4538 [astro-ph.CO]].

[76] J. J. Gomez-Cadenas, J. Martin-Albo, M. Sorel, P. Ferrario, F. Monrabal, J. Munoz-Vidal, P. Novella and A. Poves, JCAP **1106** (2011) 007 [arXiv:1010.5112].

[77] S. Plaszczynski, PoS IDM **2010** (2011) 066 [arXiv:1012.2215 [astro-ph.CO]].

[78] [The KamLAND-Zen Collaboration], arXiv:1201.4664.

[79] C. Arnaboldi *et al.* [CUORICINO Collaboration], Phys. Rev. C **78** (2008) 035502 [arXiv:0802.3439].

[80] R. Arnold *et al.* [NEMO Collaboration], Phys. Rev. Lett. **95** (2005) 182302 [hep-ex/0507083].

[81] H. V. Klapdor-Kleingrothaus and I. V. Krivosheina, Mod. Phys. Lett. A **21** (2006) 1547.

[82] J. Adam *et al.* [MEG Collaboration], Phys. Rev. Lett. **107** (2011) 171801 [arXiv:1107.5547].

[83] LEP2 SUSY Working Group: http:// lepsusy.web.cern.ch/ lepsusy/ www/ sleptons_summer04/ slep_final.html

[84] B. Aubert *et al.* [BABAR Collaboration], Phys. Rev. Lett. **104** (2010) 021802 [arXiv:0908.2381].

[85] V. Cirigliano, B. Grinstein, G. Isidori and M. B. Wise, Nucl. Phys. B **728** (2005) 121 [hep-ph/0507001]; S. Davidson and F. Palorini, Phys. Lett. B **642** (2006) 72 [hep-ph/0607329]; M. B. Gavela, T. Hambye, D. Hernandez and P. Hernandez, JHEP **0909** (2009) 038 [arXiv:0906.1461]; R. Alonso, G. Isidori, L. Merlo, L. A. Munoz and E. Nardi, JHEP **1106** (2011) 037 [arXiv:1103.546].

[86] Z. -z. Xing, H. Zhang and S. Zhou, Phys. Rev. D **77** (2008) 113016 [arXiv:0712.1419 [hep-ph]].

[87] J. C. Hardy and I. S. Towner, Phys. Rev. C **79** (2009) 055502 [arXiv:0812.1202 [nucl-ex]] ; M. Antonelli, V. Cirigliano, G. Isidori, F. Mescia, M. Moulson, H. Neufeld, E. Passemar and M. Palutan *et al.*, Eur. Phys. J. C **69** (2010) 399 [arXiv:1005.2323 [hep-ph]] ; A. Lenz, U. Nierste, J. Charles, S. Descotes-Genon, A. Jantsch, C. Kaufhold, H. Lacker and S. Monteil *et al.*, Phys. Rev. D **83** (2011) 036004 [arXiv:1008.1593 [hep-ph]] ; R. V. Kowalewski [BaBar Collaboration], PoS BEAUTY **2011** (2011) 030.

[88] S. P. Martin and M. T. Vaughn, Phys. Rev. D **50** (1994) 2282 [Erratum-ibid. D **78** (2008) 039903] [hep-ph/9311340].

[89] N. Arkani-Hamed and H. Murayama, Phys. Rev. D **56** (1997) 6733 [hep-ph/9703259].

[90] C. Tamarit, arXiv:1204.2292 [hep-ph].

[91] S. Heinemeyer, W. Hollik and G. Weiglein, Comput. Phys. Commun. **124** (2000) 76 [hep-ph/9812320].

[92] S. Heinemeyer, W. Hollik and G. Weiglein, Eur. Phys. J. C **9** (1999) 343 [hep-ph/9812472].

[93] G. Degrassi, S. Heinemeyer, W. Hollik, P. Slavich and G. Weiglein, Eur. Phys. J. C **28** (2003) 133 [hep-ph/0212020].

[94] M. Frank, T. Hahn, S. Heinemeyer, W. Hollik, H. Rzehak and G. Weiglein, JHEP **0702** (2007) 047 [hep-ph/0611326].

[95] G. Buchalla, A. J. Buras and M. E. Lautenbacher, Rev. Mod. Phys. **68** (1996) 1125 [hep-ph/9512380].

[96] P. Paradisi, M. Ratz, R. Schieren and C. Simonetto, Phys. Lett. B **668** (2008) 202 [arXiv:0805.3989 [hep-ph]].

[97] J. F. Donoghue, H. P. Nilles and D. Wyler, Phys. Lett. B **128** (1983) 55.

[98] F. Gabbiani, E. Gabrielli, A. Masiero and L. Silvestrini, Nucl. Phys. B **477** (1996) 321 [hep-ph/9604387].

[99] F. Mescia and J. Virto, arXiv:1208.0534 [hep-ph].

[100] G. Raz, Phys. Rev. D **66**, 037701 (2002) [hep-ph/0205310].

[101] J. Brod and M. Gorbahn, Phys. Rev. Lett. **108** (2012) 121801 [arXiv:1108.2036 [hep-ph]].

[102] A. Azatov, R. Contino and J. Galloway, JHEP **1204**, 127 (2012) [arXiv:1202.3415 [hep-ph]].

[103] P. P. Giardino, K. Kannike, M. Raidal and A. Strumia, arXiv:1207.1347 [hep-ph].

[104] J. Ellis and T. You, JHEP **1209**, 123 (2012) [arXiv:1207.1693 [hep-ph]].

[105] W. D. Goldberger, B. Grinstein and W. Skiba, Phys. Rev. Lett. **100** (2008) 111802 [arXiv:0708.1463]; J. Fan, W. D. Goldberger, A. Ross and W. Skiba, Phys. Rev. D **79** (2009) 035017 [arXiv:0803.2040].

[106] K. Agashe and R. Contino, Phys. Rev. D **80** (2009) 075016 [arXiv:0906.1542]; A. Azatov, M. Toharia and L. Zhu, Phys. Rev. D **80** (2009) 035016 [arXiv:0906.1990].

[107] G. F. Giudice and O. Lebedev, Phys. Lett. B **665** (2008) 79 [arXiv:0804.1753].

[108] G. C. Branco *et al.* arXiv:1106.0034; A. J. Buras, M. V. Carlucci, S. Gori and G. Isidori, JHEP **1010** (2010) 009 [arXiv:1005.5310].

[109] S. Kanemura, T. Ota and K. Tsumura, Phys. Rev. D **73** (2006) 016006 [hep-ph/0505191].

[110] P. Paradisi, JHEP **0602** (2006) 050 [hep-ph/0508054].

[111] E. Gabrielli and B. Mele, Phys. Rev. D **83** (2011) 073009 [arXiv:1102.3361 [hep-ph]].

[112] S. Davidson and G. J. Grenier, Phys. Rev. D **81** (2010) 095016 [arXiv:1001.0434].

[113] A. Goudelis, O. Lebedev and J. -h. Park, Phys. Lett. B **707** (2012) 369 [arXiv:1111.1715].

[114] S. Chatrchyan *et al.* [CMS Collaboration], Phys. Lett. B **713**, 68 (2012) [arXiv:1202.4083 [hep-ex]].

[115] R. Aaij *et al.* [LHCb Collaboration], Physics Letters B **708** (2012) 55 [arXiv:1112.1600].

[116] E. Cervero and J. -M. Gerard, arXiv:1202.1973 [hep-ph].

[117] M. Raidal *et al.*, Eur. Phys. J. C **57** (2008) 13 [arXiv:0801.1826].

[118] V. Cirigliano, R. Kitano, Y. Okada and P. Tuzon, Phys. Rev. D **80** (2009) 013002 [arXiv:0904.0957].

[119] D. Hanneke, S. Fogwell and G. Gabrielse, Phys. Rev. Lett. **100** (2008) 120801 [arXiv:0801.1134].

[120] J. Adam *et al.* [MEG Collaboration], Phys. Rev. Lett. **107** (2011) 171801 [arXiv:1107.5547].

[121] S. M. Barr and A. Zee, Phys. Rev. Lett. **65** (1990) 21 [Erratum-ibid. **65** (1990) 2920].

[122] A. Goudelis, O. Lebedev, J. Park, Phys. Lett. B **707** 369 (2012) [arXiv:1111.1715].

[123] T. D. Lee, Phys. Rev. D **8**, 1226 (1973).

[124] G. C. Branco, P. M. Ferreira, L. Lavoura, M. N. Rebelo, M. Sher and J. P. Silva, Phys. Rept. **516**, 1 (2012) [arXiv:1106.0034 [hep-ph]].

[125] S. L. Glashow and S. Weinberg, Phys. Rev. D **15**, 1958 (1977).

[126] J. Bernabeu, G. C. Branco and M. Gronau, Phys. Lett. B **169**, 243 (1986).

[127] A. J. Buras, M. V. Carlucci, S. Gori, G. Isidori, JHEP **1010** (2010) 009. [arXiv:1005.5310 [hep-ph]].

[128] B. A. Dobrescu, P. J. Fox, A. Martin, Phys. Rev. Lett. **105** (2010) 041801. [arXiv:1005.4238 [hep-ph]].

[129] M. Jung, A. Pich, P. Tuzon, JHEP **1011** (2010) 003. [arXiv:1006.0470 [hep-ph]].

[130] B. Bhattacherjee, A. Dighe, D. Ghosh and S. Raychaudhuri, Phys. Rev. D **83** (2011) 094026 [arXiv:1012.1052 [hep-ph]].

[131] R. Barlow, [arXiv:1102.1267 [hep-ex]]; D. Asner *et al.* [Heavy Flavor Averaging Group Collaboration], [arXiv:1010.1589 [hep-ex]].

[132] A. J. Bevan *et al.* [UTfit Collaboration], Phys. Lett. **B687** (2010) 61-69. [arXiv:0908.3470 [hep-ph]].

[133] K. Nakamura *et al.* [Particle Data Group Collaboration], J. Phys. G G **37** (2010) 075021.

[134] W. -S. Hou, Phys. Rev. **D48** (1993) 2342-2344.

[135] T. Hurth, G. Isidori, J. F. Kamenik, F. Mescia, Nucl. Phys. **B808** (2009) 326-346. [arXiv:0807.5039 [hep-ph]].

[136] M. Antonelli *et al.*, Eur. Phys. J. **C69** (2010) 399-424. [arXiv:1005.2323 [hep-ph]].

[137] G. Colangelo *et al.*, [arXiv:1011.4408 [hep-lat]].

[138] J. F. Kamenik, F. Mescia, Phys. Rev. **D78** (2008) 014003. [arXiv:0802.3790 [hep-ph]].

[139] A. G. Akeroyd, S. Recksiegel, J. Phys. G **G29** (2003) 2311-2317. [hep-ph/0306037].

[140] B. A. Dobrescu and P. J. Fox, JHEP **0808** (2008) 100 [arXiv:0805.0822 [hep-ph]]; B. A. Dobrescu, P. J. Fox and A. Martin, Phys. Rev. Lett. **105** (2010) 041801 [arXiv:1005.4238 [hep-ph]].

[141] F. Ambrosino *et al.* [KLOE Collaboration], Phys. Lett. **B632** (2006) 76-80. [hep-ex/0509045].

[142] [BaBar Collaboration], arXiv:1205.5442 [hep-ex].

[143] S. Fajfer, J. F. Kamenik, I. Nisandzic and J. Zupan, arXiv:1206.1872 [hep-ph].

[144] A. Crivellin, C. Greub and A. Kokulu, arXiv:1206.2634 [hep-ph]

[145] RAaij *et al.* [LHCb Collaboration], arXiv:1211.2674 [hep-ex].

[146] A. J. Buras, J. Girrbach, D. Guadagnoli and G. Isidori, arXiv:1208.0934 [hep-ph].

[147] I. Adachi *et al.* [Belle Collaboration], arXiv:1208.4678 [hep-ex].

[148] W. Altmannshofer, M. Carena, N. Shah and F. Yu, arXiv:1211.1976 [hep-ph].

[149] A. G. Akeroyd, F. Mahmoudi and D. M. Santos, JHEP **1112**, 088 (2011) [arXiv:1108.3018 [hep-ph]].

[150] M. Bona *et al.* [SuperB Collaboration], Pisa, Italy: INFN (2007) 453 p. www.pi.infn.it/SuperB/?q=CDR [arXiv:0709.0451 [hep-ex]]. D. G. Hitlin, C. H. Cheng, D. M. Asner, T. Hurth, B. McElrath, T. Shindou, F. Ronga and M. Rama *et al.*, arXiv:0810.1312 [hep-ph]. B. O'Leary *et al.* [SuperB Collaboration], arXiv:1008.1541 [hep-ex].

[151] T. Aushev, W. Bartel, A. Bondar, J. Brodzicka, T. E. Browder, P. Chang, Y. Chao and K. F. Chen *et al.*, arXiv:1002.5012 [hep-ex]. T. Abe [Belle II Collaboration], arXiv:1011.0352 [physics.ins-det].

[152] LHCB collaboration
http://cdsweb.cern.ch/record/1333091

[153] C. Bobeth, T. Ewerth, F. Kruger and J. Urban, Phys. Rev. D **64**, 074014 (2001) [hep-ph/0104284].

[154] ATLAS collaboration
http://atlas.web.cern.ch/Atlas/Collaboration/ .
CMS collaboration
http://cms.web.cern.ch/ .
LEP 2 SUSY working group
http://lepsusy.web.cern.ch/lepsusy/ .

[155] G. F. Giudice, P. Paradisi and M. Passera, arXiv:1208.6583 [hep-ph].

[156] W. Altmannshofer and D. M. Straub, JHEP **1009**, 078 (2010) [arXiv:1004.1993 [hep-ph]].